Migrant Networks and Climate Change

Shifrah Aron-Dine
UC Berkeley

Emmanuella Kyei Manu
Stanford
(Job Market Paper) *

November 15, 2026
[link to latest version]

Abstract

Migration is a potentially important form of climate adaptation if people choose to relocate to less exposed places. However, using global data on migration and climate, we find that new emigrants follow existing diasporas and that diasporas are concentrated in places with similar climates to the origin country. To assess the implications of these patterns for future adaptation, we build a dynamic spatial model with endogenous migrant networks and spatially correlated climate risk. Networks exacerbate climate losses when they are concentrated in locations whose expected damages and climate shocks positively covary with the origin's. Quantitatively, networks increase the welfare cost of climate change for two-thirds of the world. In poor, climate-exposed countries, they raise consumption-equivalent welfare losses by 2 percentage points, roughly the cost of an additional degree of warming by 2100. Targeted migration policies improve adaptation by building networks in less exposed destinations, and earlier policies generate larger gains.

*Emails: aron-dine@berkeley.edu and kyeimanu@stanford.edu. We are especially grateful to Pete Klenow, Melanie Morten, Patrick Kehoe, and Benny Kleinman for their guidance and support. We would also like to thank Ran Abramitzky, Adrien Auclert, Adrien Bilal, Luigi Bocola, Johannes Boehm, Kirill Borusyak, Marshall Burke, Tamma Carleton, Doireann Fitzgerald, Kelsey Jack, Chad Jones, Gabriel Kreindler, Ishan Nath, Elena Pastorino, Monika Piazzesi, Stephen Redding, Esteban Rossi-Hansberg, Martin Schneider, Felix Soliman, Bryan Stuart, Chris Tonetti, and Mike Waugh for helpful comments and suggestions. Emmanuella Kyei Manu acknowledges support from the Leonard W. Ely and Shirley R. Ely Graduate Student Fellowship through a grant to the Stanford Institute for Economic Policy Research.

1. Introduction

The impacts of climate change are unequally distributed across the globe. Empirical estimates of the effect of warming predict large economic losses for countries that are already hot and potential gains for some countries with currently colder climates (Burke et al., 2015; Nath et al., 2024). Because the welfare cost of warming depends on how many people can migrate to less exposed places, migration is often viewed as a key adaptation margin (Intergovernmental Panel on Climate Change, 2022). People migrate in search of economic opportunity or in response to climate shocks, but they also tend to move toward destinations with large diaspora communities from their origin (Bartel, 1989; Beine et al., 2011; Mahajan and Yang, 2020; Stuart and Taylor, 2021; Blumenstock et al., 2025). Migrant networks may facilitate adaptation if they draw migrants toward destinations with smaller climate losses. However, they may instead limit adaptation if they draw migrants toward destinations as exposed to climate change as the origin and adjust little as the world warms.

In this paper, we quantify how migrant networks shape the welfare cost of global warming. We combine data on bilateral migration with country-level measures of climate exposure. We use these data to measure how strongly existing networks shape the destinations of new emigrants and how exposed these networks are to current warming. We then develop a dynamic spatial model in which a larger diaspora attracts additional new migrants and the network evolves endogenously with household migration choices. We estimate the key elasticities of the model, including the strength of the network, from changes in migration within corridors over time. Combining the estimated model with country-level projections of economic growth and climate damages, we quantify how much the network changes climate losses through the end of the century. Finally, we use the model to evaluate the potential for migration policy to exacerbate or mitigate climate losses through its effect on the network.

We find that migrant networks limit migration as an adaptation strategy to climate change. In the data, new migrants follow existing diasporas, which are highly persistent. These diasporas are currently concentrated in destinations whose climate resembles that of the origin. As a result, when we project the economy forward, the network adjusts little to warming. Relative to an economy in which diasporas do not affect migration costs, the network raises the climate loss of the average household by 1.20 percentage points of lifetime consumption, equivalent to 0.7°C of additional warming. In the economy with the migrant network, climate losses are nearly identical to those in an economy with no migration, where every household experiences the economic losses of its origin.

Migration policy changes where households live and therefore their exposure to the economic effects of global warming, and the migrant network amplifies these effects. We find that restricting immigration into high-income destinations with small climate losses lowers welfare and raises climate losses, especially for origins that face large losses themselves and have large diasporas in these destinations. Even temporary immigration restrictions can have persistent effects. Broadly easing immigration restrictions can lower climate losses, in particular for origins that gain access to

destinations less exposed to climate change. However, it does so by moving very large numbers of people between countries. A targeted climate visa program for the most affected origins can deliver large gains by building networks in destinations that gain from warming.

We first document that, globally, new emigrants follow the existing migrant network. Using bilateral migrant stocks and flows over the last three decades, we show that destinations with a larger share of an origin's diaspora receive a larger share of its new emigrants. To separate the effect of the migrant network from confounding bilateral factors, we use a modified version of the instrument of Burchardi et al. (2019). The instrument isolates quasi-random variation in the size of an origin's diaspora in a particular destination. This variation arises when past emigration waves out of the origin happened to coincide with immigration booms into that destination from other regions. The IV estimates imply that a 10 percent larger diaspora in a destination raises the number of new migrants from the origin to that destination by 7 percent.

Second, we document that origins and their diasporas face similar climate exposure. For each origin, we compute the average temperature experienced by its diaspora, weighting each destination by the number of migrants living there. The correlation between origin and diaspora temperature is 0.75. This correlation is driven by migrants who settle in nearby countries, where the climate is similar to that of the origin. Migrants from low-income origins live much closer to their origin than migrants from high-income origins. This suggests that migration along existing networks may offer limited scope to reduce climate exposure.

Third, we find that migrant networks have shifted toward cooler destinations as the climate has warmed. From 1995 to 2020, the average origin country warmed by 0.8°C. Over the same period, the reallocation of the network toward cooler destinations offset 62 percent of the warming in existing destinations. This shift is largest among emigrants from the hottest countries, whose diasporas now live more than 400 kilometers farther from their origin country than in 1995. These facts, however, describe only how networks responded to past warming. Quantifying how networks shape the losses from much larger future warming requires a model.

Motivated by these facts, we develop a dynamic spatial model of migration in which migrant networks evolve endogenously. The model departs from standard spatial models of climate change in three ways. First, a larger diaspora in a destination lowers the cost of migrating there for households from the same origin. Because this period's migration decisions determine next period's diaspora, the network is a state variable that shapes future migration costs. Second, we model climate damages as stochastic and correlated across countries, so the value of a destination depends on how its damages co-move with those at the origin and at other destinations. Third, we allow migration costs to fall as the origin's economy grows, to capture in reduced form the role of financial constraints in migration.

The dynamics of the model are governed by the network elasticity, that is, the response of migration to the size of the existing diaspora. Relative to a standard spatial model, the network makes migration respond more strongly and more persistently to shocks. A shock that raises the wage in a destination draws new migrants there. These migrants enlarge the diaspora, which lowers

migration costs from their origin and draws additional migrants. The larger diaspora keeps drawing migrants after a temporary shock fades and amplifies the long-run response to a permanent shock. When the network elasticity is below one, the network converges to a unique stationary distribution. When it exceeds one, the model can have multiple steady states.

We estimate the parameters that govern migration by the simulated method of moments on the global panel of migrant stocks. The response of migration to destination wages identifies the dispersion of location tastes. The persistence of migration within a corridor over time identifies how strongly the diaspora lowers migration costs. The rise in emigration from poor origins as their economies grow identifies how migration costs fall with origin income. We estimate a network elasticity of 0.74, which is small enough that the long-run network is unique but large enough that persistence and amplification through the network are quantitatively important. The estimated model also forecasts migration well out of sample.

To measure climate losses, we also need projected paths for economic growth and for the effects of climate change. For growth absent climate change, we use the income projections of the Shared Socioeconomic Pathways, with SSP3 as our baseline. For climate, we take the expected warming path and the shocks around it from the Max Planck Institute Grand Ensemble. This ensemble isolates uncertainty from climate shocks, rather than ambiguity across climate models, and allows us to construct the spatial covariance of these shocks. We translate temperature into output with an empirical damage function under which warming raises output in cold countries and lowers it in hot ones. Because the damage from a given weather shock depends on a country's temperature, the covariance of damages across countries changes over the century as countries warm. Under this path, the median country is expected to lose 13.0 percent of output by 2095 due to climate change.

With the quantified model, we find that the migrant network raises the welfare cost of climate change for most of the world. We measure the network effect by comparing climate losses in our baseline economy with losses in an economy where households face the same wages and migration costs, but the diaspora does not affect those costs. For the average household, the network raises the climate loss by 1.20 percentage points of lifetime consumption, 24 percent of the total loss. This is equivalent to 0.7°C of additional warming by the end of the century. The network effect is largest in hot and poor origins, at 3.5 points for the hottest quartile and 2.5 points for origins below the median income. For the coldest quartile, the network increases climate gains relative to an economy without the network by 0.55 points, because their diasporas are concentrated in other countries that gain from warming. In total, the network raises climate losses in countries home to 64 percent of the world's population.

Once we account for the network, migration does little to help households adapt to climate change. To show this, we compare our baseline economy with a counterfactual economy without migration, in which every household lives in its origin forever and bears that origin's climate losses. The average climate loss in the economy without migration is 5.15 percent of lifetime consumption, nearly identical to the 5.05 percent we find in the baseline economy. In the economy without the network, the average loss from climate change is much smaller, at 3.85 percent. The network

therefore limits migration as an adaptation to climate change. For most origins, diasporas in the destinations with the smallest climate losses are small, so migrating there remains costly even as climate losses grow.

We decompose the network effect on climate losses into two channels using a second-order Taylor expansion of lifetime utility around the projected climate path. The first channel, which we call anchoring, is the network's effect on a household's exposure to the projected warming trend. The second channel, which we call diversification, is the network's effect on the insurance value of migration against climate shocks. Quantitatively, anchoring accounts for nearly all of the network effect. It is well approximated by the covariance across destinations between today's diaspora and the present discounted value of trend climate losses. Diversification matters less, because the insurance value of migration is small in our framework with or without the network. The network nevertheless lowers this insurance value substantially, because it concentrates households in destinations whose climate shocks move together, both with each other and with those at the origin.

The first migration policy we consider is a temporary immigration freeze into the OECD. This counterfactual is motivated by the recent tightening of immigration restrictions by many OECD members. The freeze holds the foreign-born population of the OECD at its current level until 2060. We find that it raises the average climate loss of origins outside the OECD that are projected to experience losses from climate change by 0.34 percent. Because the network is persistent, 50 percent of this increase is incurred after the policy ends. The climate effects of the freeze are largest for origins that currently have large diasporas in the OECD and that, absent the immigration freeze, would have sent many more migrants to the OECD. For the origins with the largest diasporas in the OECD, including countries in the Caribbean, Central America, and North Africa, the policy increases climate losses by 2.31 percent.

The second policy we consider is a broad easing of immigration restrictions. Specifically, we remove the small fraction of the total migration cost associated with visa requirements for every pair of countries with an active visa requirement. This waiver is a benchmark for how far policy can lower migration costs by changing entry rules, without subsidizing migration. This policy leads to 131 million additional people migrating by 2095 and raises the welfare of the average household by 3.11 percentage points of consumption. Its effect on climate losses is much smaller. Most of migration induced by this policy is to high-income destinations, but some of these destinations, such as the Gulf states, also face large climate losses.

The final policy we consider is a targeted climate visa program. It is motivated by small programs such as the visas that New Zealand and Australia offer to Pacific Islanders. In the program we implement, OECD members that are projected to gain from warming issue 150,000 visas a year to households from poor origins with the largest projected losses. The size of the program is roughly the number of refugees resettled worldwide annually. We find that the visa holders build migrant networks in these destinations, which then draw additional migrants. The program raises the welfare of households in the treated origins by 2.67 percentage points of consumption and lowers

their climate losses by 2.6 percent. Because the network takes time to grow, delaying the program by a decade forfeits 15 percent of its reduction in climate losses.

Related literature. Our main contribution is to quantify how migrant networks shape migration as an adaptation strategy to climate change, building on and extending spatial models of climate change (Desmet and Rossi-Hansberg, 2015; Conte et al., 2021; Desmet et al., 2021; Burzyński et al., 2022; Rudik et al., 2022; Bilal and Rossi-Hansberg, 2023; Conte, 2026; Cruz and Rossi-Hansberg, 2024; Bearpark et al., 2025).[1] Within this literature, the paper closest to ours is Cruz and Rossi-Hansberg (2024), who use a global model of migration, trade, innovation, and climate damages to study how the world economy adapts to warming through many endogenous margins. We focus on migration, which these models show is a central margin of adaptation, and abstract from the other forms of endogenous adaptation.[2] In these models, households are anonymous, so a household that migrates becomes identical to the residents of its new location, and migration costs are fixed over the transition. In our model, a household keeps its origin as a persistent state, which substantially changes the welfare cost of climate change. Persistent worker types play a similar role in Seo and Oh (2024), where they make sectoral shocks much more costly than in models without type persistence. In addition, the persistent states of households in our model are linked through the migrant network, because each household's migration lowers the migration costs of later households from the same origin.

We also contribute to a large empirical literature showing that existing networks shape where migrants settle (Bartel, 1989; Card, 2001; Edin et al., 2003; Munshi, 2003; Beine et al., 2011; Beaman, 2012; Mahajan and Yang, 2020; Stuart and Taylor, 2021; Blumenstock et al., 2025). Most of the evidence for the effect of migrant networks on migration comes from specific migration episodes or narrower geographic settings. We add global evidence on this relationship using a push-pull instrument adapted from Burchardi et al. (2019) to bilateral migration between countries. Despite the use of past settlement patterns as an instrument in their own right (Altonji and Card, 1991; Card, 2001), migrant networks are not included in quantitative spatial models of migration. A notable exception is Carrington et al. (1996), who study the Great Migration of African Americans from the South to the North in a two-region model where moving costs fall with the stock of earlier migrants. We embed the same mechanism in a model with many origins and destinations, so that the network determines not only whether households migrate but also where they go. Our model also adds correlated climate risk and is estimated on global data, which allows us to characterize when the long-run network is unique and to study the network transition as climate damages grow.

Our framework also connects to the development literature on migrant networks and

[1] Related work studies other margins of adaptation to a changing climate. Balboni (2025) studies how infrastructure investment shapes the persistence of coastal cities exposed to rising seas, and Krusell and Smith (2022) study savings and energy use across many regions as warming changes their productivity. See Desmet and Rossi-Hansberg (2024) and Balboni and Shapiro (2025) for reviews of these models and Carleton et al. (2024) for a broader review of climate adaptation.

[2] A related empirical literature estimates how long-run climate trends (Cattaneo and Peri, 2016; Beine and Parsons, 2017; Jessoe et al., 2018) and extreme climate events (Hornbeck, 2012; Gröger and Zylberberg, 2016; Deryugina et al., 2018; Mahajan and Yang, 2020; Aron-Dine, 2025) affect migration.

risk-sharing. A central result in this literature is that households use migration and family ties across space to insure against location-specific shocks (Rosenzweig and Stark, 1989; Bryan et al., 2014; Lagakos et al., 2023; Borusyak et al., 2026). At the same time, access to insurance at the origin can reduce incentives to migrate (Munshi and Rosenzweig, 2016; Morten, 2019; Meghir et al., 2022). Closest to our mechanism, Schwartzman (2025) considers how the insurance value of migration depends on the spatial covariance of shocks, showing that migration within the Philippines is directed toward destinations whose income shocks are less correlated with those at the origin. We show that the migrant network can work against this motive, because it concentrates households in destinations whose climate shocks move with those at the origin. We characterize this channel formally and quantify it for every country.[3]

The remainder of the paper is organized as follows. Section 2 describes the data and documents three facts on migrant networks and their climate exposure. Section 3 develops a dynamic spatial model of migration with endogenous migrant networks and climate change. Section 4 quantifies the model. Section 5 measures the effect of the migrant network on the welfare cost of climate change. Section 6 evaluates migration policy as climate policy. Section 7 concludes.

2. Migrant Networks and Climate Exposure

The first part of the paper documents three empirical patterns that motivate our analysis. First, new emigrants follow the existing network in international migration. Second, these networks are relevant for climate adaptation because origins and their networks face similar climates. However, our third fact shows that network reallocation over the past decades offset some of the warming that the diaspora would have otherwise faced. Together, these facts suggest that existing migrant networks may shape future climate-induced migration, and motivate a structural model that can assess whether network-driven migration facilitates or limits future adaptation to climate change.

2.1 Data

Migrant stocks and flows. We use data on migrant stocks from the United Nations Global Migration Database (United Nations, Department of Economic and Social Affairs, Population Division, 2021). This is the most comprehensive source of international migration statistics available. The database provides bilateral migration matrices that capture the stock of foreign-born populations residing in destination countries at 5–year intervals from 1990 to 2020 across over 200 countries. Our measure of bilateral migration flows comes from Abel and Cohen (2019) pseudo-Bayesian demographic-accounting series which builds on the UN bilateral migrant stock

[3] A related literature studies diversification against spatially correlated shocks in production and trade, including plant location within the firm (Castro-Vincenzi, 2024), supplier networks (Castro-Vincenzi et al., 2024), and the policy choice between diversification and reshoring (Grossman et al., 2023). We study diversification through migration, where the set of destinations available to a household is shaped by the migrant network.

data.[4] Their approach explicitly accounts for births and deaths in the migrant population and employs a statistical estimation procedure to infer the most likely migration flows consistent with observed stocks.[5] Appendix B.1 contains a discussion of the data construction and sources of potential systematic measurement error. To assess these concerns, Appendix A reports the main results across different subsamples of the data.

Climate data. We use data from the Berkeley Earth Surface Temperature (BEST) dataset (Rohde and Hausfather, 2020). This dataset has daily temperature measurements at 1°×1° spatial resolution from 1970-2020. BEST combines records from more than 30,000 weather stations and adjusts the raw station data for known measurement issues. We combine the gridded temperature data with high-resolution population data to obtain a measure of the daily temperature experienced by an average person in a country. We then aggregate these data to annual measures of average temperature and extreme heat, including the number of days above specific temperature thresholds. Appendix B.1 describes the data construction and the additional climate measures used in robustness exercises.

2.2 Fact 1: New emigrants follow the existing network

The data show that existing diaspora communities play an important role in explaining both the size and the destination of migration flows. Figure 1a illustrates this relationship using global bilateral migration over the last quarter century. For each origin–destination pair (o, d) and period t, we plot a binscatter of the share of origin-o flows going to destination d against the share of origin-o's pre-existing diaspora located in d five years earlier. There is a strong positive relationship between contemporaneous flows and past migrant stocks. This pattern is robust over time and across levels of economic development (see Appendix A.1).

The positive correlation in Figure 1a may not reflect the effect of the existing diaspora on subsequent migration. Persistent differences across origin–destination pairs, such as distance, common language, or destination wages, can affect both stocks and flows.

To address these concerns, we implement an IV strategy following Burchardi et al. (2019) who study the impacts of ancestry on foreign investment flows across US counties. The instrument exploits the interaction of push and pull factors that coincide in a time-period to channel migrants from an origin-o into a destination-d. When a large emigration wave from origin o coincides with a period in which destination d is attractive to migrants more generally, more migrants from o settle in d. Because migrant stocks accumulate past flows, these historical push–pull interactions generate differences in the distribution of the origin-o diaspora across destinations.[6] We adapt this logic to

[4] Differencing migrant stocks can generate spurious zeros and mismeasure flows because stock changes also reflect deaths, naturalization, and data revisions, and may miss onward migration.

[5] They use a pseudo-Bayesian approach to mix two inference strategies: The first attempts to maximize matrix diagonals (stayers) while still respecting the migrant accounting identity imposed by a start and ending stocks. The second approach attempts to spread flows more smoothly across destinations given the same margins. They find that this approach performs best against the limited sample of reported global flows measures.

[6] Burchardi et al. (2019) provide an example with nineteenth-century German migration to the Midwest, where a

Figure 1: Role of Networks in Migration and Climate Exposure

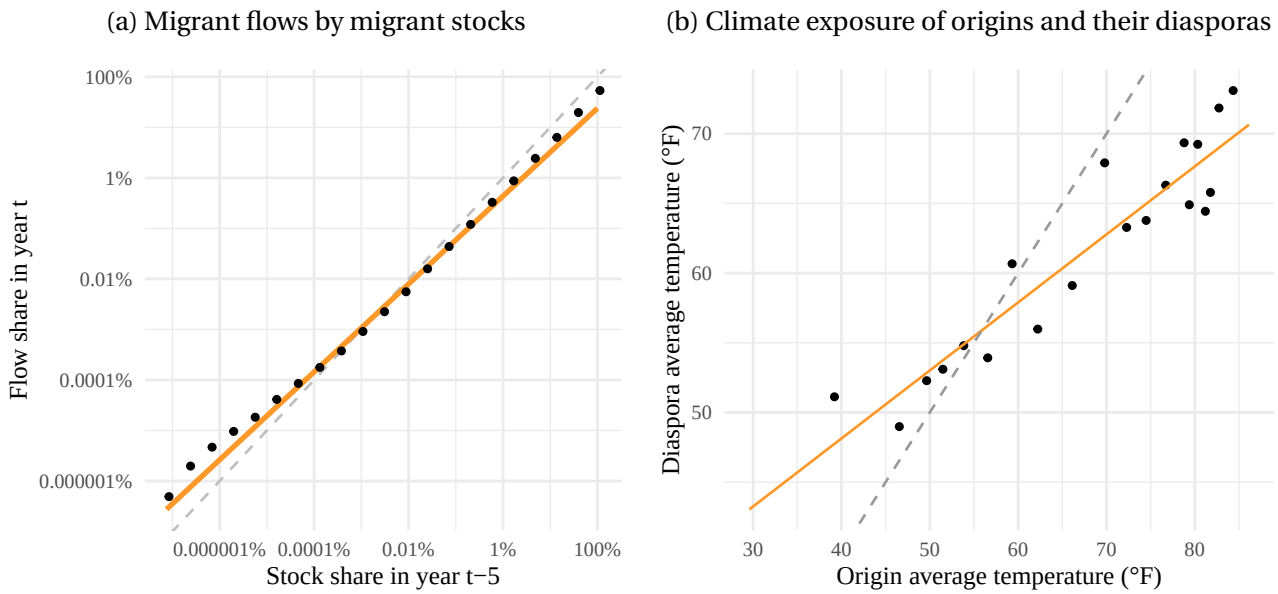

Notes: Panel (a) uses data on migrant stocks from UN Global Migration Database, flows from Abel and Cohen (2019) estimates. The figure shows a binscatter plot of flows and lagged migrant stocks for an origin-o and destination d pair using data from 1990-2020. The orange line plots the line of best fit and the dashed gray line shows the 45 degree line. Panel (b) bins origin-country temperature against the average temperature of its diaspora. The solid line is the line of best fit and the dashed line is the 45-degree line.

bilateral international migration. Our push factor captures an origin country specific emigration wave, while our pull factor captures the contemporaneous attractiveness of a destination country to migrants from other countries.

Interacting total emigration from o with total immigration into d would mechanically load the $o \rightarrow d$ flow into both components of the instrument. Therefore, we follow the leave-out construction in Burchardi et al. (2019). They construct the origin push factor excluding migration to the destination US county Census region and the destination pull factor excluding migrants from the origin's continent. In our global setting, we use the analogous geographic leave-out at the UN subregion level. The push factor excludes migration from o to destinations in d's UN subregion, while the pull factor excludes migrants from origins in o's UN subregion.

The identifying assumption is that, conditional on the fixed effects, the push–pull interaction affects future $o \rightarrow d$ migration only through the migrant stock and is uncorrelated with other time-varying bilateral determinants of migration. One concern is that the push–pull interaction could be correlated with a persistent shock that continues to push migrants out of o while also keeping d relatively attractive. The geographic leave-out helps limit this concern. For such a shock to violate the exclusion restriction, it would also need to raise emigration from o toward destinations

German emigration wave coincided with strong destination pull. There are similar examples in our data. For example, migration from Pakistan to Turkey increased after the 2010 Pakistan floods and during Turkey's 2010–2015 immigration reforms. Appendix B.3 discusses additional case studies.

outside d's subregion and, at the same time, make d attractive to migrants from origins outside o's subregion.

We instrument for migrant stocks in year $t-5$ using the history of push–pull interactions up until year $t-5$. Appendix B.2 contains more details on constructing the instrument. We then estimate

$$\log\left(\text{flows}_{od,t}\right) = \beta \log\left(\widehat{\text{stocks}}_{od,t-5}\right) + \delta_o + \delta_d + \delta_{od} + \varepsilon_{od,t} \tag{1}$$

where $\text{flows}_{od,t}$ is the level of the migrant flows and $\widehat{\text{stocks}}_{od,t-5}$ is the instrumented lagged level of the migrant stock. δ_o and δ_d are origin and destination fixed effects that absorb time-invariant push and pull factors common across destinations and origins, respectively. The origin-destination pair fixed effect, δ_{od}, absorbs stable bilateral characteristics such as distance, shared language, and colonial history. The specification including origin-destination pair fixed effects identifies the network effect from within-corridor changes over time. We report heteroskedasticity-robust standard errors clustered at the origin–destination pair level.

Table 1: Elasticity of Flows to Stocks

	OLS			IV	
	(1)	(2)	(3)	(4)	(5)
$\log\left(\text{stocks}_{od,t-5}\right)$	0.882***	0.830***	0.089***	0.723***	0.723***
	(0.002)	(0.003)	(0.006)	(0.111)	(0.112)
o, d		✓	✓		✓
$o \times d$			✓	✓	✓
First stage F-stat				11.8	11.7

Notes: The table reports estimates of the elasticity of bilateral migration flows to lagged migrant stocks from 1990 to 2020. Migrant stocks are from the UN and gross flows from Abel and Cohen (2019). Columns (1)–(3) report OLS estimates; columns (4)–(5) instrument for lagged stocks using the leave-out push–pull instrument of Burchardi et al. (2019). Standard errors are clustered at the origin–destination pair level. * p<0.05, ** p<0.01, *** p<0.001.

The coefficient β measures the elasticity of bilateral migration flows to the lagged diaspora stock. Table 1 reports the estimates. Columns (1)–(3) show the OLS results.[7] In column (1), which includes no fixed effects, a 10% larger lagged migrant stock is associated with 8.3% higher subsequent flows. The coefficient decreases when we include origin–destination fixed effects in column (3). This is because migrant stocks are highly persistent over our relatively short panel, so o–d fixed effects absorb much of the identifying variation. The IV estimates in columns (4) and (5) correct for the attenuation in the OLS estimates.[8] The IV estimate implies that a 10% increase in the migrant stock raises subsequent bilateral flows by 7.2%.[9]

[7] The PPML estimates, reported in Table A1 in Appendix A.1, are similar to the OLS results.

[8] In addition to measurement error, OLS may be biased downward by time-varying bilateral factors, such as labor-market congestion or policy responses to larger migrant stocks.

[9] This estimate is in line with related work. Beine et al. (2011) find an elasticity of 0.76 for 1990–2000 flows to OECD destinations relative to 1990 stocks, while Beine and Parsons (2015) estimate an OLS coefficient of 0.40. Stuart and Taylor (2021)'s estimates imply roughly 0.5 additional Black migrants and 0.1 additional white migrants per diaspora member over a five-year period during the Great Migration. Our estimate implies about 0.3 additional migrants per diaspora member over the same horizon.

To illustrate the magnitude of the network effect, we ask how much of the variation in migration flows across destinations is associated with differences in existing diaspora stocks, after removing destination factors that makes some locations more attractive. For each origin-year, we use our elasticity to estimate the share of the variance in migration flows associated with differences in lagged diaspora stocks. The covariance decomposition shows that the network accounts for 59% of the remaining variation in log flow shares across destinations, after accounting for destination fixed effects.

2.3 Fact 2: Origins and their networks face similar climates

Having established that migrant networks shape destination choices, we next examine whether they also shape migrants' climate exposure across destinations. In this section, we focus on climate as measured by temperature. Average temperature is the standard measure in the damage-function literature, which estimates how warming affects economic activity (Dell et al., 2012; Burke et al., 2015; Nath et al., 2024). We report robustness to other measures of climate in Appendix A.2. The key takeaway is that migrants are located in destinations with similar climate as the origin. Countries that are more exposed to high temperatures also have diasporas concentrated in similarly exposed destinations.

Let T_t^ℓ denote the average temperature of the country ℓ in period t and let $s_t^{o,d}$ denote the share of migrants from origin o residing in destination d at time t[10]. Then, origin o's diaspora's temperature is

$$\bar{T}_t^o \equiv \sum_{d \neq o} s_t^{o,d} T_t^d. \tag{2}$$

Intuitively, $\bar{T}_t^o$ measures the climate conditions experienced by the average member of origin o's diaspora at time t. We plot this against the origin country's average temperature in Figure 1b. Appendix A.2 also plots the full distribution of diaspora temperature conditional on origin temperature.

Figure 1b shows a strong positive relationship between origin and diaspora temperature, with a correlation coefficient of 0.67. Migrants from hot countries tend to be in destinations that are also hot. Appendix A.2 shows the same relationship across subsamples of the data and using alternative measures of climate exposure.

The positive correlation is consistent with gravity. Migration is concentrated toward nearby destinations, and climate is spatially correlated, so origins and diasporas have similar climates. Migrant networks are geographically concentrated near the origin, with differences by origin-country income. Migrants from low-income countries are closer to home: the average migrant from a low-income country lives 2,700 km from the origin, compared with 3,800 km for migrants from high-income countries. Appendix A.2 shows migration distances separately by origin-country income group. Nearby destinations are valuable when shocks are country-specific,

[10] Such that $\sum_{d \neq o} s_t^{o,d} = 1$.

which is consistent with the strong role of distance in many historical migration episodes, including refugee flows (Moore and Shellman, 2007).[11] Climate exposure, however, is spatially correlated across neighboring countries. As a result, networks concentrated in nearby destinations may provide limited protection against climate change.

2.4 Fact 3: Migrant networks show some adaptation with warming

Average global temperatures have increased by 1.5°F from 1995 to 2020 (Rohde and Hausfather, 2020). A key question for understanding the role of networks is whether people have adapted to warming to date by migrating to cooler destinations and, in doing so, shifted diaspora networks toward countries with lower exposure. Our central finding is that migration patterns over the past three decades have partially offset the climate exposure of networks. We find that most changes in diaspora-network exposure reflect evolving climate conditions in existing destinations, but a reallocation of migrant networks toward safer destinations mitigated some of that increasing exposure.

To formalize this analysis and distinguish changes in $\bar{T}_t^o$ driven by warming in destinations versus shifts in the migrant network, we decompose the change in the diaspora exposure of an origin country, $\Delta\bar{T}^o = \bar{T}^o_{2020} - \bar{T}^o_{1995}$, as:

$$\Delta\bar{T}^o = \underbrace{\sum_{d\neq o} s^{o,d}_{1995}\,\Delta T^d}_{\text{warming-at-destinations}} + \underbrace{\sum_{d\neq o} \Delta s^{o,d}\,T^d_{1995}}_{\text{network reallocation}} + \underbrace{\sum_{d\neq o} \Delta s^{o,d}\,\Delta T^d}_{\text{interaction}} \tag{3}$$

The first term is the warming-at-destinations term that isolates how exposure changes if destination exposure evolves while network shares stay fixed at $s^{o,d}_{1995}$. We expect this term to be positive given the warming that has happened over this time period. The second term is a network reallocation term that isolates how exposure changes holding destination temperature at baseline levels, T^d_{1995}, while allowing network shares to shift from $s^{o,d}_{1995}$ to $s^{o,d}_{2020}$. If people are shifting migration patterns toward safer destinations, then this term should be large and negative. The interaction term captures whether the network is reallocating toward destinations whose exposure is changing the most. It is positive when the network shifts toward destinations that are warming more, and negative when they shift toward destinations that are warming less or cooling.[12]

Figure 2a plots this decomposition globally and for countries in the top and bottom quartile of our climate measure. Globally, the orange bar representing warming-at-destinations dominates. However, the blue bars representing network reallocation are negative and large. This suggests

[11] Related work shows that the value of proximity depends on the spatial scale of risk; see Rosenzweig and Stark (1989) and Kazianga and Udry (2006).

[12] We do not interpret the network-reallocation term as migration caused by climate change. In practice, it is difficult to define a "climate move," since migration may respond to events partly shaped by climate e.g. Kelley et al. (2015) link the 2007–2010 drought in Syria to the civil war. Additionally, a regression of migration on climate shocks may not recover a causal estimate since exposure to those shocks is non-random (Borusyak and Hull, 2023). Therefore, we use the decomposition to ask if the sum of all migration over the period changed the climate exposure of networks.

Figure 2: Changes in Climate Exposure and Geography of Networks

(a) Decomposing change in diaspora exposure

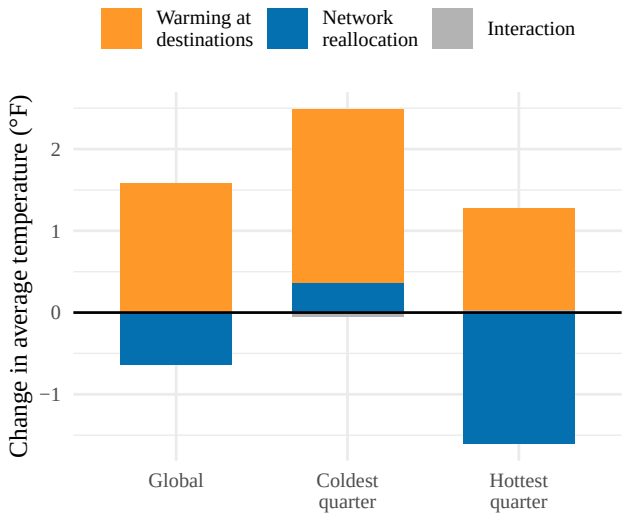

(b) Migrant distance from origin over time

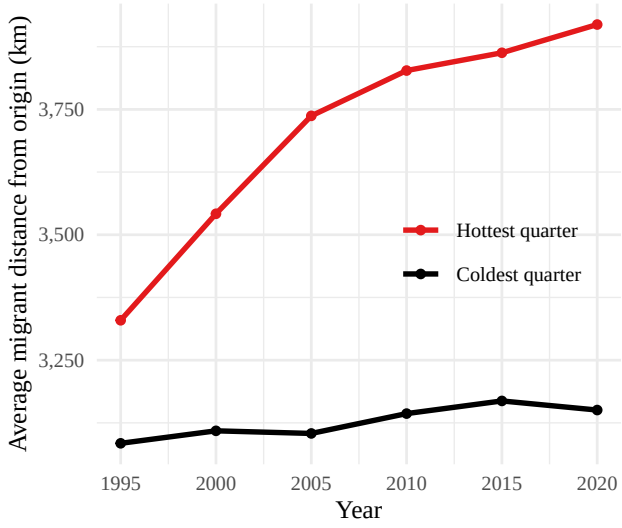

Notes: Panel (a) decomposes the change in migrant-network climate exposure from 1995 to 2020 into network reallocation (blue), warming at destinations (orange), and their interaction (grey), globally and for origins in the bottom and top temperature quartiles. Panel (b) plots migrants' average distance from the origin over time for the same quartiles. Temperature data are from BEST; bilateral distance is from GeoDist (Mayer and Zignago, 2011).

that migration has been to cooler regions. Network reallocation offset about 40% of warming, and this offset is larger for the hottest countries. This pattern could reflect networks becoming geographically dispersed over this time period. Figure 2b plots the average distance of migrants from their origin for countries in the hottest and coldest quartiles. For the hottest quartile, the average migrant is 550 km further from home in 2020 than in 1995, while the coldest quartile had little change.

The empirical evidence shows that migrant networks shape where people move and, in turn, the climate exposure of migrants' destinations. Migrants from hotter origins tend to have diasporas in similarly hot destinations, although there has been some reallocation toward cooler and more distant destinations over time. These facts describe the past role of networks, but our main question is how they will affect adaptation as climate change worsens. Answering this question requires a model that predicts how migration and migrant networks respond to future warming, allows us to compare outcomes with and without network effects, and maps changes in climate exposure into welfare. We turn to a dynamic model of migrant networks and climate change in Section 3.

3. Model of Migrant Networks and Climate Change

The findings in Section 2 suggest that migrant networks will shape adaptation to climate change. Networks can contribute to adaptation by helping move people out of the most climate-exposed

regions. But they may also limit adaptation by directing migrants to destinations facing a similar climate. We build a model to formalize both channels and measure their net effect on welfare as the difference in climate damages between an economy with migrant networks and one without. Which channel dominates depends on how strongly the network pulls migrants, on how correlated damages are between an origin and its network's destinations, and on how the network shifts as warming proceeds.

The empirical findings dictate three features absent from existing quantitative spatial models of climate change. First, new emigrants follow the existing network. In the model, a larger diaspora at a destination therefore lowers the cost of migrating there. Second, migrants settle in destinations whose climate resembles that of their origin. The value of a destination therefore depends on how its stochastic climate damages co-move with damages at home. Third, networks have shifted with recent warming. An origin's diaspora is therefore a state variable that updates with migration.

The rest of the economic environment is deliberately sparse. We abstract from trade in differentiated goods, from capital, from any fixed factor of production, from endogenous amenities, and from any market size effects. We also abstract from differences in household income within an origin, and we capture financial constraints on migration through a migration cost that falls with origin income. Including these features would change the magnitude of climate damages at a given location. Our results, however, are driven by how attractive a destination is to one origin relative to others, and a destination-wide force changes the level of damages in the same way with or without the network, leaving the interaction unchanged.

3.1 Set Up

We consider a world with N locations. Time is discrete.

Production. Competitive firms in each location ℓ produce a freely traded good with a linear technology in labor, $Y_t^\ell = A_t^\ell L_t^\ell$. The local wage is $w_t^\ell = A_t^\ell$. Productivity has three components,

$$A_t^\ell \;=\; A_0^\ell \, g_t^\ell \, z_t^\ell, \tag{4}$$

a time-invariant fundamental A_0^ℓ, a deterministic growth path g_t^ℓ, and proportional climate damages z_t^ℓ.

Climate. The climate at a location is the distribution of its temperature, and climate change is a known shift in that distribution. The temperature at location ℓ in period t is its mean plus a weather shock, $q_t^\ell = \bar{q}_t^\ell + \eta_t^\ell$. Across locations, mean temperature is the vector $\bar{\mathbf{q}}_t = (\bar{q}_t^1, \ldots, \bar{q}_t^N)$, and the weather shocks are jointly normal with covariance $\mathbf{\Gamma}_t$. We assume that weather shocks are independent across periods. Climate change is then the sequence of weather distributions $\{\bar{\mathbf{q}}_t, \mathbf{\Gamma}_t\}_{t=0}^T$. We assume that after some date T the climate stabilizes at $(\bar{\mathbf{q}}_T, \mathbf{\Gamma}_T)$. Households know this sequence, and weather shocks are the only source of risk in the model.

Following the empirical climate literature, we model climate damages as a proportional output loss that depends on temperature (Dell et al., 2012; Burke et al., 2015; Nath et al., 2024). A damage function d maps temperature into log output. Damages may persist beyond the period of the shock (Newell et al., 2021; Nath et al., 2024), so they follow an AR(1) around a trend,

$$\log z_t^\ell \;=\; \log \bar{z}_t^\ell \;+\; \psi\big(\log z_{t-1}^\ell - \log \bar{z}_{t-1}^\ell\big) \;+\; \zeta_t^\ell, \tag{5}$$

with persistence $\psi \in (-1, 1)$. The trend is the damage at the mean temperature, $\log \bar{z}_t^\ell = d(\bar{q}_t^\ell)$, and the innovation ζ_t^ℓ is the damage from the weather shock, which we assume is normally distributed with covariance $\mathbf{\Sigma}_t$.

Households. A household is characterized by its origin o, which is fixed for life. At $t = 0$, there is an initial population distribution for every origin country across locations. Let $L_t^{o,\ell}$ denote the number of households from origin o living in location ℓ at the start of period t. We abstract from population growth so the total population from o is constant over time and equal to L^o. We define $x_t^{o,\ell} = L_t^{o,\ell}/L^o$ as the share of the origin-o population living in ℓ, and call $\mathbf{x}_t^o = (x_t^{o,1}, \ldots, x_t^{o,N})$ the migrant network of origin o.[13]

Each household supplies one unit of labor inelastically and earns the wage w_t^d in its chosen location d. Households purchase a tradable consumption good at a price normalized to one in all locations. With no saving and no borrowing, households consume their wage income. Households are forward-looking, discount the future at rate $\beta < 1$, and have rational expectations. Flow utility is $\log c_t^d$ less the migration cost we describe below.[14]

In addition, households have idiosyncratic preference shocks for each potential destination, $\epsilon_t^{o,d}$. We assume these shocks are i.i.d. across households, destinations, and time, drawn from a Gumbel distribution normalized to have mean zero. The scale parameter $\nu > 0$ scales their dispersion and is common across origins. These assumptions imply a common elasticity of migration to utility differences.

Households from origin o also pay a utility cost $\kappa_t^{o,d}$ in every period they live in location d, with $\kappa_t^{o,o} = 0$.[15] We interpret the migration cost as capturing pecuniary and nonpecuniary costs

[13] Because the model is written in shares, any demographic process proportional to $L_t^{o,\ell}$ leaves $\mathbf{x}_t^o$, and hence all decisions, unaffected. We abstract from two demographic channels. First, we abstract from differential fertility across origins or over time (e.g., Doepke et al., 2023; Barreca et al., 2018). Including this would make L^o time-varying and add a location-specific drift to the law of motion (9). Second, we abstract from any assimilation of o-origin descendants into destination communities (e.g., Abramitzky et al., 2014; Bisin and Verdier, 2011). We could model this as a per-period hazard with which a household exits the co-ethnic network. This would slowly erodes the effective network stock but is unlikely to be quantiatively important over the horizon of the rest of the century.

[14] We assume the climate affects only productivity and not the amenity of living in a location. Cruz and Rossi-Hansberg (2024) estimate both effects and find they contribute about equally to welfare losses from warming. Because flow utility is log consumption, an amenity loss would enter exactly as a productivity loss of the same size in logs, so including it would raise the level of damages without changing their interaction with the network.

[15] Desmet et al. (2018) let the flow cost of moving from r to s factor into an origin and a destination component, $m(r, s) = m_1(r)m_2(s)$, with $m(r, r) = 1$. Because the costs of a household's successive moves multiply, the product becomes a cost of residing in d that depends only on the household's origin o. Our $\kappa^{o,d}$ is that object with the separability relaxed, so it need not be the difference between a destination term and an origin term.

associated with living away from a household's origin country. These include conversing in a foreign language, maintaining legal status, and living in a foreign culture with different institutions. The cost is additive in utility and independent of intermediate moves. This formulation of the cost matches our data. The migrant stocks in Section 2 record where a household was born and where it lives now, not where it lived last period. No global dataset would allow us to identify the cost of moving between two foreign countries.

Migration costs fall with the size of the diaspora and with origin country income. For $d \neq o$, the migration cost is

$$\kappa_t^{o,d} \;=\; \kappa^{o,d} - h\big(x_t^{o,d}\big) - \lambda \log\big(A_0^o\, g_t^o\big). \tag{6}$$

The function h is increasing, bounded above, and continuously differentiable. The second term is the migrant network. A larger diaspora in d lowers the cost of migrating there from o.

Based on empirical evidence that financial constraints limit migration (Bryan et al., 2014; Angelucci, 2015; Cattaneo and Peri, 2016; Bazzi, 2017; Aron-Dine, 2025; Barbosa-Alves and Britos, 2025), we allow migration costs to fall with origin country income. We do not model household financial constraints explicitly. Instead we capture them in reduced form through the last term of (6). This term lowers migration costs uniformly for households from origin o as its economy grows. Here $A_0^o g_t^o$ is origin country income absent climate change. A one percent rise in origin income lowers the cost of living abroad by λ percent of consumption. Because the cost depends on income absent climate change, a climate damage in the origin lowers the wage but does not make it harder to leave.[16]. Adding this channel would lower adaptation through migration but would not interact with the migrant network.

3.2 Migration Decisions

In the model, migration is the household's only technology for adjusting its exposure to climate change. Where a household chooses to live depends on wages and on the migration cost at each destination.

Based on evidence that the value of a network comes from migrants who are already established, we let the migration cost depend on the network at the start of the period, $\mathbf{x}_t^o$. Established migrants provide information about jobs and housing (Munshi, 2003; McKenzie and Rapoport, 2007) and job referrals (Bayer et al., 2008). Migrants who arrive at the same time do not. Beaman (2012) shows this with the random assignment of refugees across US cities. Refugees have better labor market outcomes when assigned to cities with a larger established community from their own country, and worse outcomes the larger the cohort resettled alongside them.

In each period a household observes climate damages $\mathbf{z}_t$ in every location and its preference

[16] If the cost instead depended on realized origin income, a climate shock in o would raise the cost of leaving by λ times the damage, and the response of emigration to a damage would fall from $1/\nu$ to $(1-\lambda)/\nu$. That is the trapped-population channel of Cattaneo and Peri (2016) and Barbosa-Alves and Britos (2025). We leave it out for two reasons. A period in our model is five years, long enough for a household to save for a move after a bad year, and Barbosa-Alves and Britos (2025) find that households save ahead of anticipated warming

shocks $\boldsymbol{\epsilon}_t^o$, and chooses the location d where it will live and work. A household from origin o solves

$$v_t^o\big(\mathbf{x}_t^o, \mathbf{z}_t\big) \;=\; \max_d \Big\{ \log c_t^d - \kappa_t^{o,d} + \nu\, \epsilon_t^{o,d} \;+\; \beta\, \mathbb{E}\Big[v_{t+1}^o\big(\mathbf{x}_{t+1}^o, \mathbf{z}_{t+1}\big) \,\Big|\, \mathbf{x}_t^o, \mathbf{z}_t \Big] \Big\}. \tag{7}$$

A household's choice of d in period t does not change the state it faces in period $t+1$. This is because of our assumption that the migration cost is a flow cost of residence. This means that household from o living in d faces the same residence costs for all destinations next period as a household from o in any other location d'. The expected continuation value is therefore the same for every destination the household can choose today. The forecast of future wages in d enters this continuation value, but it enters equally for every destination choice, so it cancels from the choice probabilities. The probability that a household from origin o chooses destination d is

$$\pi_t^{o,d} \;=\; \frac{\exp\big(\big[\log c_t^d - \kappa_t^{o,d}\big]/\nu\big)}{\sum_{i=1}^{N} \exp\big(\big[\log c_t^i - \kappa_t^{o,i}\big]/\nu\big)}. \tag{8}$$

Migration is reversible. A household pays $\kappa_t^{o,d}$ only as long as it lives in d. A household that emigrates from o and later returns has payed no sunk cost.[17]

Every household from origin o solves the same problem, because the choice probabilities do not depend on its current location. Next period's network is therefore the vector of choice probabilities,

$$x_{t+1}^{o,d} \;=\; \pi^{o,d}\big(\mathbf{x}_t^o, \mathbf{z}_t\big). \tag{9}$$

Households never need to forecast the network their own choices produce. Origins do not interact, because wages do not depend on who lives where and each household's migration cost depends only on the network of its own origin. Households from the same origin do interact through h. A household that moves does not take into account that it lowers next period's migration cost for every compatriot at its destination.

While the household's migration decision in the model is static, the welfare effects of climate change are not. The household's value function in (7) still contains the full expected path of wages, climate damages, and the network. Expected lifetime utility before the preference shocks are drawn, V_t^o, solves

$$V_t^o \;=\; \nu \log \sum_{d=1}^{N} \exp\Big(\big[\log c_t^d - \kappa_t^{o,d}\big]/\nu \Big) \;+\; \beta\, \mathbb{E}\big[V_{t+1}^o \,\big|\, \mathbf{x}_t^o, \mathbf{z}_t \big]. \tag{10}$$

The welfare effects of climate change therefore depend on where the network will be as climate damages grow, on how correlated future weather shocks are across the destinations open to a household from origin o, and on how quickly the network adjusts.

[17] A sunk cost of moving instead of a flow migration cost would add two things. First, households would move in anticipation of future climate damage, since the choice would depend on future as well as current payoffs. To date there is little evidence that households do so (Hoffmann et al., 2020; Aron-Dine, 2026). Second, households that had already paid to move would be more likely to stay in a destination after a bad climate realization.

Dividing (8) for destination d by the same expression for the origin country and taking logs delivers a gravity equation for migrant stocks,

$$\log\left(\frac{x_{t+1}^{o,d}}{x_{t+1}^{o,o}}\right) \;=\; \frac{1}{\nu}\left[\log\left(\frac{w_t^d}{w_t^o}\right) - \kappa^{o,d} + \lambda\log\left(A_0^o\, g_t^o\right) \;+\; h\left(x_t^{o,d}\right)\right]. \tag{11}$$

Three forces determine the size of the diaspora at d relative to the origin population. The first is the ratio of wages w_t^d/w_t^o, the finanical return to migration. The second is the migration cost that is independent of the network, $\kappa^{o,d} - \lambda\log(A_0^o g_t^o)$. The third is the size of the network in d.

3.3 Equilibrium

Given the structure of the model, the equilibrium path is unique regardless of the strength of the network.

Definition 1 (Equilibrium)**.** Given initial networks $\mathbf{x}_0^o$ and migration costs $\boldsymbol{\kappa}^o$ for all o, initial damages $\mathbf{z}_0$, fundamental productivities $\mathbf{A}_0$, growth paths $\{\mathbf{g}_t\}_{t\geq 0}$, climate paths $\{\bar{\mathbf{q}}_t, \boldsymbol{\Gamma}_t\}_{t\geq 0}$, and a sequence of weather shocks $\{\boldsymbol{\eta}_t\}_{t\geq 1}$, an equilibrium is a sequence of damages $\{\mathbf{z}_t\}_{t\geq 1}$, wages $\{\mathbf{w}_t\}_{t\geq 0}$, and networks $\{\mathbf{x}_t^o\}_{t\geq 1}$ and choice probabilities $\{\boldsymbol{\pi}_t^o\}_{t\geq 0}$ for each o such that in every period damages follow the climate process (5), wages equal local productivity (4), households optimize so that choice probabilities satisfy (8), and the population distribution is consistent with household choices, $\mathbf{x}_{t+1}^o = \boldsymbol{\pi}_t^o$ for every origin.

Proposition 1 (Existence and Uniqueness)**.** Given initial networks and damages, an equilibrium exists and is unique for any migration costs, any realization of weather shocks, and any strength of the network.

The full proof can be found in Appendix C. Intuitively, this period's wages and the inherited networks determine the household choice probabilities, and the choice probabilities determine next period's networks. Each step has a single solution. The unique equilibrium path can therefore be constructed period by period.

3.4 Network Dynamics, Steady States, and Stationary Distributions

The key object for the dynamics of the network is the response of migration to the size of the existing network. Differentiating (11), holding the share in the origin fixed, gives the elasticity of migration to the network,

$$\varepsilon_t^{o,d} \equiv \frac{\partial\log\left(x_{t+1}^{o,d}/x_{t+1}^{o,o}\right)}{\partial\log x_t^{o,d}} \;=\; \frac{x_t^{o,d}\, h'\left(x_t^{o,d}\right)}{\nu}. \tag{12}$$

The numerator is the local strength of the network. A one percent larger diaspora in d lowers the cost of migrating there for households from o by $x_t^{o,d}\, h'\left(x_t^{o,d}\right)$ percent of consumption. The denominator is the dispersion of location tastes. When ν is large, a household's idiosyncratic attachment to a

location outweighs differences in wages and networks, so few households move in response to a change in relative utility.

The migrant network makes the migration response to a shock persistent. Consider a one-time shock δ to the log relative wage of d that fades after one period. The direct response is δ/ν in the first period. Because this migration increases the size of the diaspora in d, it draws additional migrants in subsequent periods even after the shock has faded. After t periods, the log odds of living in d are still higher by $(\delta/\nu)\,\varepsilon^t$. When $\varepsilon < 1$ the effect of a one-time shock fades and the diaspora returns to the size supported by fundamentals. When $\varepsilon \geq 1$ the effect does not fade, and the size of the diaspora depends on the full history of past shocks rather than on fundamentals.

The migrant network also amplifies the migration response to a permanent change in fundamentals. Consider a permanent change δ in the log relative wage of d. The direct response is again δ/ν in the first period, but the change is now permanent, so it raises the log odds of living in d by δ/ν in every period. The direct response increases the diaspora in d and draws additional migrants in every period. The long-run change in the log odds of living in d is the sum $\sum_{t=0}^{\infty}(\delta/\nu)\,\varepsilon^t$. When $\varepsilon < 1$ the sum converges and the network multiplies the direct response to a permanent change by $1/(1-\varepsilon)$. When $\varepsilon \geq 1$ the sum does not converge, and the diaspora in d grows until the linear approximation fails, the case of Proposition 2.

Persistence and amplification matter for the effectiveness of migration as an adaptation strategy and for the role of migration policy. Amplification through the migrant network determines the magnitude of the migration response to climate change. Persistence determines whether a temporary policy, such as a border closure, has a permanent effect on where people live. Both results hold only locally, since they fix the elasticity at the current network. To characterize the long-run location of the migrant network, we first describe the steady states of the law of motion (9) in the absence of weather shocks.

Definition 2 (Steady State)**.** Hold the climate fixed at its mean, $\boldsymbol{\eta}_t = \mathbf{0}$ for all $t > T$, and the growth path for productivity in every location at $\bar{\mathbf{g}}$. A steady state for origin o is a network $\mathbf{x}^o$ that solves $\mathbf{x}^o = \boldsymbol{\pi}^o(\mathbf{x}^o, \bar{\mathbf{z}}_T)$.

Proposition 2 (Unique Steady State)**.** A steady state exists for every origin. If the elasticity of migration to the network is below one, $\varepsilon_t^{o,d} < 1$ for every $x_t^{o,d} \in [0,1]$, the steady state is unique and the network converges to it from any initial population distribution. If at a steady state $\varepsilon^{o,d}(1-x^{o,d}) > 1$ for some destination d, that steady state is unstable and (9) has more than one steady state.

The full proof can be found in Appendix C. Intuitively, when the elasticity is below one everywhere, two economies with the same fundamentals but different initial networks converge to the same steady state, at a rate equal to the elasticity. When the elasticity is above one at a steady state, two economies with the same fundamentals but slightly different initial networks move apart, and converge to different steady states. In this case, a small group of migrants who move away from the steady state generates sustained additional migration, so a network near that steady state moves away from it rather than converging back.

We now characterize the long-run location of the migrant network with weather shocks. Even after the climate has stabilized, weather shocks continue to generate migration. For example, a dry year in Ghana induces Ghanaians to migrate to Nigeria. The larger Ghanaian community makes Nigeria a more attractive destination in subsequent years even after the drought ends, so the share of Ghanaians in Nigeria falls only gradually. In a stable climate with weather shocks, the network never settles at a steady state. Instead, the distribution of the network converges. The analogous question is whether that distribution is unique.

Definition 3 (Stationary Distribution)**.** Hold the climate fixed at $(\bar{\mathbf{q}}_T, \mathbf{\Gamma}_T)$ for all $t > T$ and the growth path at $\bar{\mathbf{g}}$. A stationary distribution for origin o is a distribution μ^o over networks such that if $\mathbf{x}_t^o$ is drawn from μ^o and damages follow (5), then $\mathbf{x}_{t+1}^o$ is also distributed according to μ^o.

Proposition 3 (Unique Stationary Distribution)**.** A stationary distribution exists for every origin. If the elasticity of migration to the network is below one, $\varepsilon_t^{o,d} < 1$ for every $x_t^{o,d} \in [0,1]$, the stationary distribution is unique and the distribution of the network converges to it from any initial population distribution.

The full proof can be found in Appendix C. Intuitively, when the elasticity is below one everywhere, two economies with the same fundamentals and the same sequence of weather shocks but different initial networks converge to the same network. The distribution of the network after many periods therefore does not depend on the initial network, and the stationary distribution is unique. When the elasticity exceeds one at some steady state, the same two economies need not converge to the same network. Each economy remains near whichever stable steady state it happens to start near. Only a sequence of unusually large weather shocks can push the network into the neighborhood of a different steady state. The distribution of the network can therefore depend on the initial network.

Propositions 2 and 3 are the counterparts of the uniqueness results in the spatial equilibrium literature. Allen et al. (2020) and Kucheryavyy et al. (2023) give conditions under which a static spatial equilibrium is unique by comparing the strength of agglomeration with the dispersion of tastes. Allen and Donaldson (2020) provide the dynamic version for a single perturbation to a deterministic system. In our model with climate risk, the object is a distribution of networks instaed of a single allocation of households across locations, and there is an analogous condition which determines whether that distribution is unique.

4. Model Quantification

To quantify how much migrant networks facilitate or limit adaptation to climate change, we need three sets of inputs. First, we estimate migration elasticities and migration costs, which determine how strongly the network pulls new migrants toward the destinations of earlier migrants and how quickly the network changes in response to climate shocks. Second, we need a counterfactual path for economic growth absent global warming, because changes in the distribution of wages also induces migration for reasons unrelated to climate change. Third, we need the expected path and

the spatial covariance of climate damages. Table 2 lists all model parameters. Appendix D provides additional details on our quantification.

Table 2: Parameter Values

Parameter	Description	Value	Source
Panel A. Migration elasticities and costs			
β	discount factor	0.90	2% annual rate
$1/\nu$	international wage elasticity	0.27	Section 4.1
θ_1	network strength	2.75	Section 4.1
θ_0	network floor	1.3×10^{-8}	Section 4.1
$\kappa^{o,d}$	time-invariant migration cost		Section 4.1
λ	income elasticity of emigration costs	0.23	Section 4.1
Panel B. Economic growth absent climate change			
A_0^ℓ	productivity level		Penn World Table
g_t^ℓ	growth path		SSP3, OECD ENV-Growth
Panel C. Climate damages			
$\bar{q}_t^\ell$	expected temperature path		MPI Grand Ensemble
$\mathbf{\Gamma}_t$	weather shock covariance		MPI Grand Ensemble
$d'(\bar{q}_t^\ell)$	marginal damage		Nath et al. (2024)
$\bar{z}_t^\ell$	expected damage path		$d(\cdot)$ integrated along $\bar{q}_t^\ell$
ψ	damage persistence	0.66	Nath et al. (2024)

4.1 Migration elasticities and costs

Four objects govern how households' migration decisions respond to economic shocks. The first is the dispersion of location tastes, ν. The other three are the components of the migration cost in (6). These are the time-invariant cost of each corridor, $\kappa^{o,d}$, the network term, $h(x)$, and the elasticity of the cost to origin income, λ. We estimate ν, the parameters of h, and λ by the simulated method of moments. We recover $\kappa^{o,d}$ by inverting the model.

The network term. We parameterize the network term of the migration cost as

$$h(x) \;=\; \theta_1 \log\left(x + \theta_0\right), \tag{13}$$

where θ_1 governs the strength of the network and θ_0 the minimum diaspora size. The implied network elasticity is $\theta_1 x/(x+\theta_0)/\nu$. The elasticity is constant, θ_1/ν, for every corridor larger than θ_0 and falls to zero below θ_0. This implies that a doubling of the diaspora lowers the migration cost to a destination by the same amount independent of diaspora size. The parameter θ_0 bounds the network term at a destination with no diaspora, $h(0) = \theta_1 \log \theta_0$. Because h lowers the migration cost, a small θ_0 makes migration to a destination with no diaspora costly.

Identification and estimation. The network strength θ_1 is identified from the persistence of migration within an o-d pair over time. When a shock raises migration from o to d, the larger diaspora

lowers the cost of migrating to d for households from o in the next period, and how much of the increase in the migrant stock persists is the network elasticity, θ_1/ν. A stronger network and a weaker taste dispersion move flows in the same way, so this data moment can pin down θ_1 only together with ν. To recover θ_1, we separately identify ν from the migration response to destination wages. The network floor parameter θ_0 matters only when the diaspora is very small, $x_t^{o,d} \approx \theta_0$, such that a few additional migrants change the network term of the migration cost. The floor is therefore identified from the persistence of the smallest corridors.

The taste dispersion ν is identified from the response of migration to destination wages. When the wage in d rises by one percent, the value of living there rises by one percent of consumption for every household, so how much the stock in d rises in response pins down $1/\nu$, the wage elasticity of migration. We measure this response within a corridor over time, with corridor and origin-year effects, so persistent differences in wages across destinations are absorbed and the variation is the change in a destination's wage from 1995 to 2015. We restrict the sample for this moment estimate to migration flows into the 45 richest destinations by 1995 wage. This ensures that the moment is identified from the data least affected by measurement error.[18]

The cost elasticity λ is identified from how fast emigration from poor origins increases with their economic growth. With $\lambda = 0$ the cost of leaving a poor origin is the same in 1995 as in 2015, and the growth of its population share abroad over the sample comes only from the wage gap and the network. A positive λ means that migration costs fall with origin income, so the share abroad starts lower and rises faster. Over this period, income grew fastest for poor origins and relatively slowly for rich origins. If the wage gap and the network were all that mattered for migration, the closing wage gap would have held back emigration from poor origins, and their share abroad would have grown less over the sample than it did in the data. How much faster it grew therefore pins down λ.

Given the four parameters $\{\theta_1, \theta_0, \nu, \lambda\}$, the model has one degree of freedom left per corridor, the time-invariant component of the migration cost, $\kappa^{o,d}$. We recover it by inverting the gravity equation (11). For a corridor observed in t and $t+1$,

$$\kappa^{o,d} \;=\; \log \frac{w_t^d}{w_t^o} \;+\; \lambda \log g_t^o \;+\; \theta_1 \log\left(x_t^{o,d} + \theta_0\right) \;-\; \nu \log \frac{x_{t+1}^{o,d}}{x_{t+1}^{o,o}}, \tag{14}$$

where $\kappa^{o,o} = 0$ and g_t^o is the origin country's income relative to 2015. The recovered $\kappa^{o,d}$ therefore absorbs λ times the log of origin income in 2015, including A_0^o. Because every transition identifies the cost, we average the inversion over the 2005 to 2015 transitions that start from at least 100 migrants, so that a shock to a single transition from measurement error or other shocks outside the model is not disporportionatly reflected in the permanent cost. A corridor that is empty in 1995 or 2015, or that has no such transition, has an infinite cost and stays closed. Because the time-invariant migration cost absorbs every feature of a corridor that is constant over time, the elasticities are

[18] For most wealthy countries, the UN takes the migration stocks from population registers and annual surveys. For the other destinations it interpolates stocks between censuses. The response across all destinations is 0.07, against 0.30 in the richest quarter.

identified only from changes within a corridor over time, never from persistent differences across corridors.

Four moments identify the four parameters of these three objects, θ_1, θ_0, λ, and ν. The network moment is the coefficient on a corridor's lagged log odds against the origin, the network elasticity of Table 3. The floor moment is the same coefficient for corridors of fewer than 20 people. The wage moment is the coefficient on the destination log wage in the same regression, on transitions into the 45 richest destinations. The cost moment is the share of the population of the poorest third of origins living abroad in 2005. For each candidate parameter vector we proceed in three steps. We recover the migration cost of every open corridor from (14). We simulate the model from the observed 1995 network with observed wages. We then compute the four moments on the simulated panel with the same regressions as in the data, so each moment is matched as a regression coefficient rather than read as a parameter directly. We exclude Syria, Venezuela, Ukraine from the estimation, since migration driven by war and the collapse of the state is outside the scope of the model.

Estimates. Table 3 reports the four parameter values and the moments that identify them, in the data and in the simulated model. We estimate a wage elasticity of $1/\nu = 0.27$. This is slightly below the elasticity of international migration to the ratio of destination to origin GDP per capita in Beine and Parsons (2015), who report 0.3 across all destinations and 0.5 for destinations in the global North. Two differences in the estimation account for the gap. First, their coefficient is identified from differences in origin income, since destination-year effects absorb the destination's wage, while ours is identified from the change in a destination's wage over time within a corridor. Second, part of the response that a cross-sectional regression attributes to income is driven by the migrant network, and our estimation separates the two.

Table 3: Estimated Parameters and Targeted Moments

Parameter	Value	Moment	Data	Model
International wage elasticity, $1/\nu$	0.27	Response to destination wage, richest destinations	0.30	0.30
Network strength, θ_1	2.75	Network elasticity	0.60	0.60
Network floor, θ_0	1.3×10^{-8}	Network elasticity for small corridors	0.60	0.60
Income elasticity of migration costs, λ	0.23	Share abroad, poorest origins, 2005	4.06	4.06

We estimate a network elasticity of $\theta_1/\nu = 0.74$ for every corridor above the floor value θ_0. The network data moment in Table 3 is 0.60, below the elasticity, because the regression biases the results toward zero. With so few periods, the corridor fixed effects absorb part of the persistence itself, so the coefficient on the lagged stock is below the true elasticity. The network elasticity we recover is consistent with gravity regressions of bilateral migration on the diaspora stock reported in Beine et al. (2011); Beine and Parsons (2017) as well as our own IV estimates from Section 2. The network floor we recover is $\theta_0 = 1.3 \times 10^{-8}$. This implies that diaspora size starts to matter once a destination holds more than one migrant for every 79 million people in the origin. We estimate an

elasticity of migration costs to origin income of $\lambda = 0.23$. The implied elasticity of the probability of emigrating with respect to origin income is $(\lambda - 1)/\nu = -0.21$.

Model validation. We validate the estimated model in two ways. First, as a consistency check, we verify that the model's recovered migration costs vary across corridors with the bilateral frictions of standard gravity models. Table 4 projects the costs on bilateral frictions with origin and destination fixed effects. Countries farther apart have higher costs. Countries with a common official language, a common colonizer, or a past as one country, which proxy for similar language and institutions, have lower costs. A visa requirement raises the cost of a corridor by 0.49 log points, the same as a 39% lower wage.

Table 4: Migration Costs and Bilateral Frictions

	(1)	(2)	(3)
Log distance	1.00 (0.05)	0.93 (0.06)	0.87 (0.06)
Contiguous	−1.05 (0.14)	−0.94 (0.14)	−0.89 (0.14)
Common official language		−0.72 (0.10)	−0.68 (0.10)
Common colonizer		−0.47 (0.16)	−0.35 (0.16)
Same country in the past		−0.42 (0.15)	−0.40 (0.15)
Visa required			0.49 (0.10)
Migration corridors	4,645	4,645	4,564
R^2	0.76	0.77	0.77

Notes: Each column is a regression of the time-invariant migration cost $\kappa^{o,d}$ recovered by (14), in log wage points, on bilateral frictions, over the migration corridors open in 2015 in the data, with origin and destination fixed effects. Distance is the population-weighted bilateral distance. Distance, contiguity, common official language, common colonizer, and same country in the past are from the gravity database of Mayer and Zignago (2011). Visa required is the share of the years 1995, 2000, 2005, and 2010 in which nationals of the origin needed a visa to enter the destination, from the DEMIG VISA database (DEMIG, 2015; Czaika et al., 2018), and column (3) drops the corridors it does not cover. Standard errors clustered by origin in parentheses.

Second, the model does a good job forecasting migration patterns from 2015 to 2025, the decade after the estimation sample. We simulate the model from the observed 2015 network to 2025 with observed wages from the Penn World Table and with the estimated parameters and migration costs, and compare it with the 2020 and 2025 vintages of the UN data, which are not used in the parameter estimation. As a benchmark we also re-estimate and simulate a version of the model in which the diaspora does not affect migration costs, $\theta_1 = 0$. Figure 3(a) plots the share of the world's population living abroad over time. The baseline model predicts the share abroad almost exactly, 2.85% against 2.89% in 2025, while the restricted model with $\theta_1 = 0$ misses the moment even in the estimation sample. Figure 3(b) plots the change in the share of each corridor, in the data and in the two versions of the model. The model's predictions are not perfect, with a correlation of 0.32 with the data, but the restricted model systematically misses changes across corridors, with a correlation of −0.25.

The model misses most where migration responds to shocks outside the model. Corridors to or from Afghanistan, the Central African Republic, the Democratic Republic of the Congo, Eritrea, Ethiopia, Iraq, Libya, Myanmar, Somalia, South Sudan, Sudan, and Yemen, which experienced

Figure 3: Out-of-Sample Fit, 2015 to 2025

(a) Share of the world's population abroad

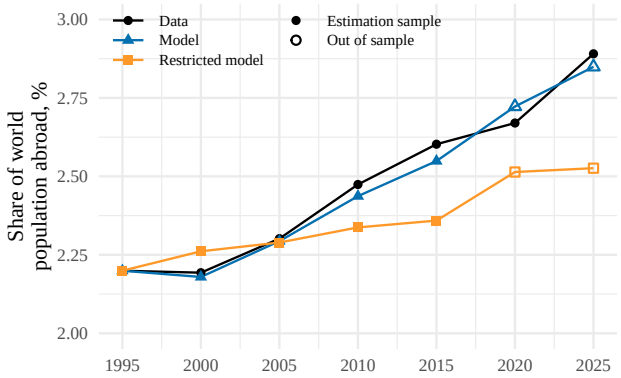

(b) Change in the share of each corridor

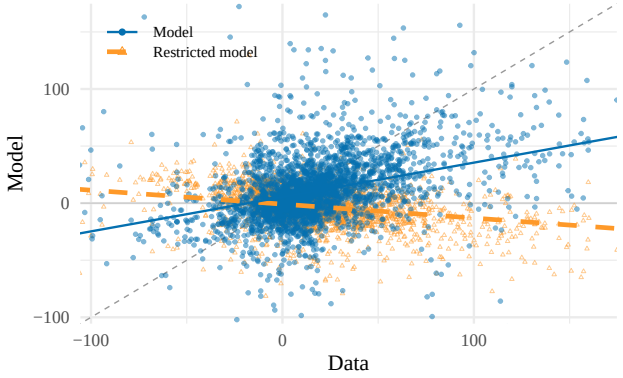

Notes: Panel (a) plots the share of the world's population living abroad, in percent, in the UN data and in the model. Filled circles mark the estimation sample, and open circles mark the years out of sample. The restricted model imposes $\theta_1 = 0$ and re-estimates the remaining migration elasticities and migration costs. Panel (b) plots the change in the log share of each corridor from 2015 to 2025 in the two versions of the model against the data, for the 2,938 corridors with at least a thousand migrants in 2015. The blue and orange lines are least-squares fits, and the gray dashed line is the 45-degree line.

armed conflict over the period are 7% of the sample but account for 38% of the squared forecast error. Migration into Germany, Japan, and Korea grew after changes in admission policy not captured in the model's estimation window. For corridors into these three destinations, the correlation with the data is −0.03 for the model and 0.10 for the restricted model. Without the conflict corridors and these three destinations, the correlation is 0.45 for the model and −0.36 for the restricted model.

4.2 Economic growth absent global warming

Migration patterns will change over the century even absent climate change, because countries' economies will grow at different rates. To separate migration driven by economic growth from migration driven by climate change, we need to predict economic growth absent global warming. We take the growth projections from the shared socioeconomic pathways, the scenarios underlying much of the climate literature (Burke et al., 2015; Carleton et al., 2022; Nath et al., 2024). The five pathways differ in their assumptions about how fast poorer countries will catch up to richer ones (Dellink et al., 2017; Riahi et al., 2017).[19] We use the growth rates implied by the income projections of the OECD's ENV-Growth model (Dellink et al., 2017; International Institute for Applied Systems Analysis, 2025), which map directly into g_t^ℓ in (4).

[19]There are two main alternative approaches to long-run growth prediction. The first is probabilistic. Müller et al. (2022) fit a Bayesian factor model to a century of growth in 113 countries and report a distribution instead of a set of pathways. However, a century of data can only weakly identify century-long persistence, so the dispersion of that distribution depends heavily on assumptions about the persistence of growth. The second is structural. Models in the tradition of Desmet et al. (2018) generate growth inside the model rather than imposing an external path, but that path then depends heavily on assumptions about local innovation and diffusion. Every approach to predicting economic growth through the end of the century must make strong assumptions.

Our baseline pathway is SSP3, the pathway of slow growth and slow catch-up that is commonly used in the climate-impacts literature. Under SSP3 the average return to migration falls dramatically over the century. In Appendix D, we report our main results under alternative pathways. Figure 4(a) plots the ratio of the ninetieth to the tenth percentile of GDP per capita across countries, through the end of the century. Figure 4(b) shows the distribution of the destination wage relative to the origin wage, in 2019 and in 2095, for every pair of countries whose origin is in the half of countries below the median of GDP per capita in 2019. The ratio of the ninetieth to the tenth percentile falls from 23 to 9.4, and the median wage ratio facing a poor origin falls from 2.7 to 2.0.

Figure 4: The Evolution of the Distribution of Relative Wages

(a) Dispersion of GDP per capita under SSP3

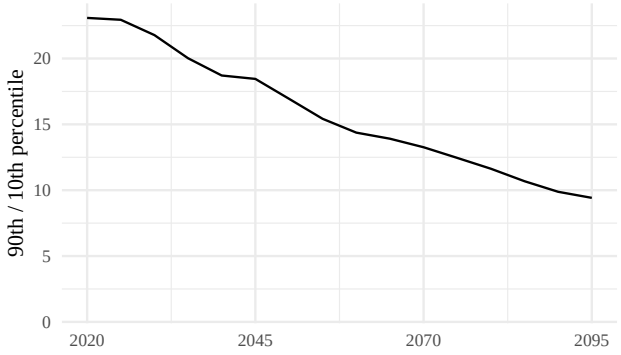

(b) Relative wage distribution, below median origins

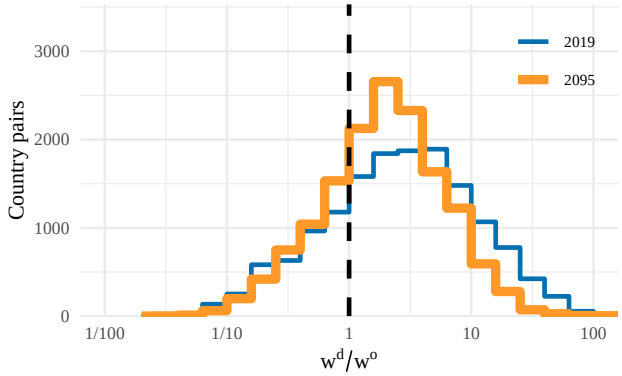

Notes: Panel (a) plots the ratio of the 90th to the 10th percentile of GDP per capita across countries under SSP3. Panel (b) plots histograms of the destination wage relative to the origin wage in 2019 and 2095 over all pairs of countries whose origin is below the median of GDP per capita in 2019.

4.3 Climate damages

We construct both the expected path of climate damages and the covariance of climate damage shocks across countries by combining the output of a climate model with an empirical damage function.

The climate path. We take the expected warming path for every country, as well as the weather shocks around that path, from the Max Planck Institute Grand Ensemble. The ensemble runs the MPI-ESM1.1 climate model 100 times under the RCP 8.5 emissions path using different initial conditions for each run (Maher et al., 2019).[20] The climate system is chaotic, so two runs with the same emissions path but slightly different initial conditions produce different weather paths for the same warming. We treat this internal climate variability as the climate risk that households face. Using large ensembles from seven climate models, Schwarzwald and Lenssen (2022) show

[20] RCP 8.5 is a pessimistic path for emissions and warming that is commonly used in the empirical damage function literature (Burke et al., 2015; Carleton et al., 2022; Nath et al., 2024). We report our main results under RCP 4.5 and other alternative projections for warming in Appendix D.

that internal variability substantially raises the uncertainty in near-term projections of mortality, corn yields, and GDP in the United States. We take the mean warming path, $\bar{q}_t^\ell$, from the average across runs. We construct the weather covariance, $\mathbf{\Gamma}_t$, as the covariance of each pair of countries' deviations from average warming, computed across runs and five-year periods and pooled into twenty-year bins.

The damage function. In the model, climate damages z_t^ℓ enter as a productivity shock that follows an AR(1) process in deviations from expected damages, $\log \bar{z}_t^\ell = d(\bar{q}_t^\ell)$. We adopt the damage function of Nath et al. (2024), who estimate the marginal damage of a degree of warming as a function of a country's temperature, $d'(q) = \beta_0 + \beta_1 q$. They find that an additional degree of warming raises output in countries with a cold climate and lowers it in countries with a hot climate. To construct our expected path for climate damages, we integrate the marginal damage from each country's 2020 temperature, so damages are zero in 2020 and $\bar{z}_t^\ell$ is output under warming relative to the no-warming path $A_0^\ell g_t^\ell$. This path of expected damages is comparable to standard measures of climate damages (Burke et al., 2015; Bilal and Känzig, 2026; Nath et al., 2024).

The covariance of damages. The covariance of damage shocks across countries follows from the covariance of weather and the slope of the damage function. Each period a location's damage deviates from its expected path by the damage from that period's weather shock, η_t^ℓ. Linearizing the damage function around the mean temperature, the damage shock is the marginal damage times the weather shock, $\zeta_t^\ell = d'(\bar{q}_t^\ell)\,\eta_t^\ell$, so the covariance of damages across locations i and j is the covariance of their weather scaled by the two marginal damages,

$$\Sigma_t^{ij} = E_{t-1}\left[\zeta_t^i \zeta_t^j\right] = d'\left(\bar{q}_t^i\right) d'\left(\bar{q}_t^j\right) \Gamma_t^{ij}. \tag{15}$$

The slopes of both countries' damage functions are evaluated at the mean temperature in period t. Therefore the covariance of damages can change over the century as countries warm, even if the covariance of weather is unaffected.

Correlated weather does not imply correlated damages. Dividing (15) by the standard deviation of damages in each location, the correlation of damages between i and j is the correlation of weather multiplied by the sign of the product of the two marginal damages. Because the marginal damage is linear in temperature, the damage function has a single peak. Two locations on the same side of it have marginal damages of the same sign, so a warm year is a cost to both or a gain to both and their damages are as correlated as their weather. Locations on opposite sides of the peak have marginal damages of opposite sign, so the same weather shock raises output in one and lowers it in the other, and their damages are negatively correlated even when their weather is highly correlated. A location with zero marginal damage suffers no economic impact from a weather shock, so its damages are uncorrelated with those of all other locations.

This method allows us to construct the covariance of damages, an object that, to our knowledge, has not been estimated for GDP damages. Damage functions estimated on panel data include

year fixed effects, which absorb the comovement of damages across countries. Bilal and Känzig (2026) recover comovement by identifying damages from global rather than local temperature, but a single global shock makes any two countries' damages perfectly correlated. Dingel and Meng (2026) recover changes in the correlation of cereal yields from ENSO events, which shift the spatial correlation of productivity across the world, but as one global index per year rather than country by country. Our question needs the whole matrix $\mathbf{\Sigma}$. A migrant network is like a portfolio of destinations, and its value depends on the covariance of each destination's damages with those at the origin.

The persistence of damage shocks. The remaining parameter of the climate process is the persistence of damage shocks, ψ. While weather shocks in our model are independent across periods, the output losses they cause are not. A bad shock may destroy capital or cause other persistent declines in output. The value of ψ matters for climate risk and not for the expected path of damages. Nath et al. (2024) identify the effect of an annual temperature deviation on GDP per capita using local projections, and find that a temperature shock lowers GDP per capita for at least a decade. They recover the persistence of damages by indirect inference on a model of catch-up to the world frontier, and their estimate implies that the deviation from trend in (5) retains 0.92 of the deviation each year, so $\psi = 0.92^5 = 0.66$ over the five-year period of the model.

Estimated damages. The expected damages we estimate are large and fall disproportionately on countries with an already hot climate. Figure 5(a) maps the expected damage $\bar{z}_t^\ell$ at the end of the century. We predict that under this warming path, the median country will lose 13.0% of output, with losses of up to 28% across the tropics. We predict that some countries will gain significantly from climate change. At high latitudes we forecast some countries may gain as much as 29% of output. The population-weighted global loss is 14.2% of GDP.[21] For the median country the loss from climate change equals 12 years of growth under SSP3.

Risk is largest where expected losses are largest, because both depend on the local slope of the damage function. Figure 5(b) shows the standard deviation of a country's damage shocks, $\sqrt{\Sigma_t^{\ell\ell}}$, in 2095. For the median country we predict it will be 0.8% of GDP, compared to 0.6% under the current climate. This increase is driven by the fact that the slope of the damage function steepens as a country warms. This modest median effect hides the fact that for some countries these shocks will be quite large. The standard deviation is 1.5% of GDP in the hottest decile of countries and it reaches 3.0% in the most exposed country, a shock the size of a deep recession every five years.

Climate damages are weakly correlated across countries, and global warming is not predicted

[21] Under the same emissions scenario Nath et al. (2024) project a loss of 16% for the world. The gap comes from the warming path, not the damage function. They cumulate damages from 2010 along a linear path to 4.3 degrees of warming for the median country, while we start in 2020 and trace the ensemble mean to 3.2 degrees. Burke et al. (2015) project a loss of 23% of world GDP per capita by 2100 under RCP 8.5. Their damage function is a permanent growth effect, so a year of warming lowers output permanently. Bilal and Känzig (2026) identify damages from global rather than local temperature and find a 12% fall in world GDP per degree of global warming, so output in 2100 is about 50% lower under 3 degrees of warming. While different in magnitude, all three estimates agree with ours on where damages fall, in countries that are hot and poor today.

Figure 5: Expected Damages and Climate Risk in 2095

(a) Expected damage

(b) Standard deviation of damages

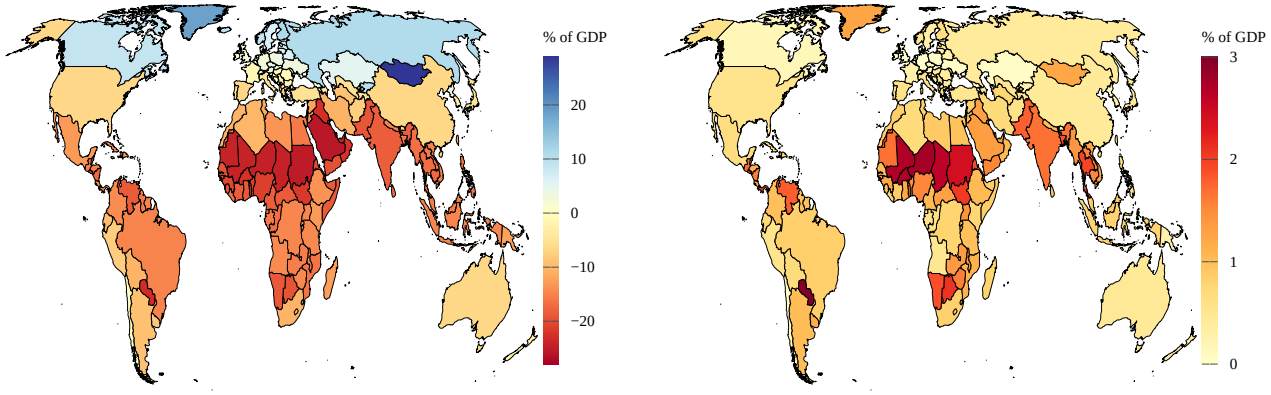

Notes: Panel (a) maps the expected damage $\bar{z}_t^\ell$, the trend of (5), in 2095, in percent of GDP per capita relative to the no-warming path. Panel (b) maps $\sqrt{\Sigma_t^{\ell\ell}}$, the standard deviation of the five-year damage shock of (15), in 2095, in percent of GDP per capita.

to significantly change these correlations. Figure 6(a) plots the distribution of the correlation of the five-year damage shock across all pairs of countries, in 2020 and in 2095. The mean correlation is 0.14 in 2020 and 0.14 in 2095. The share of country pairs with negatively correlated damages rises slightly from 35% to 37%, and the share with a correlation above 0.5 also increases from 13% to 14%. Figure 6(b) plots the mean correlation of both weather and climate damages by distance in 2095. The correlation of damages is 0.45 in the closest bin and decays quickly.

Figure 6: The Correlation of Damages

(a) Distribution in 2020 and 2095

(b) By distance between countries

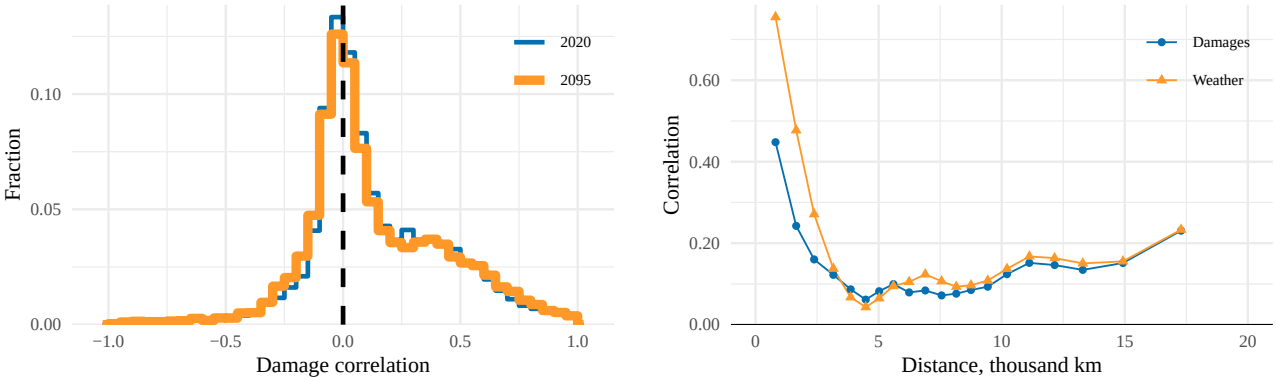

Notes: Both panels plot the correlation of the five-year damage shock, $\Sigma_t^{ij}/\sqrt{\Sigma_t^{ii}\Sigma_t^{jj}}$ from (15), over every pair of countries. Panel (a) plots the distribution of correlations in 2020 and in 2095, each as a fraction of the pairs in that year. Panel (b) is for 2095 and splits the pairs into 20 equal-count bins by the great-circle distance between the two countries' population-weighted centroids and plots, at each bin's mean distance, the mean correlation of damages and the mean correlation of weather across the pairs in the bin.

5. Migrant Networks and Climate Losses

The migrant network raises the welfare cost of climate change for the average household by 1.20 percentage points of lifetime consumption, roughly 24 percent of the total loss and the same as 0.7°C of additional warming. The effect is concentrated in hot and poor origins. For countries at high latitudes, the migrant network reduces the welfare cost of climate change. Climate losses in the baseline economy are nearly identical to those in an economy with no international migration. Nearly all of the network effect is due to the correlation of the current migrant network with the projected warming trend.

5.1 Measuring the effect of the migrant network on welfare losses from climate change

We measure the effect of the migrant network on climate losses by comparing the welfare cost of climate change across two economies. In our baseline economy, the residence cost of a destination falls with the size of the diaspora living there. In the no-network economy, households face the same wages and the same residence costs $\kappa^{o,d}$ as in the baseline economy, but the diaspora has no effect on them. The two economies start from the same initial migrant stocks but differ in how much and where households move, both before and in response to climate change. We measure the welfare cost of climate change within each economy and compare the two costs. The difference is the effect of the migrant network on climate losses.

Let $W^o \equiv V_0^o(\mathbf{x}_0^o, \mathbf{z}_0)$ be the expected lifetime utility (10) of an origin-o household at the initial network and climate. In the baseline economy, the welfare loss from climate change is

$$D^o \equiv (1-\beta)\left(W_\dagger^o - W^o\right), \tag{16}$$

where the dagger (†) denotes the no climate change benchmark, which holds the trend and the spatial covariance of the climate process (5) at their initial values, $\bar{\mathbf{z}}_t = \bar{\mathbf{z}}_0$ and $\mathbf{\Sigma}_t = \mathbf{\Sigma}_0$ for all t. We define climate losses the same way in the no-network economy, where $h \equiv 0$,

$$\tilde{D}^o \equiv (1-\beta)\left(\tilde{W}_\dagger^o - \tilde{W}^o\right), \tag{17}$$

where the tilde ($\sim$) denotes the no-network economy. The effect of the migrant network on the welfare loss from climate change is the difference between the two, $D^o - \tilde{D}^o$. This double difference nets out the cost of climate change that the two economies share and the value of the network itself in the absence of climate change, leaving only the interaction between the network and climate change.

With log utility, D^o and $\tilde{D}^o$ are exactly the consumption-equivalent welfare losses from climate change in their respective economies. Each is the fraction of consumption that a household from origin o would give up in every location and every period to avoid living in a world with climate change.[22] The difference between the two, $D^o - \tilde{D}^o$, is therefore the consumption equivalent welfare

[22] Suppose a household from origin o loses the fraction $1 - e^{-D^o}$ of its consumption in every location and every period.

loss that is due to the migrant network. Because each loss is a proportion of consumption, it does not depend on the income level of the origin. Because each is a difference within an economy, it does not depend on the level of welfare in that economy. The losses can therefore be compared across origins and across economies.

We compute the welfare levels by solving each economy forward from the observed 2020 network through 2095, along the growth path of Section 4. In the economies with climate change, the trend and the covariance of the climate process follow the projections of Section 4 through 2095 and are fixed at their 2095 values thereafter. In the economies without climate change, both stay at their 2020 values, so expected damages do not rise but weather shocks from the current climate distribution still cause losses. We average over 10,000 Monte Carlo draws of the climate process. Additional details on the computational algorithm can be found in Appendix **??**.

Table 5 reports the network effect on climate losses. Column 1 reports the consumption-equivalent welfare loss from climate change in a no-migration economy, in which every household resides in its origin. Column 2 reports the loss in the baseline economy with the migrant network, and column 3 reports the loss in the no-network economy. Column 4 reports the network effect on climate losses, the difference between columns 2 and 3. Column 5 expresses the same effect in units of additional warming.[23] The difference between columns 1 and 3 is the potential value of migration as adaptation to climate change. The difference between columns 1 and 2 shows how much of that potential adaptation is realized in the baseline economy with the migrant network. Each row is a population-weighted mean over a group of origins, for all origins and by climate exposure, GDP per capita, and region.

Table 5 shows that the migrant network increases climate losses on average, but that these effects are largest for households from hot and poor origin countries. Across all origins, the migrant network increases consumption-equivalent welfare losses from climate change by 1.20 percentage points. This is 24 percent of the average welfare loss from climate change and equivalent to an additional 0.7°C of warming by the end of the century. The network effect is heterogeneous across origins. For the hottest quartile of origins, the network raises losses by 3.5 points, and for the coolest quartile it lowers them by 0.55 points. For origins below the median GDP per capita today, the network raises losses by 2.5 points, while for wealthier origins it lowers them by 0.1 points.

The average losses reported in Table 5 mask substantial variation across countries, even within a region, so Figure 7 maps the network effect by origin. The network contributes to larger welfare losses from climate change in countries currently home to 64 percent of the world's population. The geography of the network effect mostly follows the geography of warming, with the largest increases across the Middle East, South Asia, Sub-Saharan Africa, and Southeast Asia. However,

With log utility its flow utility falls by D^o. Because the fall is the same proportion in every location, its migration decisions are unchanged. Lifetime utility falls by $D^o/(1-\beta)$, which is the welfare loss from climate change, $W^o_\dagger - W^o$, by (16).

[23] We convert consumption-equivalent losses to degrees of warming by re-solving the baseline economy under scaled warming paths. For a scaling factor s, every country's temperature path is $\bar{q}^d_{2020} + s\,(\bar{q}^d_t - \bar{q}^d_{2020})$, damages follow from the damage function of Section 4, and the average household's loss is a function of s. For each row in Table 5, we find the scaling s at which the average household's loss changes by the estimated network effect. Column 5 reports $(s-1)$ times the projected warming from 2020 to 2095.

Table 5: The Effect of Migrant Networks on Climate Losses

	Losses, % of consumption			Network effect	
	No migration	With network	Without network	pp of consumption	°C of warming
All origins	5.15	5.05	3.85	1.20	0.7
Panel A. By origin climate exposure					
Coolest quartile	1.94	1.96	2.51	−0.55	−0.3
Second quartile	3.62	3.56	3.34	0.22	0.1
Third quartile	7.32	7.06	4.69	2.37	1.3
Hottest quartile	8.95	8.79	5.29	3.50	1.9
Panel B. By origin GDP per capita					
Below median	7.71	7.56	5.04	2.52	1.4
Above median	2.54	2.48	2.62	−0.14	−0.1
Panel C. By region					
Africa	7.82	7.68	5.75	1.92	1.1
South Asia	8.47	8.43	5.17	3.26	1.8
MENA	6.49	6.03	3.87	2.16	1.2
East Asia	3.76	3.69	3.42	0.27	0.2
Latin America	5.56	5.04	3.27	1.77	1.0
Europe	−0.79	−0.67	0.71	−1.37	−0.8
North America	1.82	1.89	3.01	−1.12	−0.7

Notes: The first three columns are the lifetime welfare loss from climate change, in percent of consumption, in the economy with no migration, in the baseline economy with the migrant network, and in the economy without the migrant network affecting residence costs. The last two columns are the difference between the welfare losses in the baseline and the no-network economies, in percentage points and as the additional warming over 2020 to 2095 that would change the average household's loss by the same amount, with damages and migration re-solved. Each row is the population-weighted mean over the origins in that group.

the network effect also depends on where a country's diaspora lives. For example, Latin America is expected to experience less extreme warming than much of Sub-Saharan Africa and therefore lower climate damages, but the two regions have similar network effects. Latin American diasporas are concentrated in the origin and in nearby destinations with similar climate exposure. For origins at high latitudes, such as Canada, Scandinavia, Russia, and Mongolia, the network contributes to lower climate losses by keeping the diaspora in cold destinations that gain from warming.

In the baseline economy with the migrant network, migration is not an effective adaptation strategy for climate change. Columns 1 and 2 of Table 5 show that the average welfare loss in the no-migration economy, where every household is forced to live in its origin country forever, is nearly the same as in the baseline economy with the network. For the hottest quartile of origins, the two losses are 8.95 and 8.8 percent of lifetime consumption. Without the network, the same households and residence costs deliver a loss of 3.85 percent, so the network effect is 92 percent of the reduction in losses that migration could provide relative to the no-migration economy. Our baseline economy therefore resembles the no-migration counterfactuals of Desmet and Rossi-Hansberg (2015), Desmet et al. (2021), and Bilal and Rossi-Hansberg (2023), which find welfare losses from climate change several times larger than in their baseline economies with migration. Here, however, the migrant network endogenously keeps households in exposed places.

Figure 7: The Effect of Migrant Networks on Climate Losses

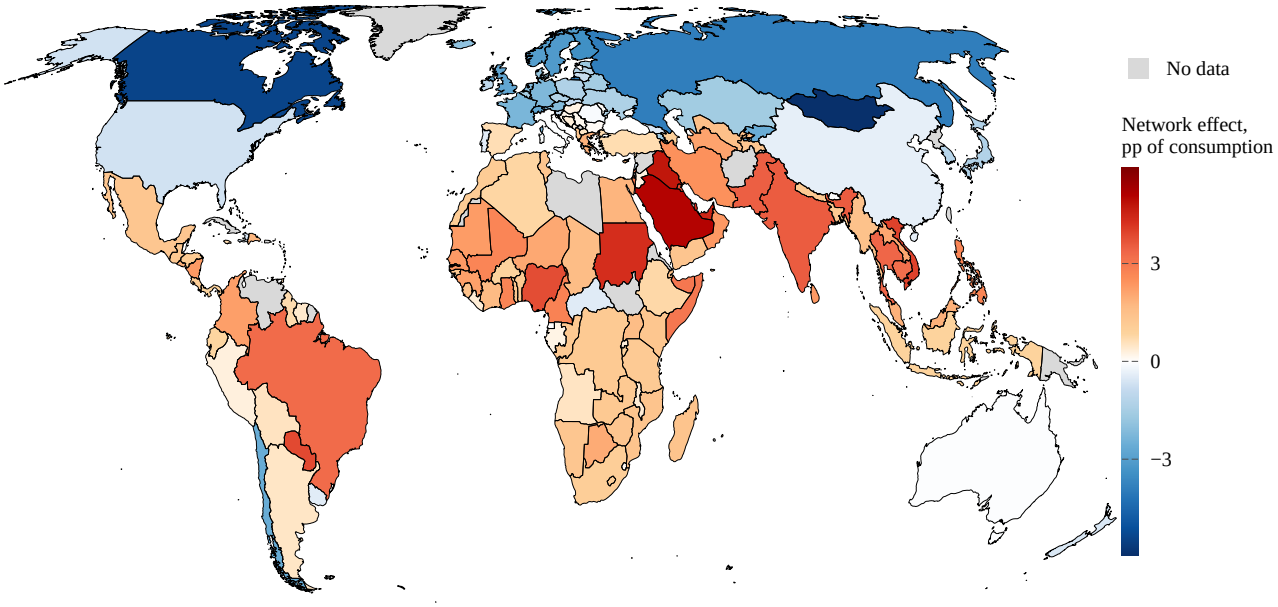

Notes: The network effect on climate losses, $D^o - \tilde{D}^o$, in percentage points of consumption, by origin country. Lifetime losses are evaluated in 2020 under the projected climate path, discounted at 2 percent a year, and averaged over the 10,000 draws of the climate process. Red is where the network raises climate losses and blue where it lowers them.

5.2 Anchoring and diversification

The network changes the welfare loss from climate change through two channels, which we call anchoring and diversification. Anchoring is the network's effect on the household's exposure to the projected warming trend, and diversification is its effect on the insurance value of migration. We separate the two by expanding W^o, the expected lifetime utility of an origin-o household, to second order in the climate shocks around the projected climate path,

$$W^o \;\approx\; V^o \;+\; \underbrace{\tfrac{1}{2}\sum_t \operatorname{tr}\!\left(\nabla^2_{\zeta_t} W^o \cdot \boldsymbol{\Sigma}_t\right)}_{\equiv\, \Omega^o}. \tag{18}$$

This expansion decomposes the value of a location into a trend and a risk term. The trend term, V^o, is the household's lifetime utility if climate change follows its projected path with no shocks. The first-order term of the expansion vanishes because the climate shocks are mean zero around the trend. The risk term, Ω^o, adjusts the trend term for the shocks around the projected path, scaling their covariance $\boldsymbol{\Sigma}_t$ by the curvature of lifetime utility. Because damages persist, a shock in period t enters lifetime utility through every later period, so the covariance that matters is that of the deviation of damages from trend, $\operatorname{Var}(\log \mathbf{z}_t - \log \bar{\mathbf{z}}_t)$, which accumulates past shocks at the rate ψ. With log utility a household that does not migrate is risk neutral in the shock, so Ω^o is nonzero only because households choose where to live after seeing the shock, and it is the option value of

moving.[24]

The network effect on the welfare loss from climate change, $D^o - \tilde{D}^o$, can be expressed as the sum of an anchoring term and a diversification term. Let Δ denote the difference between the no climate change benchmark and climate change, so that $\Delta V^o \equiv V^o_\dagger - V^o$ is the loss from the warming trend and $\Delta\Omega^o \equiv \Omega^o_\dagger - \Omega^o$ is the loss from the change in climate risk. The expansion in (18) applies to each of the four values in $D^o - \tilde{D}^o$, so to second order the network effect is the sum of the network's effect on each term:

$$D^o - \tilde{D}^o \;\approx\; (1-\beta)\Big[\underbrace{\Delta V^o - \Delta\tilde{V}^o}_{\text{anchoring}} + \underbrace{\Delta\Omega^o - \Delta\tilde{\Omega}^o}_{\text{diversification}}\Big]. \tag{19}$$

The anchoring term is the network's effect on the loss from the trend, and would be present even if the climate followed its projected path with no shocks. The diversification term is the network's effect on the loss from the shocks around that path, and is nonzero only because the network changes the option value of moving.

The network enters both terms of (19) because it changes where households choose to live. Because the diaspora enters the payoff of a destination additively, the choice probabilities (8) in the baseline economy are those of the no-network economy, reweighted by the diaspora at each destination,

$$\pi^{o,d}_t \;=\; \frac{\tilde{\pi}^{o,d}_t \, e^{h(x^{o,d}_t)/\nu}}{\mathbb{E}_{\tilde{\pi}^o_t}\big[e^{h(x^{o,d}_t)/\nu}\big]}, \tag{20}$$

where $\mathbb{E}_{\tilde{\pi}^o_t}$ is the expectation over destinations under the no-network choice probabilities $\tilde{\pi}^o_t$, which depend only on wages and residence costs. The network therefore tilts migration toward destinations with larger diasporas, which changes both the household's exposure to the warming trend and the destinations it would move to after a shock. The anchoring term follows from applying this tilt to the loss from the trend.

The anchoring term can be written as the covariance across countries between the network tilt and the present value of trend climate losses:

$$\Delta V^o - \Delta\tilde{V}^o \;\approx\; -\sum_t \beta^t \, \frac{\mathrm{Cov}_{\tilde{\pi}^o_t}\big(e^{h(x^{o,d}_t)/\nu},\ \log \bar{z}^d_t\big)}{\mathbb{E}_{\tilde{\pi}^o_t}\big[e^{h(x^{o,d}_t)/\nu}\big]} \;\approx\; -\frac{\mathrm{Cov}_{\tilde{\pi}^o_0}\Big(e^{h(x^{o,d}_0)/\nu},\ \sum_t \beta^t \log \bar{z}^d_t\Big)}{\mathbb{E}_{\tilde{\pi}^o_0}\big[e^{h(x^{o,d}_0)/\nu}\big]}, \tag{21}$$

where $-\log \bar{z}^d_t$ is the trend loss at destination d in period t relative to the 2020 climate. The first approximation applies the envelope theorem at each date t. To first order the loss from trend climate damages is the expected damage where the household chooses to live. Given the start-of-period population distribution, the two economies differ only through the network's effect on residence costs, and the difference in expected climate losses can be expressed as a covariance between the

[24] Flow utility at a destination d is $\log c^d_t + h(x^{o,d}_t) - \kappa^{o,d}_t$, and with wages equal to productivity, $\log c^d_t = \log A^d_0 + \log g^d_t + \log z^d_t$. The climate shock ζ^d_t enters $\log z^d_t$ additively by (5), so flow utility is linear in the shock. The only curvature from the shock comes through the choice of location, since with the logit structure the destination payoffs enter lifetime utility as $\nu \log \sum_d \exp(\cdot)$ in (10).

network tilt and the expected loss.[25] The second approximation holds the choice probabilities at their 2020 values, so the sum collapses into a single covariance between the network tilt today and the present value of the trend loss at each destination.

The date 0 approximation of the anchoring term captures nearly all of the network effect on climate losses. Figure 8(a) shows the approximation against the full network effect. The approximation misses where the network is predicted to change the most over the century, and this endogenous response means the effect is slightly smaller than the approximation predicts at the extremes, such as Iraq and Mongolia. The approximation works so well because migrant networks are very persistent. In the data the corridors with a large diaspora in 1995 are the corridors with a large diaspora in 2025, despite the many economic and political shocks of the intervening years. Since the model is estimated to match the data, this same persistence feature holds. The network effect is therefore well approximated by the covariance between the network tilt and the present value of trend losses at date 0, which is a function of the initial diaspora and the projected climate path.

Figure 8: The Anchoring Effect of the Migrant Network on Climate Losses

(a) Date 0 approximation

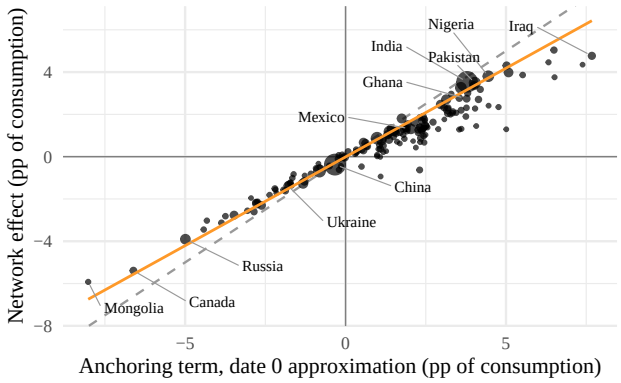

(b) Correlation of origin and diaspora losses

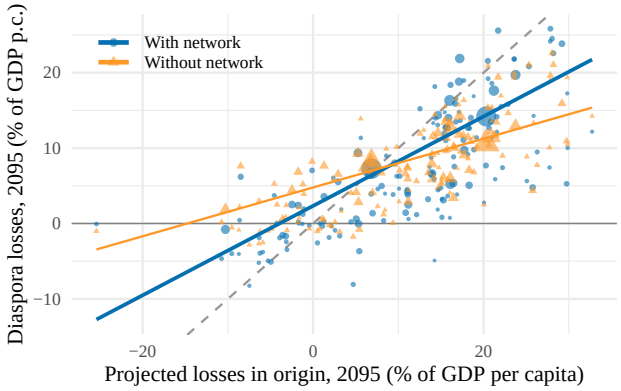

Notes: Each point is an origin country and the dashed line shows the 45-degree line in both panels. Panel (a) plots the network effect from the full solution of the model against the date 0 approximation, both in percentage points of consumption. Points size corresponds to initial population, and the orange line shows the population-weighted least squares fit. Panel (b) plots the projected loss in 2095 averaged over an origins diaspora against the projected loss in the origin, in percent of GDP per capita, with the network (blue circles) and without it (orange triangles). The lines show population-weighted least squares fits for the two economies.

The anchoring component of the network effect is large both because the network tilts households toward destinations whose climate impacts mirror those in the origin country and because trend losses are large relative to the losses from climate shocks. The diversification term is four orders of magnitude smaller than the anchoring term. When the network shapes migration choices, households are concentrated in a narrow set of destinations whose climates resemble their origin's, so the present value of trend losses where the network places households is 5.77 percent of consumption, against 5.80 percent of consumption in the origin country. Without the network,

[25] Appendix C.5 provides the derivation.

migration destinations are determined by wages, residence costs, and idiosyncratic taste shocks, so a given origin's households are spread across a much broader set of destinations with less correlated climate impacts, and the present value of trend losses falls to 4.27 percent of consumption. Figure 8(b) shows the same comparison for every origin's diaspora, with trend losses in 2095 at the origin on the horizontal axis and trend losses where the diaspora lives on the vertical axis, with and without the network. The anchoring term is therefore largest for hot and poor origins whose diasporas live in the Gulf, South Asia and neighboring countries that warm as they do, and negative for high-latitude origins whose diasporas live in cold countries that gain from warming.

The diversification term can be written as the covariance across pairs of countries between the relative network tilt and the present value of the relative change in how damage shocks co-move across the two countries:

$$\Delta\Omega^o - \Delta\tilde{\Omega}^o \;\approx\; \sum_t \beta^t \, \frac{1}{4\nu} \, \frac{\mathrm{Cov}_{\tilde{\pi}^o_t}\Big(e^{[h(x^{o,i}_t)+h(x^{o,j}_t)]/\nu},\; \sum_{s\le t} \psi^{2(t-s)}\, \Delta\big(\Sigma^{ii}_s + \Sigma^{jj}_s - 2\Sigma^{ij}_s\big)\Big)}{\mathbb{E}_{\tilde{\pi}^o_t}\big[e^{h(x^{o,i}_t)/\nu}\big]\, \mathbb{E}_{\tilde{\pi}^o_t}\big[e^{h(x^{o,j}_t)/\nu}\big]}, \tag{22}$$

where $\Sigma^{ii}_t + \Sigma^{jj}_t - 2\Sigma^{ij}_t$ is the variance of the difference between the climate shocks at i and j, and each pair of countries is weighted by the product of their no-network choice probabilities. The Δ appears because the economy without climate change also has shocks, so migration has option value in both economies and climate change matters only through the change in the distribution of shocks. The sum over s appears because a shock has persistence ψ and therefore the gap between i and j at date t accumulates every shock since date 0. Take the pair of the origin o and a destination d, which provides insurance when $\Sigma^{oo}_t + \Sigma^{dd}_t - 2\Sigma^{od}_t$ is large, which requires the shocks at o and d to be large and Σ^{od}_t to be small or negative, so that a household in the origin has somewhere better to move after a bad shock. A destination whose shocks co-move with the origin's, so that Σ^{od}_t is close to Σ^{oo}_t and Σ^{dd}_t, provides no insurance. The covariance sums this comparison over every pair of countries, weighted by the network tilt for that pair, so the migrant network increases climate losses through this term when it concentrates households in destinations whose shocks co-move with the origin's so that the diaspora is less diversified. The approximation in (22) again applies the envelope theorem at each date, now with the tilt reweighting each country in the pair.

Climate risk adds little to expected losses from climate change for any origin, with or without the network, so the diversification term is small. Because we assume log utility, a household that does not migrate is risk neutral about the climate shock. The dispersion of losses in Figure 9(a), which the network raises from 0.13 to 0.54 percentage points of consumption, therefore carries no welfare cost in itself, since the shock enters log consumption additively and averages out in expected utility. Climate risk affects the welfare cost of climate change only through the option value of moving after a shock.[26] Figure 9(b) plots this option value term in the two economies against the size of the shock

[26]The gain from re-sorting is the log-sum over destinations of the realized shocks, $\nu \log \sum_d \pi^{o,d}_t \exp(\zeta^d_t/\nu)$, where $\pi^{o,d}_t$ are the choice probabilities along the trend. Expanding around $\boldsymbol{\zeta}_t = 0$, the first-order term is the mean shock, which is zero, and the second-order term is the variance of the shock across the destinations the household would choose, divided by 2ν.

in the origin. Although the levels are small in both economies, the network removes most of the option value, leaving 6% of its no-network value, because it concentrates households in destinations whose shocks co-move with the origin's.[27] The network therefore makes the baseline economy look similar to an economy with no international migration where the insurance value is zero.

Figure 9: The Network and Climate Risk

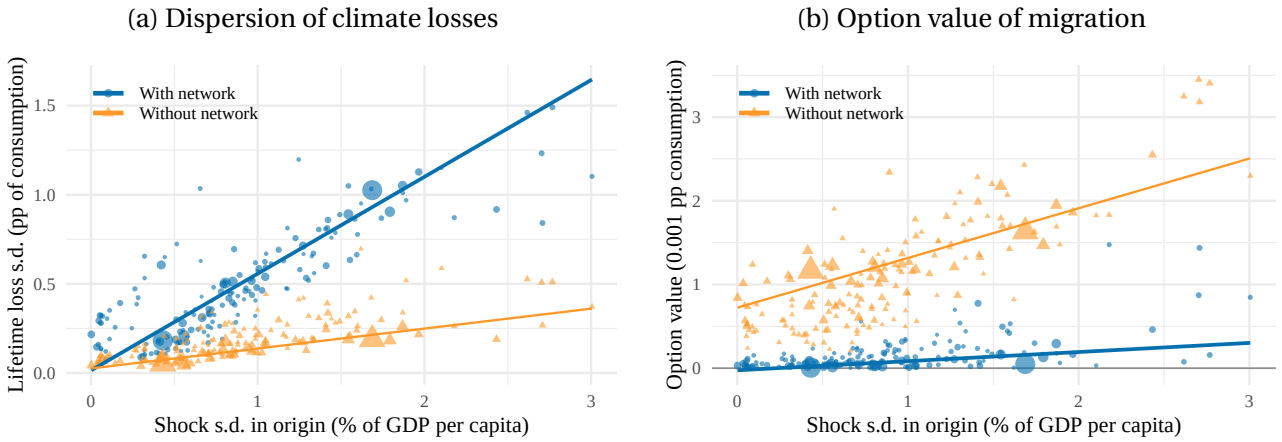

Notes: Each point is an origin country, in an economy with the migrant network (blue circles) and without it (orange triangles). The lines show the population-weighted least squares fit. The x axis in both panels is the standard deviation of the climate shock in the origin in 2095, in percent of GDP per capita. Panel (a) plots the standard deviation of lifetime losses across the 10,000 climate draws, in percentage points of consumption. Panel (b) plots the option value of migration in the climate economy, in thousandths of a percentage point of consumption.

6. Counterfactual Migration Policies

Migration policy is climate policy because it changes where households live and therefore their exposure to the economic effects of global warming. The migrant network amplifies the impact of a migration policy, because a policy that restricts or expands migration opportunities also changes the diaspora, which in turn shapes the destination choices of future migrants. We use the estimated model to evaluate three policies: a freeze on immigration into the OECD, a uniform relaxation of immigration policy, and a climate visa program for the origins most exposed to global warming. Restrictions raise climate losses, especially for origins with large existing networks in the OECD, and because a restriction stops those networks from growing, its effects outlast its implementation. Easing restrictions lowers losses on average, but only by moving a very large number of people,

[27] Three changes to the model would increase the value of diversification. Alternative preferences such as power utility with a coefficient of relative risk aversion above one would make households dislike the variance of consumption. Epstein–Zin preferences that price persistent risk would make the diaspora's location a hedge against long-lived damages and increase the option value of migration. A sunk cost of moving would change the location choice from a static choice period by period to a dynamic one. In that case a diversified diaspora would be worth more as insurance. Although these extensions would change the level of the diversification term, in each case the network would still lower the insurance value of migration, given the initial network that countries are endowed with in the data and the persistence of the network.

while a targeted visa program reduces the climate losses of the most exposed origins with fewer migrants.

6.1 Immigration restrictions

The first counterfactual policy we consider is a temporary freeze on immigration into the 38 member countries of the OECD. The counterfactual is motivated by the recent tightening of immigration policy in the United States, the United Kingdom, Canada, Australia, and many member states of the European Union.[28] We implement the freeze as a temporary addition $\bar{\tau}$ to the residence cost of every corridor from an origin outside the OECD to a destination inside it. The additional cost is in place from 2020 to 2055 and is zero from 2060 onward. We choose $\bar{\tau}$ so that the size of the foreign-born population in the OECD in 2060 equals its 2020 level. This requires $\bar{\tau} = 0.79$ log points, larger than the residence cost of a visa requirement implied by Table 4.

Table 6 column (1) reports the effect of the immigration freeze on the climate losses of the origins outside the OECD. The table also reports three additional counterfactual restrictions. Column (2) is a permanent freeze, in which $\bar{\tau}$ never falls to zero. Columns (3) and (4) report the effect of a full ban, which raises the residence cost of every migration corridor into the OECD until no one enters, for the same window and permanently. Because households pay the residence cost in every period, the ban also implies that every foreign-born resident leaves the OECD. The ban is an extreme policy, but it serves as an upper bound on how far immigration restrictions by wealthy countries can raise climate losses. Panel A averages over all origins outside the OECD, and Panels B to D repeat the statistics for three regions that span the range of exposure to the OECD's restriction, the Caribbean and Central America, with 12.2% of its population living in the OECD in 2020, the Middle East and North Africa with 2.6%, and Sub-Saharan Africa with 0.6%.

For each counterfactual we focus on the change in the loss from climate change, because a restriction lowers welfare whether or not the climate changes. Let P^o denote the expected lifetime utility of a household from origin o with the policy in effect, and $P^o_\dagger$ the same object without climate change, the counterparts of W^o and $W^o_\dagger$. If we compared welfare with the policy to welfare without it, $(1-\beta)(P^o - W^o)$, the difference would combine the loss of access to high-wage destinations with the change in the impact of climate change. We instead isolate the climate effect by reporting the difference between the losses from climate change with and without the policy, $D^o_P - D^o$, where $D^o_P \equiv (1-\beta)(P^o_\dagger - P^o)$. The first row of the table reports this difference in percentage points of

[28] The United States suspended refugee admissions in January 2025 and restricted entry from nineteen countries in June 2025 (White House, 2025a; White House, 2025b). In 2025, the United Kingdom raised the skill and salary thresholds for work visas (Home Office, 2025). Canada recently cut its permanent-resident targets for 2025 to 2027 by 20% and capped international student visas (IRCC, 2024). In 2023, Australia raised English fluency requirements for students and set a target of reducing net migration by 50% (Australian Government, 2023). In 2024, New Zealand tightened its work visa scheme (Immigration New Zealand, 2024). In the European Union, Germany introduced additional border controls in September 2024 (BMI, 2024). In 2024, Finland suspended asylum applications at its eastern border (EUAA, 2025). In 2025, Austria suspended family reunification for refugees (Parlament Österreich, 2025). Also in 2025, Poland suspended the right to apply for asylum at its border with Belarus (Ministry of the Interior of Poland, 2026). In 2026, the Netherlands adopted a two-tier asylum system (Eerste Kamer, 2026). OECD (2025) presents a systematic review of recent immigration policy changes across the OECD.

consumption, so that a positive number means the policy raises the loss from climate change. The second row expresses the same change in percent of the no-policy loss D^o. The third row reports the change in welfare from the policy, $(1-\beta)(P^o - W^o)$, in percentage points of consumption.

The fourth row of Table 6 isolates the part of the change in climate losses driven by the migrant network. Households pay the residence cost in every period, so when a restriction is lifted, the cost of every corridor returns to its no-policy value. After the policy is lifted, the only difference from the no-policy economy is a smaller migrant network in the OECD. Any loss incurred after the restriction is lifted relative to the no-policy economy therefore comes through the network. This row reports the share of the loss incurred after 2060, discounted to 2020. The value is not reported for the permanent restrictions. The last two rows for each panel report how many fewer people from these origins live in the OECD than without the policy at the start of 2060 and of 2095.

A temporary migration freeze raises the climate losses of the origins outside the OECD by only a small amount on average. The headline numbers are small because only 1.2% of the population of countries outside the OECD lives in an OECD country in 2020, and the climate loss of an origin averages over all its households, most of which never migrate. The losses from the permanent freeze, the temporary ban, and the permanent ban are all still small but several times larger. Even for the temporary immigration freeze, however, the cost outlasts the policy, since the origins outside the OECD incur 50% of it after the freeze is lifted. The full welfare cost of these restrictions is also much larger than the climate losses alone, since these policies reduce the option value of moving to a high-income destination, irrespective of climate change. For the average household outside the OECD, the welfare loss from the restriction is equivalent to 1.23 percentage points of permanent consumption.

The largest climate costs from the policy fall on the origins with the largest migrant networks in OECD countries. Figure 10 maps the change in each origin's climate loss under the temporary freeze in percentage points of consumption. The effects are largest in the Caribbean and Central America and in Iraq and several Gulf states. The impact is smaller across Sub-Saharan Africa and South Asia. The results largely trace the share of each origin's population living in the OECD in 2020. Panels B, C, and D of Table 6 provide additional numbers for three regions that span the range of population shares in the OECD. The table shows that the temporary freeze raises the climate loss of the Caribbean and Central America, with 12.2% of its population in the OECD, by 2.17%, of the Middle East and North Africa, with 2.6%, by 1.03%, and of Sub-Saharan Africa, with 0.6%, by 0.25%. For a few origins the temporary immigration freeze reduces climate losses. In Russia and many Central Asian countries, warming is predicted to raise incomes, so households that are prevented by the policy from moving to the OECD remain in a country that gains from global warming.

Although the average climate impacts of these policies are small, they nonetheless have large impacts on the distribution of people across the globe. By 2060 the temporary immigration freeze results in 58.7 million fewer immigrants in the OECD. By 2095 the number falls to 7.6 million, because immigration resumes but with a smaller migrant network than in the baseline economy. The temporary ban results in 127 million fewerer immigrants in the OECD by 2060 and 104 million

Table 6: Restricting Immigration into the OECD

	Freeze		Full ban	
	Until 2060 (1)	Permanent (2)	Until 2060 (3)	Permanent (4)
Panel A. All origins outside the OECD (1.2% of origin population living in the OECD in 2020)				
Change in climate loss, $D_P^o - D^o$, pp of consumption	0.019	0.062	0.103	0.136
Change in climate loss, % of D^o	0.33	1.08	1.77	2.36
Change in welfare, pp of consumption	−1.23	−2.05	−4.38	−4.89
Share of the loss incurred after 2060, %	49.5	–	78.2	–
Fewer immigrants in the OECD in 2060, millions	58.7	58.7	127	127
Fewer immigrants in the OECD in 2095, millions	7.6	68.3	104	142
Panel B. Caribbean and Central America (12.2% of origin population living in the OECD in 2020)				
Change in climate loss, $D_P^o - D^o$, pp of consumption	0.110	0.458	1.01	1.60
Change in climate loss, % of D^o	2.17	9.00	19.8	31.5
Change in welfare, pp of consumption	−11.6	−20.3	−50.4	−57.8
Share of the loss incurred after 2060, %	25.3	–	71.7	–
Fewer immigrants in the OECD in 2060, millions	6.0	6.0	17.6	17.6
Fewer immigrants in the OECD in 2095, millions	0.4	6.6	12.5	18.9
Panel C. Middle East and North Africa (2.6% of origin population living in the OECD in 2020)				
Change in climate loss, $D_P^o - D^o$, pp of consumption	0.062	0.256	0.439	0.588
Change in climate loss, % of D^o	1.03	4.23	7.26	9.74
Change in welfare, pp of consumption	−3.24	−5.88	−12.0	−13.5
Share of the loss incurred after 2060, %	49.4	–	82.8	–
Fewer immigrants in the OECD in 2060, millions	13.8	13.8	30.0	30.0
Fewer immigrants in the OECD in 2095, millions	1.7	19.1	30.7	40.8
Panel D. Sub-Saharan Africa (0.6% of origin population living in the OECD in 2020)				
Change in climate loss, $D_P^o - D^o$, pp of consumption	0.019	0.057	0.088	0.110
Change in climate loss, % of D^o	0.25	0.74	1.14	1.44
Change in welfare, pp of consumption	−0.60	−0.95	−1.93	−2.12
Share of the loss incurred after 2060, %	52.6	–	78.0	–
Fewer immigrants in the OECD in 2060, millions	9.2	9.2	18.2	18.2
Fewer immigrants in the OECD in 2095, millions	1.8	12.6	17.7	23.6

Notes: Each column is one restriction on migration into the OECD, in effect from 2020 until 2060 or permanently. The freeze raises residence costs into the OECD so that the OECD's population born outside it stays at its 2020 level. The full ban stops migration into the OECD and expels residents born outside it. Rows report, for the origins in each panel, the change in the climate loss D^o of (16) caused by the policy, in percentage points of permanent consumption and in percent of the no-policy loss, the change in lifetime welfare with climate change in percentage points of permanent consumption, the discounted share of that loss incurred after 2060, and how many fewer people from these origins live in the OECD at the start of 2060 and of 2095 than without the policy. Panel titles give the share of each panel's population living in the OECD in 2020. All numbers are population weighted.

by 2095. A temporary restriction therefore has a persistent effect on where people live, because the network does not immediately recover when the restriction is lifted.

The migrant network makes the effects of a temporary restriction persistent. While the immigration freeze is in place, households that could otherwise migrate to the OECD either stay in their origin or settle in other destinations. The additional climate loss incurred during the policy window is 0.16% of the no-policy loss. Once the policy is lifted, residence costs return to their no-policy values, but the OECD's diaspora is smaller than it would be otherwise. This implies that fewer households are drawn to the OECD by their diaspora, and the loss incurred after 2060

Figure 10: Change in Climate Loss from OECD Immigration Freeze

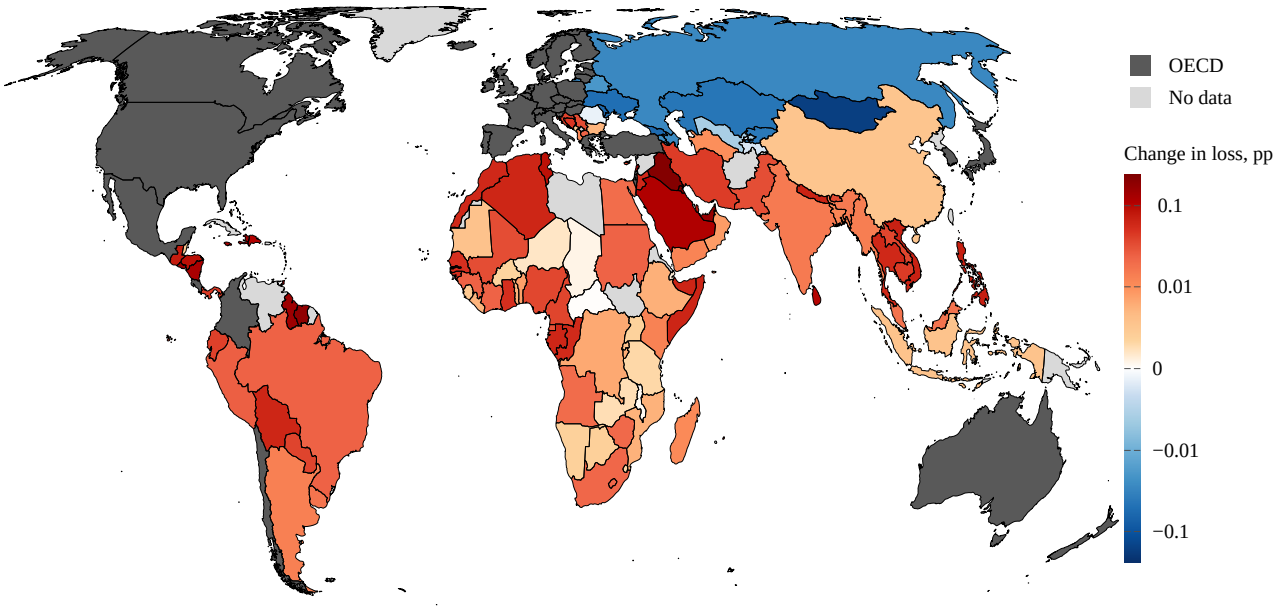

Notes: The map shades each origin outside the OECD by the change in its climate loss under the temporary freeze, $D^o_P - D^o$, in percentage points of permanent consumption. Origins whose loss rises are red and origins whose loss falls are blue, on a scale that is logarithmic on each side of zero. OECD members are shaded dark gray.

adds another 0.16% of the no-policy loss. Figure 11 shows the two phases for all origins and for the Caribbean and Central America. Panel (a) shows that the number of immigrants in the OECD remains below its no-policy level for decades after the policy is lifted, and panel (b) shows that the climate loss decays with the population gap.

Figure 11: Restricting Immigration into the OECD

(a) Immigrants living in the OECD

(b) Change in climate loss

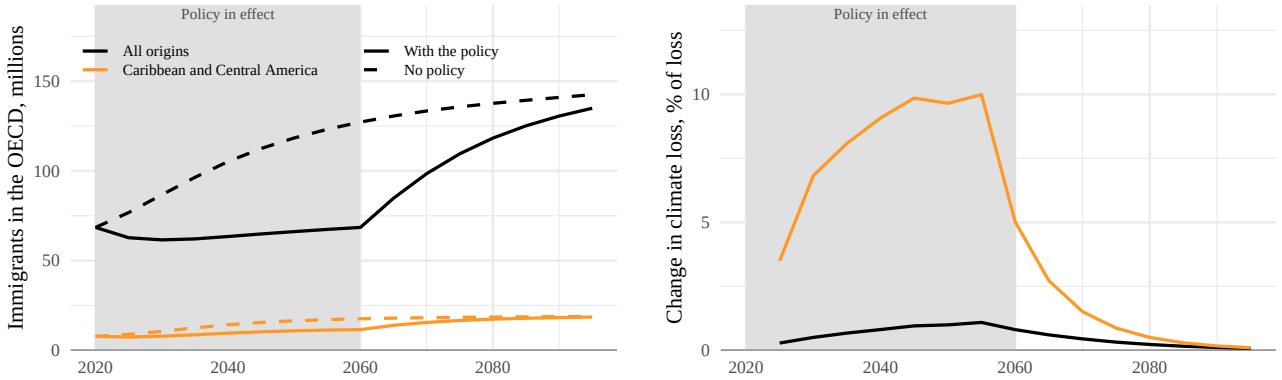

Notes: Both panels are for the temporary immigration freeze, and the shaded area is the policy window, 2020 to 2060. Black lines are all origins outside the OECD and orange lines are the Caribbean and Central America. Panel (a) plots the number of people from the group living in the OECD, in millions, with the freeze in solid lines and without it in dashed lines. Panel (b) plots the change from no policy in the group's climate loss that falls in one five-year period, in percent of the group's climate loss in that period without the policy. All statistics are population weighted.

6.2 Easing immigration restrictions

The second counterfactual policy we consider is a global easing of the immigration restrictions. In Table 4, we find that immigration restrictions in the form of visa requirements contribute 0.49 log points, or 6%, of the median residence cost. The remainder of the residence cost reflects more fundamental origin and destination characteristics such as distance, language, and institutions. We therefore consider two experiments. The first is a visa waiver, where we remove the estimated cost of a visa requirement from all corridors in which the destination requires a visa for households from that origin in the DEMIG data. This amounts to relaxing residence costs on 56% of migration corridors. The second type of policy we consider is a uniform reduction in residence costs of 5% and 10%. This policy represents a general easing of entry rules globally. We assume both policies are permanent, so residence costs fall in 2020 and remain at the lower level in every later period. In all of these counterfactuals, we assume there are no congestion forces, so these gains are an upper bound.

Table 7 reports the effect of the three experiments on climate losses. Each column reports results for one of the three experiments. Similarly to Table 6, Panel A reports global aggregates and the remaining panels report results for specific regions. The first two rows report the change in the climate loss, $D_P^o - D^o$, in percentage points of permanent consumption and in percent of the no-policy loss D^o. The third row reports the change in welfare, $(1-\beta)(P^o - W^o)$, in percentage points of permanent consumption. The fourth row reports the share of the change in the climate loss due to network amplification, the difference in utility when the network held at its no-policy path with the same cut in residence costs. The last row reports the number of people living in a different country in 2095 than they would without the policy.

Relaxing immigration restrictions reduces climate losses by only a small amount on average. We estimate that the visa waiver lowers the average household's climate loss by 0.032 percentage points of consumption, or 0.64% of the no-policy loss. The effect is between the reductions from the 5 and the 10% uniform cuts in residence costs. Network amplification accounts for a significant share of these changes. Even though the average reductions in climate losses are small, they imply very large population movements, with between 107 and 244 million additional people living in a different country by 2095. The waiver raises the welfare of the average household by 3.11 percentage points of permanent consumption, and 3.07 points of this gain remain in a world without climate change. The main effect of relaxing visa requirements is therefore increased migration from low- to high-income countries, and some of these high-income destinations are also projected to experience large climate losses.

The small reduction on average masks the fact that the effect of the policy on climate losses is heterogeneous. Figure 12 maps the change in climate losses from the visa waiver for each origin. The visa waiver policy reduces an origin's climate loss when the destinations that require a visa are less exposed to warming than the origin, and raises it when those destinations are more exposed or when the origin itself gains from warming. The gains from the policy are largest in the Caribbean and Central America, where the waiver lowers climate losses by 4.84%, followed by the Middle East

Table 7: Easing Immigration Restrictions

	Visa waiver	Uniform cut in residence costs	
		5 percent	10 percent
Panel A. All origins (2.8% of origin population living abroad in 2020)			
Change in climate loss, $D_P^o - D^o$, pp of consumption	−0.032	−0.024	−0.057
Change in climate loss, % of D^o	−0.64	−0.48	−1.13
Change in welfare, pp of consumption	3.11	2.61	5.91
Share due to network amplification, %	65.2	70.5	73.6
Additional migration by 2095, millions	131	107	244
Panel B. Caribbean and Central America (12.0% of origin population living abroad in 2020)			
Change in climate loss, $D_P^o - D^o$, pp of consumption	−0.248	−0.086	−0.176
Change in climate loss, % of D^o	−4.84	−1.68	−3.43
Change in welfare, pp of consumption	15.6	5.27	11.1
Share due to network amplification, %	41.9	51.1	51.3
Additional migration by 2095, millions	4.7	1.7	3.6
Panel C. Middle East and North Africa (4.3% of origin population living abroad in 2020)			
Change in climate loss, $D_P^o - D^o$, pp of consumption	−0.143	−0.072	−0.157
Change in climate loss, % of D^o	−2.37	−1.19	−2.60
Change in welfare, pp of consumption	8.05	4.62	10.2
Share due to network amplification, %	62.8	66.1	67.8
Additional migration by 2095, millions	23.2	12.4	27.0
Panel D. Sub-Saharan Africa (2.2% of origin population living abroad in 2020)			
Change in climate loss, $D_P^o - D^o$, pp of consumption	−0.067	−0.053	−0.125
Change in climate loss, % of D^o	−0.87	−0.69	−1.63
Change in welfare, pp of consumption	2.90	2.61	5.96
Share due to network amplification, %	71.5	71.6	74.7
Additional migration by 2095, millions	41.4	38.1	87.2

Notes: Each column is one permanent easing of residence costs from 2020. The visa waiver removes the estimated cost of a visa requirement from every corridor that requires a visa in the DEMIG data. The uniform cuts lower the residence cost of every open corridor by 5 and by 10 percent. Rows report, for the origins in each panel, the change in the climate loss D^o of (16) caused by the policy, in percentage points of permanent consumption and in percent of the no-policy loss, the change in lifetime welfare with climate change in percentage points of permanent consumption, the share of the change in the climate loss that disappears when the network term in utility is held on its no-policy path with the same cut in costs, and the number of people living in a different country in 2095 than they would without the policy. Panel titles give the share of each panel's population living abroad in 2020. All numbers are population weighted.

and North Africa at 2.37% and Sub-Saharan Africa at 0.87%.[29]

The uniform cuts show the same ranking across regions. By 2095 the waiver moves 41 million people from Sub-Saharan Africa, 23 million from the Middle East and North Africa, and 5 million from the Caribbean and Central America.

6.3 Climate visas

The third counterfactual policy we consider is a global climate visa program. No country is currently obliged to admit people displaced by climate change. UN climate negotiations have not yet

[29] Losses rise in Egypt, Jordan, Yemen, Nepal, and Bangladesh, where the destinations that require a visa are mainly the Gulf states. The Gulf states lose 26% of output to warming by 2095, against 13 to 20% in these origins, so the waiver moves their households toward destinations with higher climate losses.

Figure 12: Change in Climate Loss from the Visa Waiver

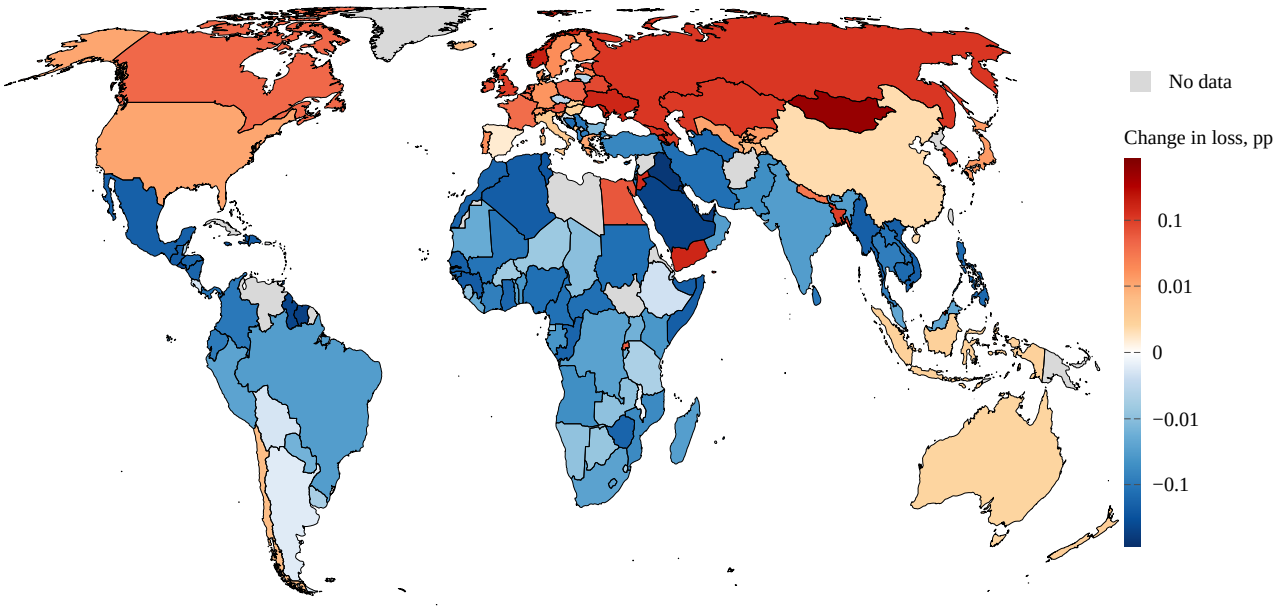

Notes: The map shades each origin by the change in its climate loss under the visa waiver, $D_P^o - D^o$, in percentage points of permanent consumption. Origins whose loss rises are red and origins whose loss falls are blue.

produced a comprehensive climate migration policy (UNFCCC, 2010; UNFCCC, 2015). The only active climate migration programs are quite small.[30] There are, however, potential benefits for wealthy countries that participate in such a program. Many rich countries that are expected to be climate winners face aging populations, shrinking labor forces, and underfunded pension systems (OECD, 2023). Admitting additional working-age immigrants from the countries most exposed to climate change would both ease these challenges and reduce the global welfare losses from climate change.

Our proposed visa program is designed to move households from poor origins with large projected climate losses to rich destinations with projected gains from warming. Figure 13(a) maps the proposed origins and the destinations for our climate visa program. The treated origins are Sudan, Niger, Chad, Mali, Mauritania, Paraguay, Iraq, Burkina Faso, Nigeria, Togo, Benin, Guinea, El Salvador, Guinea-Bissau, Yemen, Senegal. Combined, these countries had a population of 475 million people in 2020, and their average projected loss from climate change is 9.9% of consumption. The destinations are 21 high-income OECD members with a projected gain from warming. In our baseline program, the destinations issue 150,000 visas each year in proportion to their population, the same order of magnitude as the number of refugees resettled worldwide

[30] New Zealand admits 650 Pacific Islanders a year under its Pacific Access Category (Immigration New Zealand, 2026). Australia admits up to 3,000 a year under its Pacific Engagement Visa (Department of Home Affairs, 2026) and up to 280 Tuvaluans a year under its treaty with Tuvalu, which names the existential threat of climate change (DFAT, 2023; Prime Minister of Australia, 2024). Majumdar (2025) imagines a near future in which such programs are the main route out of climate-stricken countries.

annually.

This is a permanent policy, and we assume visa holders reside in the destination permanently. We also assume that the destinations introduce no immigration restrictions alongside the program, so additional migrants are able to relocate as the diaspora in these destinations grows. Figure 13(b) plots, over time, the number of people from the treated origins who live in the destinations because of the program. It distinguishes between visa holders and migrants who move because of network amplification. We estimate that by 2095 the program would move 12.0 million people to the destinations directly through visas, and an additional 21.4 million people would migrate because of the network effect. This is an amplification of roughly 1.8 migrants for every visa holder.

Figure 13: Climate Visas

(a) Treated origins and destinations

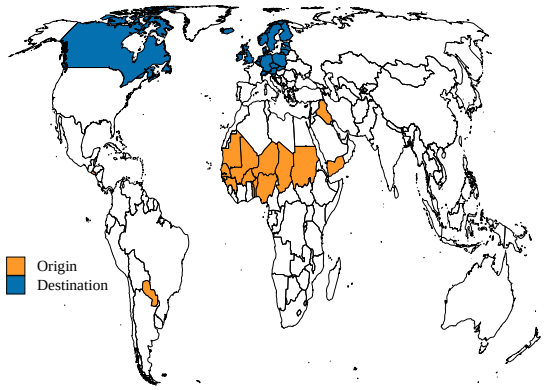

(b) Visa holders and network amplification

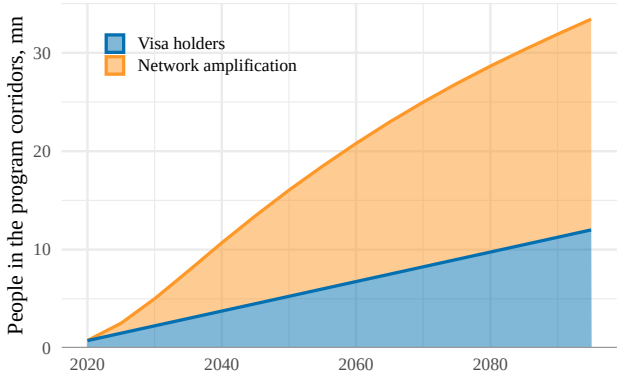

Notes: Panel (a) maps the origins (orange) and destinations (blue), selected as described in the text. Panel (b) plots the number of visa holders living in the destinations and the number of additional migrants due to network amplification in millions, for the baseline program of 150 visas per year launched in 2020.

Table 8 reports the effect of the visa program on the climate losses of the treated origins, together with more detailed statistics on migration. We report results for the baseline program and six other visa program sizes ranging from 15 thousand to 1.5 million visas a year. Panel A reports the effect on the treated origins' climate loss. The first two rows report the change in the loss, $D^o_P - D^o$, in percentage points of consumption and in percent of the no-policy loss. The third row reports the change in welfare of the households from o that do not receive a visa, in percentage points of consumption. The fourth row reports the share of the change in the climate loss due to network amplification, the part that disappears when the network term in utility is held on its no-policy path and the same visas are issued. Panel B reports more statistics on migration by 2095. It lists the annual quota as a share of each destination's population, the number of visa holders, the additional migrants added by network amplification, and the share of new migrants in the population of the origins and of the average destination.

The program has small effects on climate losses because it moves only a small share of the origins' population. The headline program reduces the treated origins' losses by 2.61%, or 0.258 percentage points of consumption. By 2095, its visa holders and the migrants who follow them are

Table 8: Climate Visas, by Program Size

	Visas a year, thousands						
	15	38	75	150	375	750	1,500
Panel A. Climate loss of the treated origins							
Change in climate loss, $D^o_P - D^o$, pp of consumption	−0.113	−0.142	−0.184	−0.258	−0.451	−0.735	−1.25
Change in climate loss, % of D^o	−1.15	−1.44	−1.86	−2.61	−4.57	−7.44	−12.6
Change in welfare, pp of consumption	1.00	1.38	1.87	2.67	4.52	6.95	11.0
Share due to network amplification, %	93.6	87.4	80.5	72.2	60.2	51.2	42.5
Panel B. Migration by 2095							
Annual quota, % of destination population	0.005	0.011	0.023	0.045	0.114	0.227	0.455
Visa holders, millions	1.2	3.0	6.0	12.0	30.0	60.0	120
Network amplification, millions	9.0	11.7	15.4	21.4	34.9	51.8	77.2
Program migrants, % of origin population	0.52	0.75	1.09	1.70	3.31	5.70	10.1
Program migrants, % of destination population	2.65	3.85	5.62	8.83	17.4	30.3	53.9

Notes: Each column is the climate visa program at one size, the number of visas issued each year across all destinations. The fourth column is the baseline program. Panel A reports, for the treated origins, the change in the climate loss D^o of (16) in percentage points of consumption and in percent of the no-policy loss, the change in lifetime welfare with climate change of the households without a visa in percentage points of consumption, and the share of that change in the climate loss due to network amplification. Panel B reports the annual quota in percent of each destination's population, the visa holders and the migrants added by network amplification in millions, and the two together in percent of the origins' population and of the average destination's population. All numbers are population weighted.

only 1.70% of the origins' population. Larger programs undo more of the loss, but the reduction rises much less than in proportion to the number of visas. The largest program, 1.5 million visas a year, reduces the losses by 12.6%, and by 2095 its migrants are 10.1% of the origins' population and 53.9% of the average destination's population. A program large enough to change climate losses meaningfully must dramatically change the composition of the destination countries' populations.

Network amplification accounts for 72.2% of the headline reduction and 93.6% of the reduction from the smallest program. Network amplification accounts for a larger share of total migrants for the smallest program because the network term is concave in the diaspora. Therefore a visa program that grows a tiny diaspora community will generate more migrants per visa issued than a larger program. The amplification rests on three assumptions. The destinations do not respond to the program with new restrictions, households respond to the new diasporas with the parameter values of the baseline economy, and corridors that hold no migrants in 2020 open at the residence cost predicted by the gravity regression in Table 4.

The third row of Panel A shows that the program also generates large welfare gains, most of which do not come from its effect on climate losses. A household in the treated origins that does not receive a visa gains the equivalent of 2.67 percentage points of consumption in every period under the headline program, an order of magnitude more than the program's effect on its climate loss. Without climate change the same household would still gain 2.48 points. Most of the program's value therefore comes from the option value of moving to a high-income destination, rather than from a reduction in climate losses.

Delaying program implementation is costly because it delays the growth of the network. Figure

14(a) plots the reduction in the treated origins' climate loss in each period for the same baseline program launched in 2020, 2030, 2040, 2050, and 2060. A program launched in 2030 reduces the treated origins' lifetime losses by 15% less than one launched in 2020, and one launched in 2040 by 28% less. Forgone network growth accounts for 65% of the benefit lost by a 2040 launch. Fewer visa holders are placed before the decades in which climate damages are projected to be largest, so the effect of the holders themselves falls by 35%.

An alternative way to measure the cost of delayed program implementation is how many more visas would have to be issued to achieve the same reduction in climate losses. Figure 14(b) reports the number of visas a year that a program launched in each year must issue to match the 2020 launch on the baseline program of 150,000 visas a year. A program launched in 2030 must issue 201 thousand visas a year, one launched in 2040 must issue 274 thousand, and one launched in 2050 must issue 384 thousand, 2.6 times as many as the 2020 program. Part of this increase only keeps the total number of visas equal over a shorter window, the dashed line in the figure, which reaches 240 thousand a year for a 2050 launch. The remaining 144 thousand a year compensate for the amplification the later program forgoes, because its visa holders have fewer decades in which to draw further households.

Figure 14: Cost of Delayed Policy Implementation

(a) Reduction in climate loss, by launch year

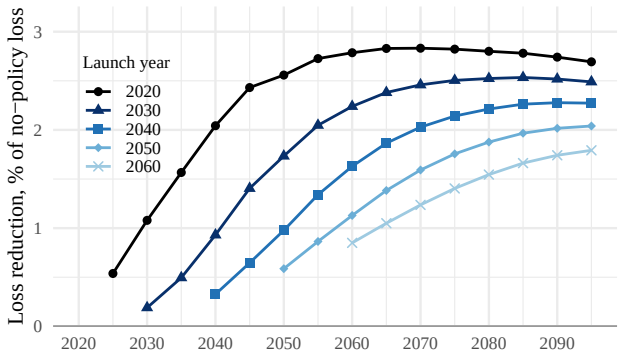

(b) Additional annual visas to match a 2020 launch

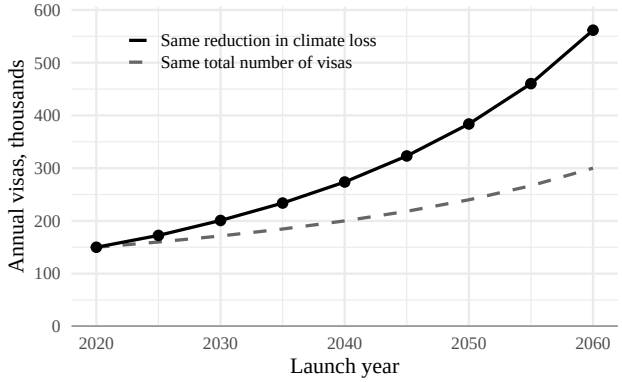

Notes: Panel (a) plots, for a program of 150 thousand visas a year launched in 2020, 2030, 2040, 2050, and 2060, the reduction in the treated origins' climate loss in percent of the no-policy climate loss in that period. Panel (b) plots, for each launch year, the number of visas a year that a program launched in that year must issue to reduce the treated origins' lifetime climate loss by as much as the program of 150 thousand visas a year launched in 2020, in thousands. The dashed line shows the number of visas a year that would result in the same total number of visas as the 2020 program over the shorter policy window.

7. Conclusion

Whether migration will help people adapt to climate change depends not only on how many move but on where they go. Our estimates show that migrant networks raise the welfare cost of climate change for origins home to 64 percent of the world's population. Relative to an economy in which

migrant networks do not affect migration choices, the network raises the average climate loss by the equivalent of 0.7°C of additional warming by the end of the century. Because new migrants follow the diaspora and diasporas are located in climates similar to their origins, the network steers new migrants toward destinations that face the same warming as the origin. Nearly all of this increase can be explained by the spatial covariance between current diasporas and projected climate losses. We find that with the migrant network, climate losses are nearly identical to those in an economy with no migration.

Our results suggest that models without migrant networks significantly understate the welfare cost of global warming. Spatial models of climate change find that migration substantially reduces the welfare cost of warming (Desmet and Rossi-Hansberg, 2015; Bilal and Rossi-Hansberg, 2023; Conte, 2026; Cruz and Rossi-Hansberg, 2024; Bearpark et al., 2025). For tractability, these models treat households as anonymous, so a household that migrates becomes identical to the residents of its new location. We show that migrant networks are straightforward to add to this class of models and are quantitatively important. In our model, the network eliminates 92 percent of the reduction in climate losses that migration would otherwise provide. Researchers should therefore be cautious in using these models to produce estimates of the social cost of carbon.

The same force that raises the cost of climate change also makes migration policy a more effective tool for climate adaptation. However, the gains from programs on the scale of current UN refugee resettlement remain small. In our targeted climate visa counterfactual, OECD members that gain from warming issue 150,000 visas a year to households from the poor origins with the largest projected climate losses. The program reduces the climate losses of these origins by only 2.61 percent. Most of this reduction comes from network amplification of the program. New migrants who are drawn by the larger diasporas in these destinations account for 72.2 percent of the effect of the policy.

Our results suggest that, if countries can agree on a global climate visa program, the most effective version would be implemented as soon as possible, target origins with large climate losses and small diasporas, and be as large as is politically feasible. Because migrant networks take time to grow, in our model, a decade of policy delay forfeits 15 percent of the program's reduction in climate losses. Targeting origins with large projected losses raises the climate loss that each migrant avoids. Because the network term is concave in the diaspora, each visa draws the most additional migrants where the origin's diaspora in the destination is small. The reduction in climate losses rises from 2.61 percent at 150,000 visas a year to 12.6 percent at 1.5 million visas a year. Because no international agreement currently obliges countries to admit people displaced by climate change (UNFCCC, 2010, 2015; United Nations General Assembly, 2018), the scale of such a program will depend on the political constraints faced by visa-issuing countries.

Finally, our results point to two directions for future research. First, using migrant stocks observed at a five-year frequency, we show that migrant networks are adapting slowly to global warming. Data at this frequency cannot reveal whether networks facilitate short-run migration after a large climate shock such as a flood. Annual bilateral flows, with information on return and

onward moves, would allow researchers to measure the value of the diaspora as insurance after a shock. Second, our damage functions, like most in the literature, map annual average temperature into output. Extreme events such as hurricanes, droughts, and floods are likely to account for a large share of climate damages and of climate-related displacement (Hornbeck, 2012; Gröger and Zylberberg, 2016; Mahajan and Yang, 2020; Aron-Dine, 2025). Better data or new methods are needed to estimate damage functions for these extremes and their spatial covariance.

References

Abel, Guy J. and Joel E. Cohen, "Bilateral international migration flow estimates for 200 countries," *Scientific Data*, June 2019, *6*, 82.

Abramitzky, Ran, Leah Platt Boustan, and Katherine Eriksson, "A Nation of Immigrants: Assimilation and Economic Outcomes in the Age of Mass Migration," *Journal of Political Economy*, 2014, *122* (3), 467–506.

Allen, Treb and Dave Donaldson, "Persistence and Path Dependence in the Spatial Economy," Working Paper 28059, National Bureau of Economic Research November 2020. Revised November 2022.

_ , Costas Arkolakis, and Yuta Takahashi, "Universal Gravity," *Journal of Political Economy*, 2020, *128* (2), 393–433.

Altonji, Joseph G. and David Card, "The Effects of Immigration on the Labor Market Outcomes of Less-Skilled Natives," in John M. Abowd and Richard B. Freeman, eds., *Immigration, Trade, and the Labor Market*, University of Chicago Press, 1991, pp. 201–234.

Angelucci, Manuela, "Migration and Financial Constraints: Evidence from Mexico," *Review of Economics and Statistics*, 2015, *97* (1), 224–228.

Aron-Dine, Shifrah, "Rebuild or Relocate? Recovery after Natural Disasters," 2025. Working paper.

_ , "Natural Disaster Expectations and Household Adaptation," *AEA Papers and Proceedings*, May 2026, *116*, 527–531.

Balboni, Clare, "In Harm's Way? Infrastructure Investments and the Persistence of Coastal Cities," *American Economic Review*, 2025, *115* (1), 77–116.

_ and Joseph S. Shapiro, "Spatial Environmental Economics," in Dave Donaldson and Stephen J. Redding, eds., *Handbook of Regional and Urban Economics*, Vol. 6, Elsevier, 2025, pp. 585–652.

Barbosa-Alves, Mauricio and Braulio Britos, "Climate Change and International Migration," 2025. Working paper, May 2025.

Barreca, Alan, Olivier Deschenes, and Melanie Guldi, "Maybe Next Month? Temperature Shocks and Dynamic Adjustments in Birth Rates," *Demography*, 2018, *55* (4), 1269–1293.

Bartel, Ann P., "Where Do the New U.S. Immigrants Live?," *Journal of Labor Economics*, 1989, *7* (4), 371–391.

Bayer, Patrick, Stephen L. Ross, and Giorgio Topa, "Place of Work and Place of Residence: Informal Hiring Networks and Labor Market Outcomes," *Journal of Political Economy*, December 2008, *116* (6), 1150–1196.

Bazzi, Samuel, "Wealth Heterogeneity and the Income Elasticity of Migration," *American Economic Journal: Applied Economics*, 2017, *9* (2), 219–255.

Beaman, Lori A., "Social Networks and the Dynamics of Labour Market Outcomes: Evidence from Refugees Resettled in the U.S.," *The Review of Economic Studies*, January 2012, *79* (1), 128–161.

Bearpark, Tom, Aditya Bhandari, and Jordan Rosenthal-Kay, "The Economic Geography of Climate Risk," 2025. Working paper, November 2025.

Beine, Michel and Christopher Parsons, "Climatic Factors as Determinants of International Migration," *Scandinavian Journal of Economics*, 2015, *117* (2), 723–767.

_ and Christopher R. Parsons, "Climatic factors as determinants of international migration: Redux," *CESifo Economic Studies*, 2017, *63* (4), 386–402.

_ , Frédéric Docquier, and Çağlar Özden, "Diasporas," *Journal of Development Economics*, 2011, *95* (1), 30–41.

Bilal, Adrien and Diego R. Känzig, "The Macroeconomic Impact of Climate Change: Global Versus Local Temperature," *Quarterly Journal of Economics*, 2026, *141* (2), 889–944.

_ and Esteban Rossi-Hansberg, "Anticipating Climate Change Across the United States," Working Paper 31323, National Bureau of Economic Research June 2023.

Bisin, Alberto and Thierry Verdier, "The Economics of Cultural Transmission and Socialization," in "Handbook of Social Economics," Vol. 1, Elsevier, 2011, pp. 339–416.

Blumenstock, Joshua E., Guanghua Chi, and Xu Tan, "Migration and the Value of Social Networks," *The Review of Economic Studies*, January 2025, *92* (1), 97–128.

Borusyak, Kirill and Peter Hull, "Nonrandom Exposure to Exogenous Shocks," *Econometrica*, 2023, *91* (6), 2155–2185.

_ , Rafael Dix-Carneiro, and Brian K. Kovak, "Understanding Migration Responses to Local Shocks," NBER Working Paper 35921, National Bureau of Economic Research 2026.

Bryan, Gharad, Shyamal Chowdhury, and Ahmed Mushfiq Mobarak, "Underinvestment in a Profitable Technology: The Case of Seasonal Migration in Bangladesh," *Econometrica*, 2014, *82* (5), 1671–1748.

Burchardi, Konrad B., Thomas Chaney, and Tarek A. Hassan, "Migrants, Ancestors, and Foreign Investments," *The Review of Economic Studies*, 2019, *86* (4), 1448–1486.

Burke, Marshall, Solomon M. Hsiang, and Edward Miguel, "Global non-linear effect of temperature on economic production," *Nature*, October 2015, *527*, 235–239.

Burzyński, Michał, Christoph Deuster, Frédéric Docquier, and Jaime de Melo, "Climate Change, Inequality, and Human Migration," *Journal of the European Economic Association*, 2022, *20* (3), 1145–1197.

Card, David, "Immigrant Inflows, Native Outflows, and the Local Labor Market Impacts of Higher Immigration," *Journal of Labor Economics*, 2001, *19* (1), 22–64.

Carleton, Tamma A., Esther Duflo, B. Kelsey Jack, and Guglielmo Zappalà, "Adaptation to climate change," in Lint Barrage and Solomon Hsiang, eds., *Handbook of the Economics of Climate Change*, Vol. 1, Elsevier, 2024, pp. 143–248.

Carleton, Tamma, Amir Jina, Michael Delgado, Michael Greenstone, Trevor Houser, Solomon Hsiang, Andrew Hultgren, Robert E. Kopp, Kelly E. McCusker, Ishan Nath, James Rising, Ashwin Rode, Hee Kwon Seo, Arvid Viaene, Jiacan Yuan, and Alice Tianbo Zhang, "Valuing the Global Mortality Consequences of Climate Change Accounting for Adaptation Costs and Benefits," *The Quarterly Journal of Economics*, 2022, *137* (4), 2037–2105.

Carrington, William J., Enrica Detragiache, and Tara Vishwanath, "Migration with Endogenous Moving Costs," *American Economic Review*, September 1996, *86* (4), 909–930.

Castro-Vincenzi, Juanma, "Climate Hazards and Resilience in the Global Car Industry," 2024. Working paper, June 2024.

_ , Gaurav Khanna, Nicolas Morales, and Nitya Pandalai-Nayar, "Weathering the Storm: Supply Chains and Climate Risk," NBER Working Paper 32218 March 2024. Revised September 2025.

Cattaneo, Cristina and Giovanni Peri, "The Migration Response to Increasing Temperatures," *Journal of Development Economics*, 2016, *122*, 127–146.

Conte, Bruno, "Climate Change and Migration: The Case of Africa," *Journal of the European Economic Association*, 2026.

_ , Klaus Desmet, Dávid Krisztián Nagy, and Esteban Rossi-Hansberg, "Local Sectoral Specialization in a Warming World," *Journal of Economic Geography*, 2021, *21* (4), 493–530.

Cruz, José-Luis and Esteban Rossi-Hansberg, "The Economic Geography of Global Warming," *The Review of Economic Studies*, 2024, *91* (2), 899–939.

Czaika, Mathias, Hein de Haas, and María Villares-Varela, "The Global Evolution of Travel Visa Regimes," *Population and Development Review*, 2018, *44* (3), 589–622.

Dell, Melissa, Benjamin F. Jones, and Benjamin A. Olken, "Temperature Shocks and Economic Growth: Evidence from the Last Half Century," *American Economic Journal: Macroeconomics*, 2012, *4* (3), 66–95.

Dellink, Rob, Jean Château, Elisa Lanzi, and Bertrand Magné, "Long-term economic growth projections in the Shared Socioeconomic Pathways," *Global Environmental Change*, 2017, *42*, 200–214.

DEMIG, "DEMIG VISA, Version 1.4, Online Edition," International Migration Institute, University of Oxford 2015.

Deryugina, Tatyana, Laura Kawano, and Steven Levitt, "The Economic Impact of Hurricane Katrina on Its Victims: Evidence from Individual Tax Returns," *American Economic Journal: Applied Economics*, 2018, *10* (2), 202–233.

Desmet, Klaus and Esteban Rossi-Hansberg, "On the Spatial Economic Impact of Global Warming," *Journal of Urban Economics*, 2015, *88*, 16–37.

_ and _ , "Climate Change Economics over Time and Space," *Annual Review of Economics*, 2024, *16*, 271–304.

_ , Dávid Krisztián Nagy, and Esteban Rossi-Hansberg, "The Geography of Development," *Journal of Political Economy*, 2018, *126* (3), 903–983.

_ , Robert E. Kopp, Scott A. Kulp, Dávid Krisztián Nagy, Michael Oppenheimer, Esteban Rossi-Hansberg, and Benjamin H. Strauss, "Evaluating the Economic Cost of Coastal Flooding," *American Economic Journal: Macroeconomics*, 2021, *13* (2), 444–486.

Dingel, Jonathan I. and Kyle C. Meng, "Spatial Correlation, Trade, and Inequality: Evidence from the Global Climate," *Review of Economics and Statistics*, 2026, pp. 1–46.

Doepke, Matthias, Anne Hannusch, Fabian Kindermann, and Michèle Tertilt, "The Economics of Fertility: A New Era," in "Handbook of the Economics of the Family," Vol. 1, Elsevier, 2023, pp. 151–254.

Edin, Per-Anders, Peter Fredriksson, and Olof Åslund, "Ethnic Enclaves and the Economic Success of Immigrants—Evidence from a Natural Experiment," *The Quarterly Journal of Economics*, February 2003, *118* (1), 329–357.

Gröger, André and Yanos Zylberberg, "Internal Labor Migration as a Shock Coping Strategy: Evidence from a Typhoon," *American Economic Journal: Applied Economics*, 2016, *8* (2), 123–153.

Grossman, Gene M., Elhanan Helpman, and Hugo Lhuillier, "Supply Chain Resilience: Should Policy Promote International Diversification or Reshoring?," *Journal of Political Economy*, 2023, *131* (12), 3462–3496.

Hoffmann, Roman, Anna Dimitrova, Raya Muttarak, Jesús Crespo Cuaresma, and Jonas Peisker, "A Meta-Analysis of Country-Level Studies on Environmental Change and Migration," *Nature Climate Change*, 2020, *10* (10), 904–912.

Hornbeck, Richard, "The Enduring Impact of the American Dust Bowl: Short- and Long-Run Adjustments to Environmental Catastrophe," *American Economic Review*, 2012, *102* (4), 1477–1507.

Intergovernmental Panel on Climate Change, *Climate Change 2022: Impacts, Adaptation and Vulnerability. Working Group II Contribution to the Sixth Assessment Report of the IPCC*, Cambridge, UK and New York, NY: Cambridge University Press, 2022.

International Institute for Applied Systems Analysis, "SSP Scenario Explorer, basic drivers," https://ssp.apps.ece.iiasa.ac.at 2025. GDP from OECD ENV-Growth 2025, population from IIASA-WiC POP 2025.

Jessoe, Katrina, Dale T. Manning, and J. Edward Taylor, "Climate Change and Labour Allocation in Rural Mexico: Evidence from Annual Fluctuations in Weather," *The Economic Journal*, 2018, *128* (608), 230–261.

Kazianga, Harounan and Christopher Udry, "Consumption Smoothing? Livestock, Insurance and Drought in Rural Burkina Faso," *Journal of Development Economics*, 2006, *79* (2), 413–446.

Kelley, Colin P., Shahrzad Mohtadi, Mark A. Cane, Richard Seager, and Yochanan Kushnir, "Climate Change in the Fertile Crescent and Implications of the Recent Syrian Drought," *Proceedings of the National Academy of Sciences*, 2015, *112* (11), 3241–3246.

Krusell, Per and Anthony A. Smith Jr., "Climate Change Around the World," Working Paper 30338, National Bureau of Economic Research 2022.

Kucheryavyy, Konstantin, Gary Lyn, and Andrés Rodríguez-Clare, "Grounded by Gravity: A Well-Behaved Trade Model with Industry-Level Economies of Scale," *American Economic Journal: Macroeconomics*, 2023, *15* (2), 372–412.

Lagakos, David, Ahmed Mushfiq Mobarak, and Michael E. Waugh, "The Welfare Effects of Encouraging Rural–Urban Migration," *Econometrica*, 2023, *91* (3), 803–837.

Mahajan, Parag and Dean Yang, "Taken by Storm: Hurricanes, Migrant Networks, and US Immigration," *American Economic Journal: Applied Economics*, April 2020, *12* (2), 250–277.

Maher, Nicola, Sebastian Milinski, Laura Suarez-Gutierrez, Michael Botzet, Mikhail Dobrynin, Luis Kornblueh et al., "The Max Planck Institute Grand Ensemble: Enabling the Exploration of Climate System Variability," *Journal of Advances in Modeling Earth Systems*, 2019, *11* (7), 2050–2069.

Mayer, Thierry and Soledad Zignago, "Notes on CEPII's Distances Measures: The GeoDist Database," Working Paper 2011-25, CEPII December 2011.

McKenzie, David and Hillel Rapoport, "Network Effects and the Dynamics of Migration and Inequality: Theory and Evidence from Mexico," *Journal of Development Economics*, 2007, *84* (1), 1–24.

Meghir, Costas, A. Mushfiq Mobarak, Corina Mommaerts, and Melanie Morten, "Migration and Informal Insurance: Evidence from a Randomized Controlled Trial and a Structural Model," *Review of Economic Studies*, 2022, *89* (1), 452–480.

Moore, Will H. and Stephen M. Shellman, "Whither Will They Go? A Global Study of Refugees' Destinations, 1965–1995," *International Studies Quarterly*, 2007, *51* (4), 811–834.

Morten, Melanie, "Temporary Migration and Endogenous Risk Sharing in Village India," *Journal of Political Economy*, 2019, *127* (1), 1–46.

Müller, Ulrich K., James H. Stock, and Mark W. Watson, "An Econometric Model of International Growth Dynamics for Long-Horizon Forecasting," *Review of Economics and Statistics*, 2022, *104* (5), 857–876.

Munshi, Kaivan, "Networks in the Modern Economy: Mexican Migrants in the U.S. Labor Market," *The Quarterly Journal of Economics*, May 2003, *118* (2), 549–599.

_ and Mark Rosenzweig, "Networks and Misallocation: Insurance, Migration, and the Rural–Urban Wage Gap," *American Economic Review*, 2016, *106* (1), 46–98.

Nath, Ishan B., Valerie A. Ramey, and Peter J. Klenow, "How Much Will Global Warming Cool Global Growth?," Working Paper 32761, National Bureau of Economic Research July 2024.

Newell, Richard G., Brian C. Prest, and Steven E. Sexton, "The GDP-Temperature Relationship: Implications for Climate Change Damages," *Journal of Environmental Economics and Management*, 2021, *108*, 102445.

Riahi, Keywan et al., "The Shared Socioeconomic Pathways and their energy, land use, and greenhouse gas emissions implications: An overview," *Global Environmental Change*, 2017, *42*, 153–168.

Rohde, Robert A. and Zeke Hausfather, "The Berkeley Earth Land/Ocean Temperature Record," *Earth System Science Data*, 2020, *12*, 3469–3479.

Rosenzweig, Mark R. and Oded Stark, "Consumption Smoothing, Migration, and Marriage: Evidence from Rural India," *Journal of Political Economy*, 1989, *97* (4), 905–926.

Rudik, Ivan, Gary Lyn, Weiliang Tan, and Ariel Ortiz-Bobea, "The Economic Effects of Climate Change in Dynamic Spatial Equilibrium," 2022. SocArXiv preprint, July 2022.

Schwartzman, Matthew, "Risk Management and Aggregate Migration Flows," 2025. Working paper.

Schwarzwald, Kevin and Nathan Lenssen, "The Importance of Internal Climate Variability in Climate Impact Projections," *Proceedings of the National Academy of Sciences*, 2022, *119* (42), e2208095119.

Seo, Jaeeun and Ryungha Oh, "Sectoral Shocks and Labor Market Dynamics: A Sufficient Statistics Approach," December 2024. Working paper.

Stuart, Bryan A. and Evan J. Taylor, "Migration Networks and Location Decisions: Evidence from US Mass Migration," *American Economic Journal: Applied Economics*, July 2021, *13* (3), 134–175.

UNFCCC, "The Cancun Agreements: Outcome of the Work of the Ad Hoc Working Group on Long-term Cooperative Action under the Convention," 2010. Decision 1/CP.16, paragraph 14(f).

_ , "Adoption of the Paris Agreement," 2015. Decision 1/CP.21, paragraph 49.

United Nations, Department of Economic and Social Affairs, Population Division, "International Migrant Stock 2020: Destination and Origin," Dataset, POP/DB/MIG/Stock/Rev.2020 2021. Accessed 27 July 2026.

United Nations General Assembly, "Global Compact for Safe, Orderly and Regular Migration," 2018. Resolution A/RES/73/195, adopted 19 December 2018.

Supplemental Appendix

A Additional Tables and Figures **57**

A.1 Additional Evidence on Flows–Stocks Relationship 57

A.2 Additional Evidence on Diaspora Climate Exposure 57

B Data **62**

B.1 Data Construction and Limitations 62

B.2 Constructing the Instrument 64

B.3 Examples of Variation Underlying the Instrument 65

C Model Proofs and Derivations **68**

C.1 Proof of Proposition 1: Existence and Uniqueness of Equilibrium 68

C.2 Proof of Proposition 2: Unique Steady State 68

C.3 Proof of Proposition 3: Unique Stationary Distribution 68

C.4 Persistence and Amplification with N Destinations 69

C.5 Second Order Expansion of Welfare 69

D Quantification and Computation **72**

D.1 Differences across Shared Socioeconomic Pathways 72

D.2 The Damage Process 73

D.3 Quantitative Implications of Estimated Network Elasticity 73

D.4 Comparison with Cruz & Rossi-Hansberg (2024) Quantification 74

D.5 Monte Carlo Simulation of Climate Path 75

A. Additional Tables and Figures

A.1 Additional Evidence on Flows–Stocks Relationship

This appendix provides additional evidence on the relationship between migrant stocks and subsequent migration flows documented in Section 2. We first show that the positive relationship is visible in the raw data and is similar across alternative transformations, time periods, and country income groups. We then report alternative estimates that account for the large number of zero bilateral flows.

Figure A1 provides additional evidence on the flows–stocks relationship. Figure A1a plots bilateral flow shares against lagged stock shares. One concern is that this relationship could be driven by the normalization used to construct the shares. Figure A1b therefore plots migrant flows against lagged stocks in levels and shows the same positive relationship. Another concern is that the quality and coverage of the migration data vary across countries and over time. The aggregate relationship could therefore be driven by particular parts of the sample. Figures A1c and A1d plot the relationship separately by year and by UN income group. The positive relationship is present across these subsamples, suggesting that it is not driven by a particular time period or income group.

We also show that our results are robust to including corridors with zero migration flows. Our main specification is estimated in logs using OLS so that the estimates are directly comparable to the 2SLS estimates in Table 1. A limitation of this specification is that bilateral flows are frequently zero and are therefore dropped when taking logs. As a robustness check, we estimate the relationship using Poisson pseudo–maximum likelihood (PPML), which retains zero-flow observations and allows the conditional variance of flows to vary with the covariates.

Table A1 reports the results. As in the OLS specifications, lagged migrant stocks are strongly positively associated with subsequent flows. The estimated elasticity is 0.77 without fixed effects and 0.73 with origin and destination fixed effects, compared with 0.88 and 0.83 in the corresponding OLS specifications. The coefficient falls once origin–destination fixed effects are included, again reflecting the limited within-corridor variation in migrant stocks, but remains positive and precisely estimated. Overall, the positive flows–stocks relationship is not driven by dropping corridors with zero migration flows.

A.2 Additional Evidence on Diaspora Climate Exposure

This appendix provides additional evidence on the relationship between origin-country climate exposure and the exposure of its diaspora. We first show the distributions underlying the averages reported in the main text. We then examine whether the relationship differs across time periods and country income groups, given differences in the coverage and quality of the migration data. Finally, we repeat the analysis using alternative measures of climate exposure.

Figure A2 shows the distributions behind the averages reported in Section 2. Figure A2a plots the distribution of diaspora temperature conditional on origin-country temperature. As origin

Figure A1: Migrant Flows by Migrant Stocks

(a) Flow shares and stock shares

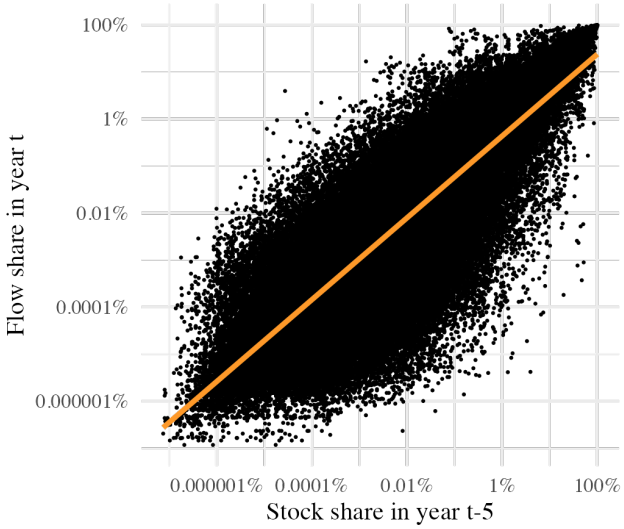

(b) Flows and stocks in levels

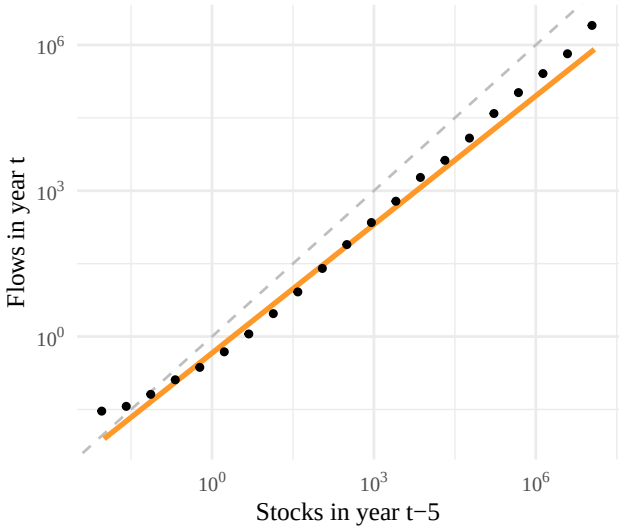

(c) Flow shares and stock shares, by year

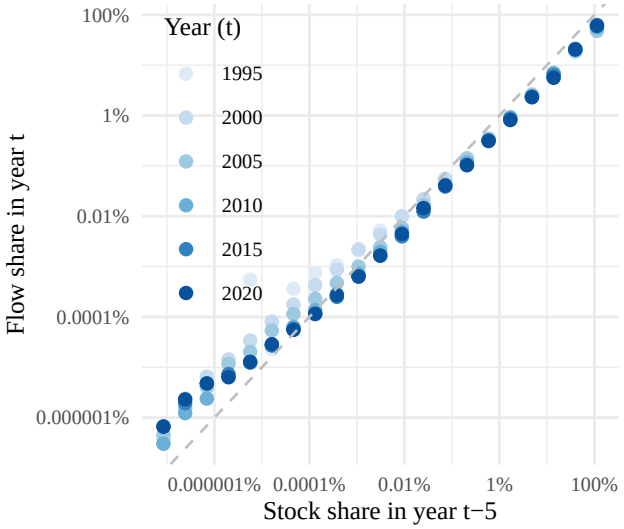

(d) Flow shares and stock shares, by UN income group

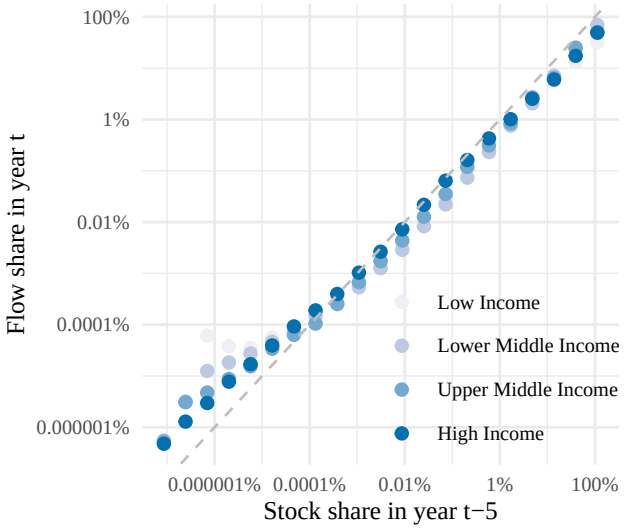

Notes: Migrant stock data are from the UN Global Migration Database and migrant flows are from Abel and Cohen (2019). Panel (a) plots bilateral migrant flow shares against lagged migrant stock shares. Panel (b) plots the same relationship in levels. Panels (c) and (d) report binscatters of flow shares against lagged stock shares separately by year and by UN income group, respectively. The dashed gray line denotes the 45-degree line.

Table A1: Elasticity of Flows to Stocks, PPML Estimates

	(1)	(2)	(3)	(4)	(5)
$\log(\text{stocks}_{od,t-5})$	0.770***	0.731***	0.789***	0.211***	0.183***
	(0.014)	(0.015)	(0.011)	(0.034)	(0.027)
o, d		✓		✓	
$o \times t, d \times t$			✓		✓
$o \times d$				✓	✓

Notes: The table reports PPML estimates of the elasticity of bilateral migration flows with respect to lagged migrant stocks from 1990 to 2020. PPML is estimated in levels and includes observations with zero flows. Migrant stocks are from the UN and gross flows from Abel and Cohen (2019). Standard errors are clustered at the origin–destination pair level. * p<0.05, ** p<0.01, *** p<0.001.

temperature rises, the distribution of diaspora temperature shifts toward higher temperatures. Figure A2b reports the distribution of migrants' distance from their origin by income group. The distribution shifts toward larger distances as origin-country income rises: migrants from low-income countries are concentrated much closer to home, while migrants from middle- and high-income countries are spread over a wider range of distances. Migrants from poorer countries are systematically closer to home across the distribution.

Figure A2: Distribution of Climate Exposure and Geography of Migrant Networks

(a) Climate exposure of origins and their diasporas

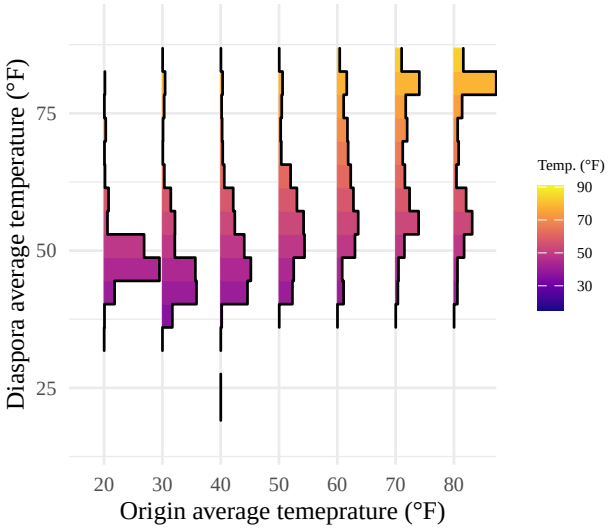

(b) Spatial concentration of migrant networks

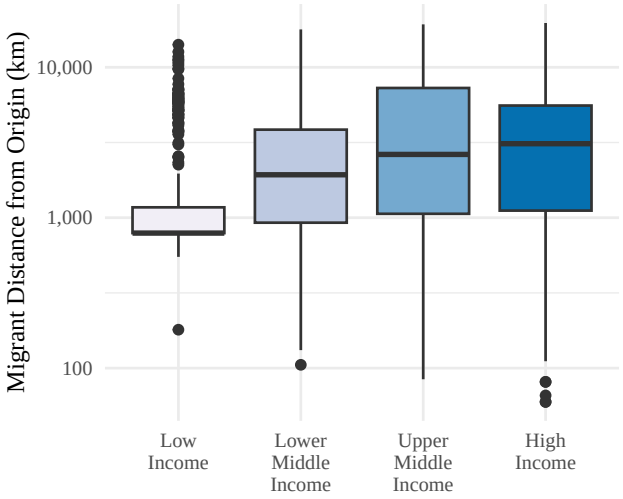

Notes: Panel (a) plots the distribution of diaspora average temperature by origin-country temperature. Origins are grouped by their average temperature, and each vertical histogram shows the distribution of diaspora temperatures for origins in that group. Diaspora temperature is the migrant-stock-weighted average temperature across an origin's destination countries. Colors indicate diaspora temperature in degrees Fahrenheit. Panel (b) plots distribution of migrants' distance from their origin by UN income group. Temperature is from BEST and bilateral distance from GeoDist (Mayer and Zignago, 2011).

The migration data vary in coverage and quality across countries and over time, raising the

possibility that the aggregate relationship is driven by particular parts of the sample. Figure A3 therefore plots the origin–diaspora exposure relationship separately by year and by UN income group. The positive relationship is present across periods and income groups.

Figure A3: Diaspora Network and Origin Country Climate Exposure

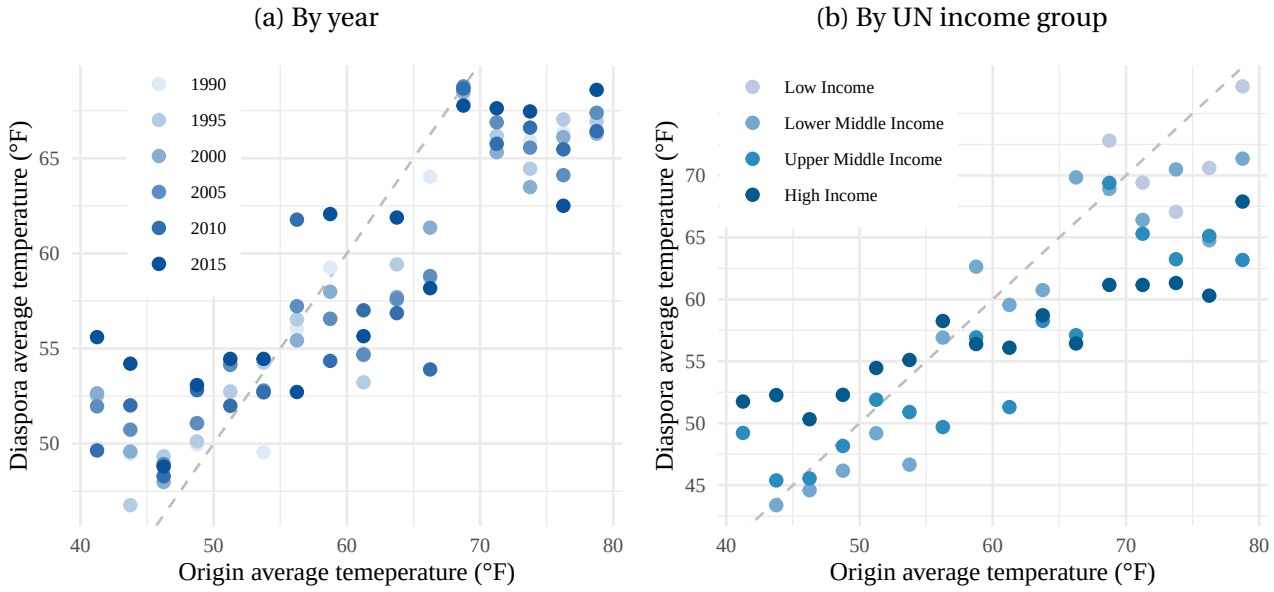

Notes: The figures show a binscatter of the relationship between diaspora exposure against origin exposure. Panel (a) plots relationship by year. Panel (b) plots the same relationship by the UN classifications of income groups. The gray dashed line is the 45-degree line.

Our baseline measure of climate exposure is average temperature. Temperature is measured more consistently across space and time than many other climate variables, particularly precipitation, which varies more sharply across space and is harder to interpolate in areas with sparse station coverage (Dell et al., 2014). Figure A4 shows that the origin–diaspora relationship is not specific to average temperature. We find similar positive relationships using measures of extreme heat, coastal exposure, extreme rainfall, and natural disasters. Appendix B describes the construction and sources of these measures.

Figure A4: Origin–Diaspora Exposure Relationship Under Alternative Climate Measures

(a) Temp. of 10 Hottest Days

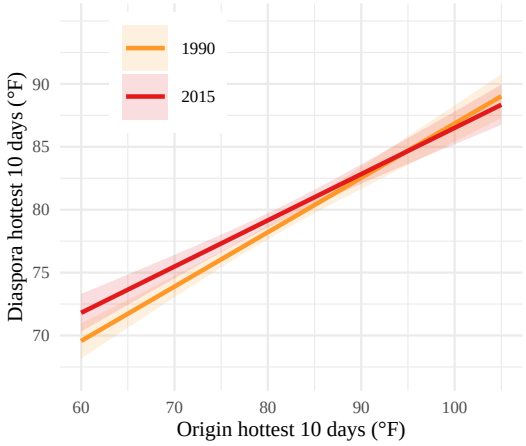

(b) Number of Hot Days

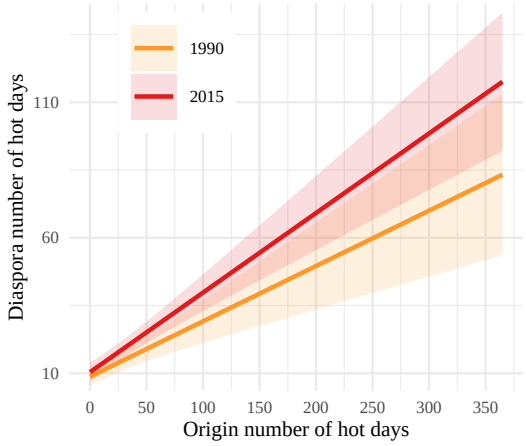

(c) Temp. of Hottest Day, ERA5

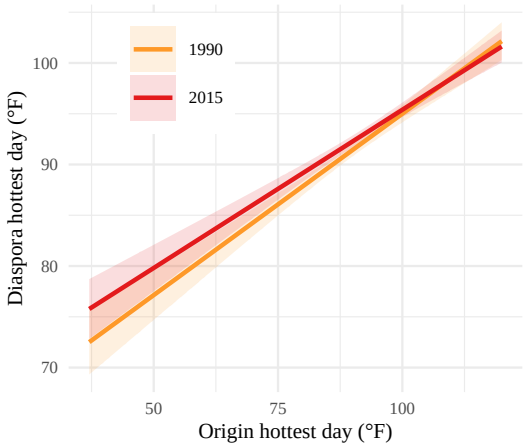

(d) Low-Elevation Coastal Population

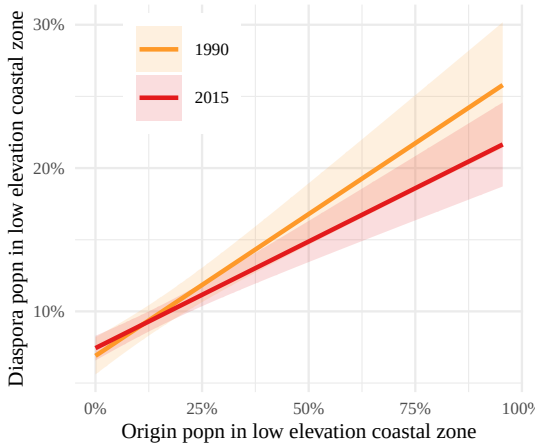

(e) Extreme 1-Day Rainfall

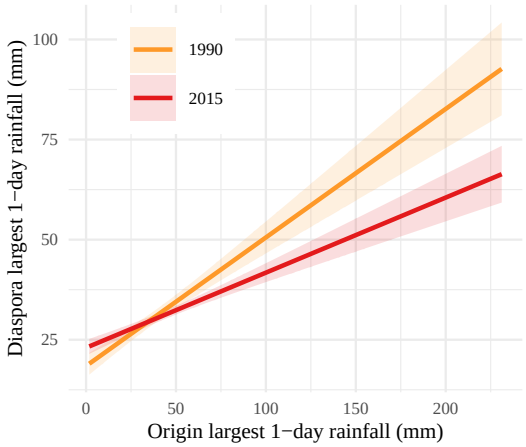

(f) Natural Disaster Count

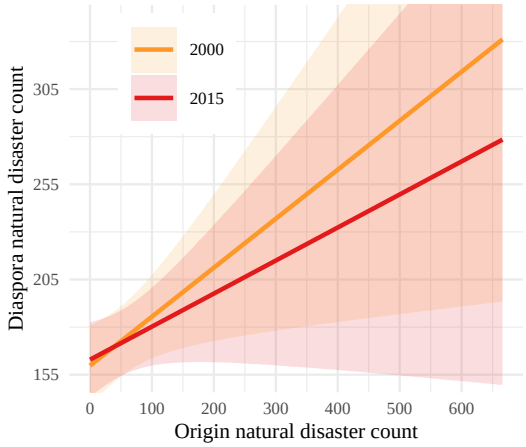

Notes: Each panel relates origin-country climate exposure to the migrant-weighted average exposure of its diaspora. Lines show OLS fitted values using the 1990 network (orange) and 2015 network (red); shaded areas are 95% confidence intervals. Migrant stocks are from the UN Global Migration Database (UNDESA, Population Division, 2021). See Appendix B for variable definitions and data sources.

B. Data

B.1 Data Construction and Limitations

Migrant stocks. The UN global bilateral migration data are constructed through a systematic harmonization of national censuses and population registers across over 200 countries and territories, spanning multiple decades. The harmonization process attempts to address inconsistencies in national data collection methods, definitions of migrants (including distinctions between foreign-born and foreign nationals), and reporting periods, thereby enabling cross-country comparisons and longitudinal analysis.

However, the data have several important limitations and sources of potential systematic measurement error. First, countries vary significantly in how they define and measure migrants for example, birthplace versus citizenship. This distinction is particularly problematic when comparing countries with and without birthright citizenship policies. For instance, a second-generation immigrant born in the United States would not be counted as a migrant under a birthplace definition, whereas the child of immigrants born in Germany (prior to recent reforms) might be counted as foreign even if they have never lived elsewhere. This implies much greater persistence over time in the stock of people from origin-o in Germany than in the United States even if actual migration patterns are similar. Such systematic differences could bias our estimates of migration persistence and network effects across destination countries.

Second, the data are typically drawn from five-year or decennial censuses, which may miss temporary migration episodes and provide limited information on the precise timing of migration. Third, undocumented migrants are systematically undercounted in official statistics, with the degree of undercount likely varying across countries based on enforcement regimes, survey methodology, and migrants' willingness to participate in census activities. Finally, data quality and availability remain particularly limited for developing countries and earlier time periods, potentially biasing our sample toward wealthier destinations and more recent decades. To address concerns about sample composition and data quality, we demonstrate that our main results are robust across different time periods and country income classifications.

Temperature data. We construct country-level temperatures from the Berkeley Earth daily land temperature product (Rohde and Hausfather, 2020), which reports daily average temperature on a one-degree grid as an anomaly relative to the 1951–1980 climatology. We recover the daily temperature of each grid cell by adding the anomaly to the climatology. We then aggregate grid cells to the country level, weighting each cell by the population living in the part of the cell that falls within the country's borders. Country boundaries come from Esri's World Countries shapefile. Population weights come from the Gridded Population of the World version 3 count grid for 1990 (CIESIN, 2005). This gives daily population-weighted temperature series for each country from 1970 to 2019, representing the temperature experienced by an average person in the country. From these data, we construct three measures of temperature exposure:

- *Average temperature*, our headline measure, is the mean daily temperature within a country-year.
- *Temperature of the 10 hottest days* captures extreme heat and is defined as the average temperature across the ten hottest days of each country-year.
- *Number of hot days* counts the number of days in a country-year with temperatures above 30°C.[31]

A limitation of the Berkeley Earth data is that temperatures are interpolated from weather-station records, and station coverage is sparse in parts of Sub-Saharan Africa and South Asia. Temperature estimates in these regions are therefore measured with more error. Our approach of using annual averages of the population-weighted temperature series addresses this concern by smoothing out much of the day-to-day measurement error.

Other climate variables. We show robustness to the following alternative measures of climate exposure. These measures use different data sources and capture dimensions of climate other than average temperature.

- *Temperature of hottest day, ERA5:* We use the temperature of the hottest day of the year. The data come from the ERA5 reanalysis (Hersbach et al., 2020), using country-level, area-weighted aggregates from the World Bank Climate Change Knowledge Portal. Unlike Berkeley Earth, ERA5 combines a global weather model with satellite and station observations and is therefore less dependent on local weather-station coverage. This measure captures exposure to extreme heat.
- *Low elevation coastal population:* We use the share of a country's population living in the Low Elevation Coastal Zone, defined as land at or below ten meters above sea level that is contiguous with the coast. The measure comes from Version 3 from CIESIN (2021), which combines elevation data with gridded population counts. It provides a measure of exposure to sea-level rise and coastal flooding.
- *Extreme 1-day rainfall:* We use the largest one-day precipitation total in each year, corresponding to the Rx1day index. These data also come from ERA5 through the World Bank Climate Change Knowledge Portal and are aggregated by area. This measure captures exposure to extreme rainfall and flooding.
- *Natural disaster count:* We count the number of floods, storms, heatwaves, droughts, and wildfires recorded in each country-year by EM-DAT, the international disaster database

[31] There is an extensively documented negative relationship between extreme high temperatures and many outcomes related to welfare. Mortality risk rises non-linearly with high temperatures (Deschênes and Greenstone, 2011; Gasparrini et al., 2015; Barreca et al., 2016; Vicedo-Cabrera et al., 2021; Carleton et al., 2022). Agricultural yields suffer (Schlenker and Roberts, 2009), worker productivity declines (Chen and Yang, 2019), schooling and learning is disrupted (Park et al., 2020), among many other negative effects.

maintained by the Centre for Research on the Epidemiology of Disasters (Delforge et al., 2025). EM-DAT includes events that kill at least ten people, affect at least one hundred people, or lead to a declaration of emergency or a call for international assistance. Unlike the other measures, this variable records realized disaster events rather than meteorological conditions. Because reporting is less complete in earlier periods and in poorer countries, we use it as a complementary measure rather than as our main measure of climate exposure.

B.2 Constructing the Instrument

We follow the construction in Burchardi et al. (2019), who motivate their instrument from a reduced-form law of motion for migrant stocks. In their framework, the stock of migrants from origin o in destination d evolves with migration flows, which depends on the interaction of origin-specific push and destination-specific pull factors, as well as the existing migrant stock. Iterating this law of motion forward expresses the migrant stock in period t as a function of the history of push–pull interactions and higher-order interactions generated by the dependence of migration on past stocks. We follow the same logic and estimate a first stage that projects $\text{stocks}_{od,t}$ on the history of leave-out push–pull interactions, principal components summarizing the higher-order terms, and the initial migrant stock. We refer the reader to Burchardi et al. (2019) for the full derivation.

Similar to Burchardi et al. (2019), we define a leave-out push factor as the total outflow from o to destinations excluding all destinations in the UN sub-region where d is located, denoted by $r(d)$:

$$\text{push}_{o,t}^{-r(d)} \equiv \sum_{d' \notin r(d)} \text{flows}_{od',t}. \tag{B1}$$

This construction ensures the push measure does not mechanically load on o–d migration. Analogously, we define a leave-out pull factor as destination d's share of inflows from origins outside of all origins in o's sub-region, $r(o)$:

$$\text{pull}_{d,t}^{-r(o)} \equiv \frac{\sum_{o' \notin r(o)} \text{flows}_{o'd,t}}{\sum_{o' \notin r(o)} \sum_{d''} \text{flows}_{o'd'',t}}. \tag{B2}$$

That is, pull is measured using migrants from other UN sub-regions, so it captures destination-year attractiveness that is not mechanically driven by flows from o. For each period $\tau \in \{1995, 2000, 2005, 2010, 2015\}$, the resulting push–pull interaction is

$$Z_{od,\tau} \equiv \text{push}_{o,\tau}^{-r(d)} \times \text{pull}_{d,\tau}^{-r(o)}. \tag{B3}$$

For our first stage for migrant stocks we use the history of push–pull interactions to instrument

for stocks in year t, $\text{stocks}_{od,t}$:

$$\log\left(\text{stocks}_{od,t}\right) = \delta_o + \delta_d + \delta_{od} + \sum_{\tau=1995}^{t} \alpha_\tau \, Z_{od,\tau} + \sum_{k=1}^{K} \lambda_k \, \text{PC}_k + u_{od,t}. \tag{B4}$$

where $u_{od,t}$ is the error term and δ_o, δ_d, and δ_{od} are the fixed effects. The interaction terms $Z_{od,\tau}$ are the leave-out push-pull terms that capture quasi-random variation in the allocation of migrants across destinations generated by the coincidence of origin-specific emigration pushes and destination-specific immigration pulls. Following Burchardi et al. (2019), we also include principal components of the higher-order interaction terms implied by the forward solution, PC_k. These terms allow past push–pull shocks to affect later migrant stocks through the evolution of the migrant network. Rather than include the full set of higher-order interactions, we summarize them using their first five principal components, which account for 96% of their variation.

Our preferred specification includes origin–destination fixed effects. Identification therefore comes from changes over time in the push–pull interactions and their higher-order terms within a corridor.

B.3 Examples of Variation Underlying the Instrument

This section provides two examples of the push–pull variation underlying the instrument. In each case, a large origin-specific push coincided with a destination-specific pull, temporarily increasing migration from the origin to the destination.

Zimbabwe and Spain + Italy Example

Zimbabwe's economy began deteriorating from 1998 to 2000, where political turmoil and economic mismanagement generated large output losses.[32] This generated strong push incentives for outward migration from Zimbabwe. This period also coincided with pull-side policy changes in key Southern European destinations: Spain implemented large-scale regularization programmes around 2000–2001, and Italy's 2002 framework facilitated legalization, especially for domestic and care work, raising the expected payoff to migrating to these destinations.[33] Figure B1 shows that Spain and Italy became relatively important destinations for Zimbabwean migrants during this period, but do not stand out in later periods.

Pakistan and Turkey Example

Pakistan experienced a major push shock with the floods that began in late July 2010 and affected more than 20 million people.[34] Over the same period, Turkey overhauled its migration governance

[32] See the IMF's 2000 Article IV report on Zimbabwe for more details.

[33] See Finotelli & Arango (2011, Documents d'Anàlisi Geogràfica) for a discussion of the determinants and effects of this program.

[34] See the report by the Asian Development Bank (2020) for more details on the damage caused by the floods.

Figure B1: Zimbabwe and Italy + Spain Example

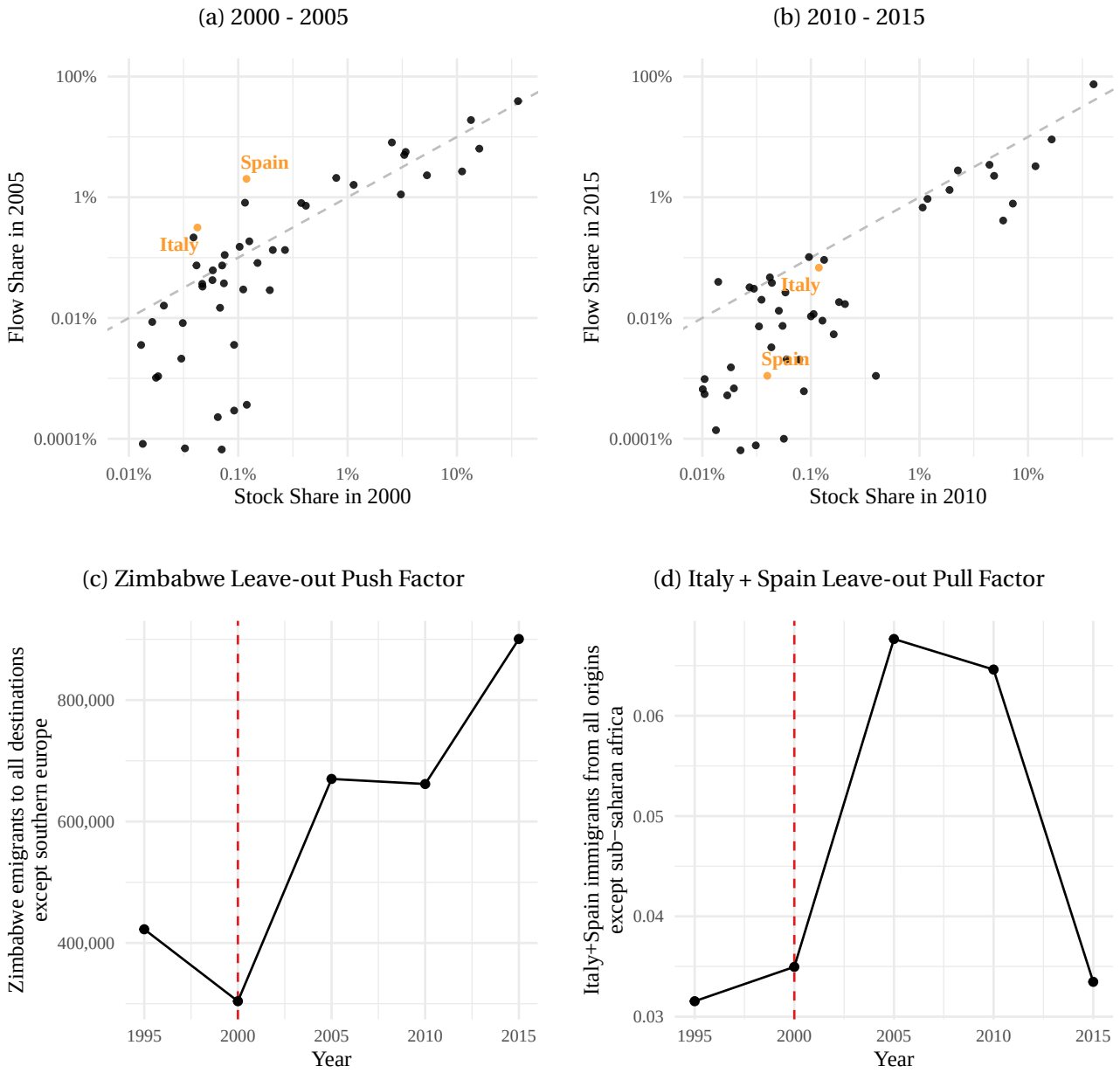

Notes: Panels (a)–(b) plot Zimbabwean flows against lagged migrant stocks across destinations, highlighting Spain and Italy. Panels (c)–(d) plot the leave-out push factor for Zimbabwe and the leave-out pull factor for Spain and Italy. Migrant stocks are from the UN Global Migration Database and flows from Abel and Cohen (2019).

by adopting a law which established a centralized framework for entry, residence, and international protection. These institutional upgrades reduced administrative uncertainty and transaction costs, raising the expected payoff from selecting Turkey as a destination.[35] Figure B2 shows that Turkey became a relatively more important destination for Pakistani migrants during this period than in the preceding period.

Figure B2: Pakistan and Turkey Example

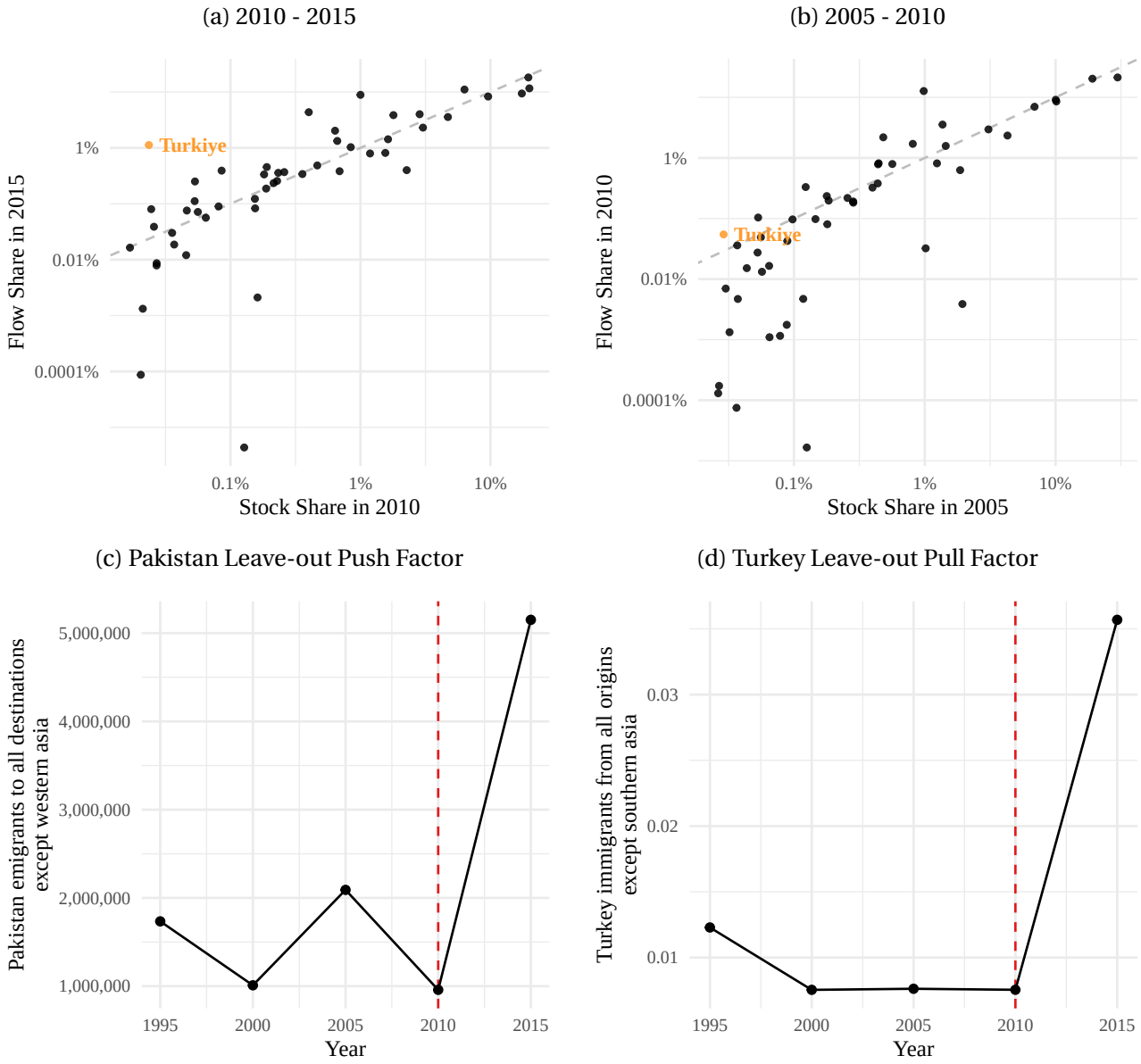

Notes: Panels (a)–(b) plot Pakistani flows against lagged migrant stocks across destinations, highlighting Turkey. Panels (c)–(d) plot the leave-out push factor for Pakistan and the leave-out pull factor for Turkey. Migrant stocks are from the UN Global Migration Database and flows from Abel and Cohen (2019).

[35] For more details on the changes, see the report by the Ministry of Interior of the Republic of Türkiye (2014).

C. Model Proofs and Derivations

C.1 Proof of Proposition 1: Existence and Uniqueness of Equilibrium

We construct the equilibrium forward. Given $\mathbf{z}_{t-1}$ and the weather shock $\boldsymbol{\eta}_t$, the climate process (5) determines $\mathbf{z}_t$ and (4) determines $\mathbf{w}_t$. Given $\mathbf{w}_t$ and the inherited network $\mathbf{x}_t^o$, the choice probabilities (8) are an explicit function of both, and the law of motion (9) determines $\mathbf{x}_{t+1}^o$. Each step has one solution, so the equilibrium exists and is unique. The network enters (8) only as a predetermined argument, so nothing in the construction restricts h.

The value function (10) is well defined along this path. Flow utility is $\nu \log \sum_d \exp([\log w_t^d + h(x_t^{o,d}) - \kappa_t^{o,d}]/\nu)$, in which h is bounded, κ and g are deterministic, and $\log z_t^d$ is normal with variance bounded by the stationary variance of (5). Its expectation is therefore finite in every period, and the discounted sum converges for $\beta < 1$.

C.2 Proof of Proposition 2: Unique Steady State

A steady state exists because $\boldsymbol{\pi}^o(\cdot, \bar{\mathbf{z}}_T)$ is a continuous map from the simplex to itself.

For uniqueness, measure the distance between two networks $\mathbf{x}$ and $\mathbf{x}'$ by the range of their log ratio across destinations, $\max_d \log(x^d/x'^d) - \min_d \log(x^d/x'^d)$, which is zero only when the networks coincide. By (8), the log choice probabilities differ at destination d by $[h(x^d) - h(x'^d)]/\nu$ plus a term common to all destinations, which drops out of the range. As a function of $\log x$, h has slope $xh'(x) = \nu\varepsilon$, so $h(x^d) - h(x'^d)$ has the sign of $\log(x^d/x'^d)$ and is at most $\nu \max_x \varepsilon$ times its size. Since both networks sum to one, the log ratio is positive somewhere and negative somewhere, so the range of the utility differences is at most $\max_x \varepsilon$ times the range of the log ratio. One step of (9) therefore shrinks the distance between any two networks by the factor $\max_x \varepsilon$. When this is below one the map is a contraction, so the steady state is unique and the network converges to it from anywhere.

For instability, the Jacobian of (9) at a steady state $\mathbf{x}$ is $(\operatorname{diag}(\mathbf{x}) - \mathbf{x}\mathbf{x}^\top)\operatorname{diag}(h'(\mathbf{x})/\nu)$, a positive semidefinite matrix times a positive diagonal one. Its eigenvalues are real and non-negative, and the largest is at least the largest diagonal entry, $\max_d \varepsilon^{o,d}(1 - x^{o,d})$. If that exceeds one, a small perturbation of $\mathbf{x}$ along the corresponding eigenvector grows, and the steady state is unstable. The map takes a convex compact set into itself, so the fixed-point indices of its steady states sum to one. A steady state with one unstable direction has index -1, so another steady state exists. With k unstable directions the index is $(-1)^k$, and the argument covers every odd k.

C.3 Proof of Proposition 3: Unique Stationary Distribution

After T the state is the network and the deviation of damages from trend, $\log \mathbf{z}_t - \log \bar{\mathbf{z}}_T$. The deviation is a Gaussian AR(1) with $|\psi| < 1$, so it has a stationary distribution, and the network lives on the simplex. The state is therefore tight and its transition is continuous, so a stationary distribution exists: any limit of the time averages of the transition probabilities from a fixed starting point is one. Integrating out the deviation gives a stationary distribution of the network.

For uniqueness, take two economies with the same weather shocks but different initial states. Their deviations differ by ψ^t times the initial difference, which vanishes. Their networks are updated each period by the same map, and the argument above shows that map shrinks the distance between any two networks by $\max_x \varepsilon$ whatever the damages, since damages enter both economies identically. When $\max_x \varepsilon < 1$ the two networks converge for every sequence of shocks. The distribution of the network after many periods therefore does not depend on the initial state, so the stationary distribution is unique and the distribution of the network converges to it.

C.4 Persistence and Amplification with N Destinations

The persistence and amplification results in Section 3 perturb one corridor holding the rest of the network fixed. They extend to the full system. In log shares, the linearized law of motion is

$$\frac{\partial \log x_{t+1}^{o,d}}{\partial \log x_t^{o,k}} \;=\; \left(\mathbf{1}\{d=k\} - \pi_t^{o,k}\right) \varepsilon_t^{o,k},$$

so a corridor's own response is $\varepsilon_t^{o,d}(1-\pi_t^{o,d})$, which is approximately $\varepsilon_t^{o,d}$ at the small destination shares in the data. The contraction argument in the proof of Proposition 2 bounds the decay of any perturbation of the whole network by $\max_x \varepsilon$ per period for any level of wages, so the persistence rate and the amplification factor $1/(1-\varepsilon)$ hold for the system. Under the condition of Proposition 2 they hold at every network configuration.

C.5 Second Order Expansion of Welfare

In this appendix, we derive the expressions that decompose the role of the network in climate losses into the anchoring term and the diversification term. First, define the expected lifetime utility of an origin-o household $W^o \equiv V_0^o(\mathbf{x}_0^o, \mathbf{z}_0)$. We define $\tilde{W}^o$ as expected lifetime utility in the corresponding economy without network preferences, setting $h(x) = 0$ for all x.

Taking a second-order expansion of W^o around the expected climate path $\{\bar{\mathbf{z}}_t\}$, with period-t deviations $\log \mathbf{z}_t - \log \bar{\mathbf{z}}_t \sim (\mathbf{0}, \mathbf{\Sigma}_t)$,[36]

$$V_0^o(\mathbf{x}_0^o, \{\mathbf{z}_t\}) \;\approx\; V_0^o(\mathbf{x}_0^o, \{\bar{\mathbf{z}}_t\}) \;+\; \sum_t \beta^t \, \nabla_z v_t^o \cdot (\log \mathbf{z}_t - \log \bar{\mathbf{z}}_t) \;+\; \tfrac{1}{2} \sum_t \beta^t \, (\log \mathbf{z}_t - \log \bar{\mathbf{z}}_t)' \, \nabla_z^2 v_t^o \, (\log \mathbf{z}_t - \log \bar{\mathbf{z}}_t)$$

Because the shocks are mean zero, the first order term is zero in expectation. The second order term captures the curvature of the value in each pair of shocks times their covariance

$$\tfrac{1}{2} \sum_{i,j} \frac{\partial^2 v_t^o}{\partial \log z_t^i \, \partial \log z_t^j} \, \Sigma_t^{ij} \;=\; \tfrac{1}{2} \operatorname{tr}\left(\nabla_z^2 v_t^o \cdot \mathbf{\Sigma}_t\right)$$

[36] Because choices are static, the value function is additively separable across periods in the climate path: $V_0^o = \sum_t \beta^t \, \mathbb{E}\left[\nu \log \sum_d \exp\left(\left[\log w_t^d + h(x_t^{o,d}) - \kappa_t^{o,d}\right]/\nu\right)\right]$, up to an additive constant from the Gumbel taste shocks, with $\mathbf{z}_t$ entering through wages. The second derivative of V_0^o with respect to the climate path is therefore block-diagonal by period, so cross-period covariances of the shocks drop out of the expansion.

Therefore, we can write the second order effect as

$$W^o \;\approx\; \underbrace{V_0^o(\mathbf{x}_0^o, \{\bar{\mathbf{z}}_t\})}_{\text{trend effect}} \;+\; \underbrace{\sum_t \beta^t \,\tfrac{1}{2}\,\mathrm{tr}\big(\nabla_z^2 v_t^o \cdot \boldsymbol{\Sigma}_t\big)}_{\text{uncertainty effect} \,\equiv\, \Omega^o} \tag{C1}$$

where the first term, the trend effect, is the welfare along the expected climate path $\bar{\mathbf{z}}$, and the second order effect, defined as Ω^o, is the welfare from the climate shocks. Now, we use that with the idiosyncratic Gumbel taste shocks, direct differentiation gives

$$\frac{\partial v_t^o}{\partial \log z_t^i} \;=\; \pi_t^{o,i}, \qquad \frac{\partial^2 v_t^o}{\partial \log z_t^i \,\partial \log z_t^j} \;=\; \frac{1}{\nu}\Big(\pi_t^{o,i}\,\mathbf{1}\{i=j\} - \pi_t^{o,i}\,\pi_t^{o,j}\Big)$$

Substituting this into the uncertainty term gives

$$\Omega^o \;=\; \sum_t \beta^t\,\Omega_t^o, \qquad \Omega_t^o \;=\; \frac{1}{2\nu}\sum_{i,j}\pi_t^{o,i}\,\pi_t^{o,j}\big(\Sigma_t^{ii} - \Sigma_t^{ij}\big).$$

Ω^o captures the option value of moving under log utility and that option is larger when locations' shocks are negatively correlated.

We define the network effect on climate losses as $D^o - \tilde{D}^o = (1-\beta)\big[(W_\dagger^o - \tilde{W}_\dagger^o) - (W^o - \tilde{W}^o)\big]$ where $\dagger$ represents a no-climate-change economy. The first difference in the square bracket is the network value with no warming, and the second difference is the network value with warming. Now, before deriving how these two terms enter the network effect, let us first show that network preferences tilt choices toward large diasporas. Let $\tilde{\pi}_t^{o,d}$ be migration choices in period t when $h \equiv 0$. Then,

$$\begin{aligned}\pi_t^{o,d} &= \frac{\exp\big(\big[\log w_t^d + h(x_t^{o,d}) - \kappa_t^{o,d}\big]/\nu\big)}{\sum_k \exp\big(\big[\log w_t^k + h(x_t^{o,k}) - \kappa_t^{o,k}\big]/\nu\big)} = \frac{\exp\big(\big[\log w_t^d - \kappa_t^{o,d}\big]/\nu\big)\, e^{h(x_t^{o,d})/\nu}}{\sum_k \exp\big(\big[\log w_t^k - \kappa_t^{o,k}\big]/\nu\big)\, e^{h(x_t^{o,k})/\nu}} \\ &= \frac{\tilde{\pi}_t^{o,d}\, e^{h(x_t^{o,d})/\nu}}{\sum_k \tilde{\pi}_t^{o,k}\, e^{h(x_t^{o,k})/\nu}} \;=\; \frac{\tilde{\pi}_t^{o,d}\, e^{h(x_t^{o,d})/\nu}}{\mathbb{E}_{\tilde{\pi}}\big[e^{h(x_t^{o,k})/\nu}\big]}\end{aligned}$$

That is, h tilts migration choices toward destinations with larger diasporas. Using the second order expansion, the network effect can be written as

$$D^o - \tilde{D}^o \;\approx\; (1-\beta)\Big[\Delta V^o - \Delta\tilde{V}^o \;+\; \Delta\Omega^o - \Delta\tilde{\Omega}^o\Big] \tag{C2}$$

where V^o and $V_\dagger^o$ denote welfare along the trend paths with and without climate change, so that by separability $\Delta V^o = \sum_t \beta^t\,\Delta v_t^o$ with $\Delta v_t^o \equiv v_t^o(\bar{\mathbf{z}}_t^\dagger) - v_t^o(\bar{\mathbf{z}}_t)$, and $\Delta\Omega^o = \sum_t \beta^t\,\Delta\Omega_t^o$ with $\Delta\Omega_t^o \equiv \Omega_{\dagger,t}^o - \Omega_t^o$.

Now, we derive each term. First, let us start with the losses from the expected climate path. Recall

$\Delta \log \bar{z}_t^d \equiv \log \bar{z}_t^{\dagger,d} - \log \bar{z}_t^d$, the trend damages of destination d. Then

$$\begin{aligned}
\Delta v_t^o - \Delta \tilde{v}_t^o \;&\approx\; \sum_d \pi_t^{o,d}\, \Delta \log \bar{z}_t^d \;-\; \sum_d \tilde{\pi}_t^{o,d}\, \Delta \log \bar{z}_t^d \\
&=\; \frac{\sum_d \tilde{\pi}_t^{o,d}\, e^{h(x_t^{o,d})/\nu}\, \Delta \log \bar{z}_t^d}{\mathbb{E}_{\tilde{\pi}}\left[e^{h(x_t^{o,k})/\nu}\right]} \;-\; \mathbb{E}_{\tilde{\pi}}\left[\Delta \log \bar{z}_t^d\right] \\
&=\; \frac{\mathbb{E}_{\tilde{\pi}}\left[e^{h(x_t^{o,d})/\nu}\, \Delta \log \bar{z}_t^d\right] \;-\; \mathbb{E}_{\tilde{\pi}}\left[e^{h(x_t^{o,d})/\nu}\right] \mathbb{E}_{\tilde{\pi}}\left[\Delta \log \bar{z}_t^d\right]}{\mathbb{E}_{\tilde{\pi}}\left[e^{h(x_t^{o,k})/\nu}\right]} \\
&=\; \frac{\mathrm{Cov}_{\tilde{\pi}}\left(e^{h(x_t^{o,d})/\nu},\; \Delta \log \bar{z}_t^d\right)}{\mathbb{E}_{\tilde{\pi}}\left[e^{h(x_t^{o,k})/\nu}\right]}.
\end{aligned}$$

The first line expands each per-period value to first order in trend damages, using that $\partial v_t^o / \partial \log z_t^d = \pi_t^{o,d}$. The same $\Delta \log \bar{z}_t^d$ appears in both economies because they share wages and residence costs. The second line substitutes $\pi_t^{o,d} = \tilde{\pi}_t^{o,d}\, e^{h(x_t^{o,d})/\nu} / \mathbb{E}_{\tilde{\pi}}\left[e^{h(x_t^{o,k})/\nu}\right]$. The third line multiplies and divides the second term by $\mathbb{E}_{\tilde{\pi}}\left[e^{h(x_t^{o,k})/\nu}\right]$. The last line is the definition of covariance. Summing with discount weights gives the lifetime anchoring term,

$$\Delta V^o - \Delta \tilde{V}^o \;=\; \sum_t \beta^t\, \frac{\mathrm{Cov}_{\tilde{\pi}}\left(e^{h(x_t^{o,d})/\nu},\; \Delta \log \bar{z}_t^d\right)}{\mathbb{E}_{\tilde{\pi}}\left[e^{h(x_t^{o,k})/\nu}\right]}$$

The second order term follows similar steps. Recall $\Delta\Sigma_t^{ij} \equiv \Sigma_t^{\dagger,ij} - \Sigma_t^{ij}$, the benchmark-minus-climate-change difference in the covariance of destinations i and j's shocks. Then

$$\begin{aligned}
\Delta \Omega_t^o - \Delta \tilde{\Omega}_t^o \;&=\; \frac{1}{2\nu} \sum_{i,j} \pi_t^{o,i} \pi_t^{o,j} \left(\Delta\Sigma_t^{ii} - \Delta\Sigma_t^{ij}\right) \;-\; \frac{1}{2\nu} \sum_{i,j} \tilde{\pi}_t^{o,i} \tilde{\pi}_t^{o,j} \left(\Delta\Sigma_t^{ii} - \Delta\Sigma_t^{ij}\right) \\
&=\; \frac{1}{2\nu} \left[\frac{\sum_{i,j} \tilde{\pi}_t^{o,i} \tilde{\pi}_t^{o,j}\, e^{(h(x_t^{o,i}) + h(x_t^{o,j}))/\nu} \left(\Delta\Sigma_t^{ii} - \Delta\Sigma_t^{ij}\right)}{\mathbb{E}_{\tilde{\pi}}\left[e^{h(x_t^{o,i})/\nu}\right] \mathbb{E}_{\tilde{\pi}}\left[e^{h(x_t^{o,j})/\nu}\right]} \;-\; \mathbb{E}_{\tilde{\pi}\tilde{\pi}}\left[\Delta\Sigma_t^{ii} - \Delta\Sigma_t^{ij}\right] \right] \\
&=\; \frac{1}{2\nu}\, \frac{\mathrm{Cov}_{\tilde{\pi}\tilde{\pi}}\left(e^{(h(x_t^{o,i}) + h(x_t^{o,j}))/\nu},\; \Delta\Sigma_t^{ii} - \Delta\Sigma_t^{ij}\right)}{\mathbb{E}_{\tilde{\pi}}\left[e^{h(x_t^{o,i})/\nu}\right] \mathbb{E}_{\tilde{\pi}}\left[e^{h(x_t^{o,j})/\nu}\right]}.
\end{aligned}$$

The first line uses that Ω_t^o is linear in the covariance matrix given the weights, so the difference across climate scenarios replaces Σ_t with $\Delta\Sigma_t$. The second line substitutes $\pi_t^{o,i}\pi_t^{o,j} = \tilde{\pi}_t^{o,i}\tilde{\pi}_t^{o,j}\, e^{(h(x_t^{o,i}) + h(x_t^{o,j}))/\nu} / \mathbb{E}_{\tilde{\pi}}\left[e^{h(x_t^{o,i})/\nu}\right] \mathbb{E}_{\tilde{\pi}}\left[e^{h(x_t^{o,j})/\nu}\right]$. The last line multiplies and divides the second term by $\mathbb{E}_{\tilde{\pi}}\left[e^{h(x_t^{o,i})/\nu}\right] \mathbb{E}_{\tilde{\pi}}\left[e^{h(x_t^{o,j})/\nu}\right]$, and applies the definition of covariance. Summing with discount

weights gives the lifetime diversification term,

$$\Delta\Omega^o - \Delta\tilde{\Omega}^o \;=\; \sum_t \beta^t \, \frac{1}{2\nu} \, \frac{\mathrm{Cov}_{\tilde{\pi}\tilde{\pi}}\left(e^{(h(x_t^{o,i})+h(x_t^{o,j}))/\nu},\; \Delta\Sigma_t^{ii} - \Delta\Sigma_t^{ij}\right)}{\mathbb{E}_{\tilde{\pi}}\left[e^{h(x_t^{o,i})/\nu}\right] \mathbb{E}_{\tilde{\pi}}\left[e^{h(x_t^{o,j})/\nu}\right]}$$

These expressions are to build intuition. In the quantitative exercises, we solve each economy fully and allow migration choices and the migrant network to respond endogenously to climate change.

D. Quantification and Computation

D.1 Differences across Shared Socioeconomic Pathways

The growth paths g_t^ℓ used in the quantification come from the Shared Socioeconomic Pathways (SSPs), which are five scenarios for global development over the century (Riahi et al., 2017; Dellink et al., 2017). We use SSP3 as our baseline. Migration incentives in the model depend on cross-country wage differences, and SSP3 preserves large wage gaps over the century. The 90/10 income ratio remains above 9 in 2095, compared with 3.3 under SSP5, so a fast-convergence scenario would substantially reduce migration incentives even in the absence of climate change. SSP3 is also consistent with the high-warming environment used in the quantitative exercises.[37] SSP4 generates similar cross-country income dispersion but substantially lower emissions, making it less consistent with the warming path we study.

Table D1: Growth and Convergence Across the SSPs

	SSP1	SSP2	SSP3	SSP4	SSP5
Growth in GDP per capita, 2020–2095, % per year					
poorest third	3.6	3.2	1.7	2.2	4.3
middle third	2.5	2.3	1.2	2.2	3.1
richest third	1.4	1.3	0.5	1.3	2.0
Dispersion of GDP per capita in 2095					
sd of log GDP per capita	0.51	0.60	0.87	0.97	0.48
90/10 ratio	3.6	4.6	9.4	11.7	3.3

Notes: GDP per capita projections across the five Shared Socioeconomic Pathways. Growth rates are annualized over 2020–2095. Thirds are defined by GDP per capita in 2020, and countries are weighted equally. The 90/10 ratio is the ratio of the 90th to the 10th percentile of GDP per capita across countries in 2095.

[37] In the SSP scenario matrix, SSP5 is the only baseline pathway that reaches radiative forcing of 8.5 W/m^2, while SSP3 reaches approximately 7.0 W/m^2. We follow the climate-impacts literature in pairing weak development with a high-warming path.

D.2 The Damage Process

This appendix details how we construct the trend damages (**??**) and the damage shocks entering (15) from the annual estimates of Nath et al. (2025). They estimate the response of GDP per capita to an annual temperature shock, with a marginal damage linear in the country's temperature, $d'_a(q) = \hat{\beta}_0 + \hat{\beta}_1 q$, and they find that the damage persists, decaying at an annual rate of 0.92. Our model runs at five-year periods and separates permanent warming from transitory weather, so their annual response enters the trend and the shock with different multipliers.

Trend damages. Warming is permanent, so each degree of the trend generates an accumulated effect. We scale the annual response by the ratio of the cumulative response to the annual response in Nath et al. (2025), at their ten-year horizon, so the marginal damage from permanent warming is $d'(q) = \times d'_a(q)$. We then integrate this marginal damage along the expected temperature path,

$$\log \bar{z}_t^\ell = \int_{\bar{q}_0^\ell}^{\bar{q}_t^\ell} \left(\hat{\beta}_0 + \hat{\beta}_1 q\right) dq,$$

We compute the integral in 0.1°C increments, evaluating marginal damages at each step along the temperature path. Since marginal damages are linear in temperature, this is equivalent to using the closed-form integral up to a negligible discretization error. Integrating along the path matters because the implied damage function is quadratic, so the damage from an additional degree depends on the temperature level at which it occurs.

Shock damages. The weather shock η_t^ℓ is the deviation of five-year average temperature from its expected path. If this shock persists for the full five-year period, it affects output in each year. Because the effect of each year's temperature shock decays at the annual rate 0.92, the total damage remaining at the end of the period is

$$\sum_{j=0}^{4} 0.92^j = \frac{1 - 0.92^5}{1 - 0.92} =$$

times the annual response. The marginal damage entering (15) is therefore $\times d'_a(\bar{q}_t^\ell)$. Any damage that carries into the next five-year period persists at rate $\psi = 0.92^5 = 0.66$, as in (5). Thus, both the accumulation of damages within a period and their persistence across periods are implied by the same annual persistence estimate.

D.3 Quantitative Implications of Estimated Network Elasticity

We estimate a migrant network elasticity of $\theta_1/\nu = 0.73$. An elasticity below one means that a shock to a migration corridor fades over time. Consider a migration corridor whose migrant stock is one percent above its steady state, the size its wages and residence cost support. The larger diaspora community draws more migrants in the next period, but only enough to keep the corridor θ_1/ν

percent above its steady state, and the period after that $(\theta_1/\nu)^2$ percent. Given our estimate, the half-life of a shock to the network is 11 years, and 28 percent of a one percent shock remains after twenty years. For the same reason, no corridor is in the region of Proposition 2, where the elasticity exceeds one and more than one long-run migrant network distribution exists.

Although a one-time shock to the network fades over time, the network is a source of amplification. A permanent change in a corridor's wages or residence cost moves its migrant stock nearly four times as much as it would in a model without the network. Figure D1(b) plots the long-run size of a migration corridor against its residence cost net of the wage gap, $\kappa_t^{o,d} - \log(w_t^d/w_t^o)$, the corridor's fundamentals. In the model without the network the slope is $-1/\nu$, the direct response of the corridor's migrant stock to its cost. In the baseline model with the network effect the slope is instead $-1/(\nu - \theta_1)$. A permanent bad shock to a corridor's fundamentals shrinks its migrant stock directly, and the smaller diaspora community then draws fewer migrants in every subsequent period. The migrant stock declines each period by θ_1/ν of its decline in the prior period, so the long-run impact is $1/(1-\theta_1/\nu) = 3.7$ times the direct decline.

Figure D1: Amplification from the Network Elasticity

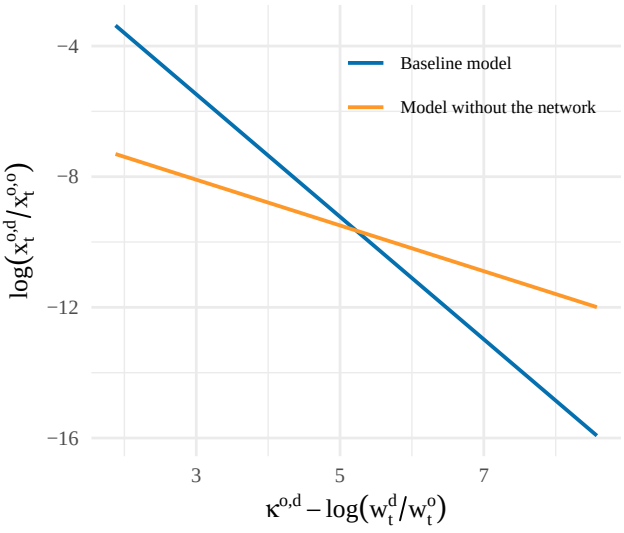

Notes: The figure plots the model's long-run relationship between the size of a corridor, $\log(x_t^{o,d}/x_t^{o,o})$, and its residence cost net of the wage gap, $\kappa^{o,d} - \log(w_t^d/w_t^o)$, through the mean of the corridors open in 2015. The blue line has slope $-1/(\nu - \theta_1)$ and the orange line, the model with the network held fixed, slope $-1/\nu$.

D.4 Comparison with Cruz & Rossi-Hansberg (2024) Quantification

Cruz and Rossi-Hansberg (2024) is the closest quantitative model of migration and climate change. This appendix summarizes the main differences between the two quantifications.

The first difference is how migration costs are modeled. In Cruz and Rossi-Hansberg (2024), the cost of living away from home is the product of an origin and a destination component, $m_o \times m_d$,

and is fixed over time. In our model, the effective cost of moving from o to d is

$$\kappa_t^{o,d} - \left[h(x_t^{o,d}) - h(x_t^{o,o})\right].$$

The first term is a residence cost, while the second depends on the size of the migrant community at the destination relative to the community left at the origin. Effective migration costs therefore change endogenously as migrant stocks evolve. Panel (a) of Figure D2 illustrates this for migration from Pakistan to Canada. In Cruz and Rossi-Hansberg (2024), the effective cost is constant over time. In our model, it falls as the Pakistani community in Canada grows.

The second difference is the path of income in the absence of climate change. In Cruz and Rossi-Hansberg (2024), growth is endogenous. Innovation is concentrated in more productive locations and diffuses across space, generating convergence over time. Their model also starts from greater spatial income dispersion, in part because the economy is defined over $1^\circ \times 1^\circ$ grid cells and therefore captures within-country inequality. In our model, growth follows the SSP3 path, under which cross-country income differences remain large. Panel (b) of Figure D2 compares the 90/10 ratio of income per capita under the two baselines. Since migration incentives depend on wage differences across locations, the two growth paths imply different incentives to migrate later in the century.

There are other differences between the two frameworks. First, Cruz and Rossi-Hansberg (2024) model the world at the $1^\circ \times 1^\circ$ grid-cell level, while we model 161 countries. Their framework therefore allows substantial adjustment through within-country migration, whereas our model focuses on international migration, where migrant networks, borders, and migration policy are directly relevant. Second, their climate path is deterministic, while our model includes weather shocks through $\mathbf{\Sigma}_t$. This additional uncertainty generates an option value of migration and the diversification channel studied in Section 5.

D.5 Monte Carlo Simulation of Climate Path

The welfare objects in Section 5 are expectations of lifetime welfare over realized climate paths in four economies. We compute these expectations by Monte Carlo. A simple Monte Carlo simulation generates first-order variation around the expected climate path that may dominate the second-order effect of climate risk that we want to measure. The diversification channel is a second-order object,

$$\Omega^o = \mathbb{E}[W^o(\mathbf{z})] - W^o(\bar{\mathbf{z}}) \approx \tfrac{1}{2}\,\mathrm{tr}\left(\nabla^2 W^o \mathbf{\Sigma}\right).$$

The first-order term, $\nabla W^o \cdot (\mathbf{z} - \bar{\mathbf{z}})$, has expectation zero and therefore does not enter Ω^o. However, it enters every simulated path. With S draws, its sample mean is of order $\frac{|\nabla W^o||\mathbf{z}-\bar{\mathbf{z}}|}{\sqrt{S}}$. The diversification channel, by contrast, is second order in the climate deviations and is therefore of order $|\mathbf{z} - \bar{\mathbf{z}}|^2$. A standard Monte Carlo simulation must therefore average away first-order variation in order to recover a second-order object. Since the first-order sampling error declines only at rate $1/\sqrt{S}$, this requires a very large number of simulations.

Figure D2: Comparison with Cruz and Rossi-Hansberg (2024)

(a) Effective cost, Pakistan to Canada

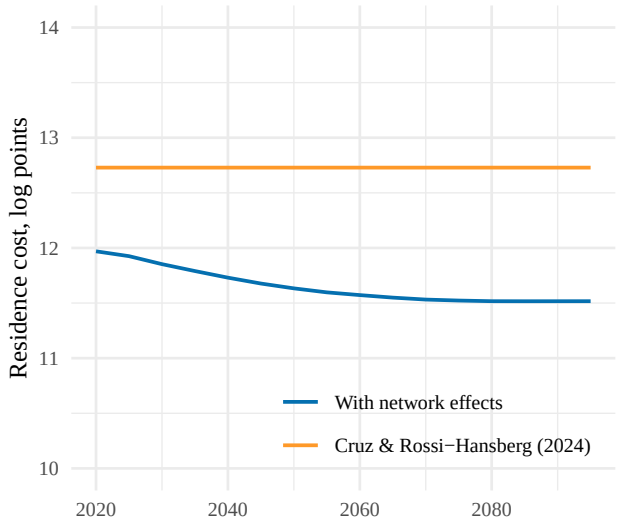

(b) Income convergence absent climate change

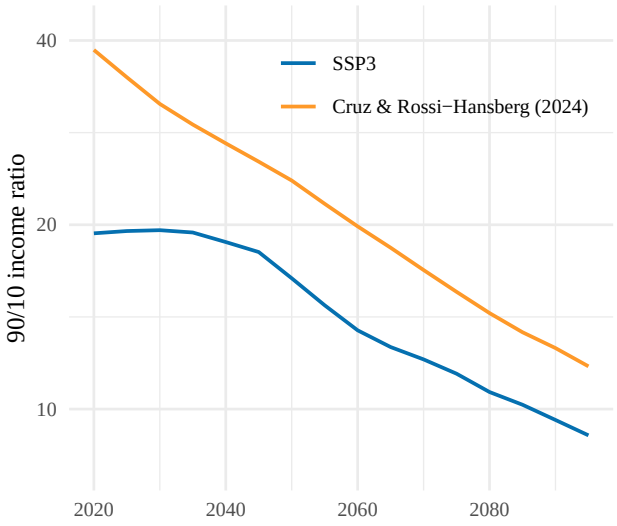

Notes: Panel (a) plots the effective cost of the Pakistan–Canada corridor over the century. Panel (b) plots the 90/10 ratio of income per capita in the baseline without climate change.

Our simulation procedure is designed to remove this first-order variation rather than average it away. We address this in two ways. First, we use the same climate draws across all counterfactual economies, which reduces noise when we take welfare differences. Second, we pair each climate path with its mirror image, so that the first-order variation cancels within the pair.

Step 1: Hold the random draws fixed across economies. We factor each covariance matrix as $\mathbf{\Sigma}_t = \mathbf{L}_t \mathbf{L}_t^\top$. For each simulation path $s = 1, \ldots, S$ and period t, we draw a vector of independent standard normal shocks $\boldsymbol{\eta}_{s,t}$ using a fixed seed.[38] We use the same draws in all four economies. This means that when we compare welfare across economies, each economy faces the same underlying realization of climate risk. Using common draws therefore reduces sampling error in the welfare differences that define the network effect. It does not eliminate the first-order term, however, because the response of welfare to a given climate realization differs across economies.

Step 2: Construct comparable climate and no-climate paths. Under climate change, innovations $\boldsymbol{\zeta}_{s,t} = \mathbf{L}_t \boldsymbol{\eta}_{s,t}$ feed into the climate process around the projected trend $\bar{\mathbf{z}}_t$, with the economy starting on the trend in the base year. The no-climate-change benchmark uses the same $\boldsymbol{\eta}_{s,t}$, but holds the climate trend and covariance matrix at their base-year values. The two scenarios therefore differ only in the evolution of the climate process. We also verify that realized productivity remains strictly positive along every simulated path.

[38] Each $\mathbf{\Sigma}_t$ is estimated from one hundred ensemble runs. A small number of eigenvalues are slightly negative because of sampling error, so we construct the factorization from the eigendecomposition after setting negative eigenvalues to zero.

Step 3: Remove the first-order component using antithetic paths. For every draw $\boldsymbol{\eta}_{s,t}$, we also simulate the antithetic draw $-\boldsymbol{\eta}_{s,t}$. Because the innovations are symmetrically distributed, the two draws have the same distribution, so averaging welfare across the pair does not change expected welfare. Around the deterministic climate path, however, the first-order term enters with opposite signs and cancels exactly. All other odd-order terms cancel as well. The pair average therefore retains the second-order term, along with higher even-order terms, while removing the main source of simulation noise. This allows us to estimate the diversification channel with $S = 10{,}000$ antithetic pairs rather than the orders of magnitude more draws required by a plain Monte Carlo simulation.

Step 4: Solve the four economies on each climate path. For every draw and its mirror, we solve the model forward in four cases: with and without the effect of the migrant network on migration decisions, and with and without climate change. With $S = 10{,}000$ antithetic pairs, this gives $2 \times 2 \times 2S = 80{,}000$ simulated economy-paths. The no-network economy sets $h \equiv 0$ and leaves all other parameters, including residence costs, unchanged. Along each path, we construct log wages from the trend and realized climate damages, compute migration probabilities using the inherited migrant network, update the migrant network, and calculate lifetime welfare.

Expected welfare and the average network effect are computed by first averaging within antithetic pairs and then across pairs. These welfare levels give D^o and $\tilde{D}^o$, and hence the network effect $D^o - \tilde{D}^o$.

For the tail results, we keep the original and antithetic draws as separate climate realizations rather than averaging them within pairs. Quantiles are therefore calculated from the distribution of realized losses across the $2S$ climate paths, with the same realization used across counterfactual economies.

Finally, we solve each economy once along the deterministic climate trend, setting $\boldsymbol{\zeta} = \mathbf{0}$. This gives the anchoring component directly. We define the remaining part of the simulated network effect as the diversification component. The resulting numerical decomposition is exact by construction, while the analytical decomposition in the text gives its second-order approximation.

References

Abel, Guy J. and Joel E. Cohen, "Bilateral international migration flow estimates for 200 countries," *Scientific Data*, June 2019, *6*, 82.

Barreca, Alan, Karen Clay, Olivier Deschênes, Michael Greenstone, and Joseph S. Shapiro, "Adapting to Climate Change: The Remarkable Decline in the US Temperature-Mortality Relationship over the Twentieth Century," *Journal of Political Economy*, 2016, *124* (1), 105–159.

Burchardi, Konrad B., Thomas Chaney, and Tarek A. Hassan, "Migrants, Ancestors, and Foreign Investments," *The Review of Economic Studies*, 2019, *86* (4), 1448–1486.

Carleton, Tamma, Amir Jina, Michael Delgado, Michael Greenstone et al., "Valuing the Global Mortality Consequences of Climate Change Accounting for Adaptation Costs and Benefits," *The Quarterly Journal of Economics*, 2022, *137* (4), 2037–2105.

Chen, Xiaoguang and Lu Yang, "Temperature and industrial output: Firm-level evidence from China," *Journal of Environmental Economics and Management*, 2019, *95*, 257–274.

CIESIN, "Gridded Population of the World, Version 3 (GPWv3): Population Count Grid," 2005.

_ , "Low Elevation Coastal Zone (LECZ) Urban-Rural Population and Land Area Estimates, Version 3," Dataset, Version 3.00 2021.

Cruz, José-Luis and Esteban Rossi-Hansberg, "The Economic Geography of Global Warming," *The Review of Economic Studies*, 2024, *91* (2), 899–939.

Delforge, Damien, Valentin Wathelet, Regina Below, Cinzia Lanfredi Sofia, Margo Tonnelier, Joris A. F. van Loenhout, and Niko Speybroeck, "EM-DAT: The Emergency Events Database," *International Journal of Disaster Risk Reduction*, 2025.

Dell, Melissa, Benjamin F. Jones, and Benjamin A. Olken, "What Do We Learn from the Weather? The New Climate-Economy Literature," *Journal of Economic Literature*, 2014, *52* (3), 740–798.

Dellink, Rob, Jean Château, Elisa Lanzi, and Bertrand Magné, "Long-Term Economic Growth Projections in the Shared Socioeconomic Pathways," *Global Environmental Change*, 2017, *42*, 200–214.

Deschênes, Olivier and Michael Greenstone, "Climate Change, Mortality, and Adaptation: Evidence from Annual Fluctuations in Weather in the US," *American Economic Journal: Applied Economics*, 2011, *3* (4), 152–185.

Gasparrini, Antonio, Yuming Guo, Masahiro Hashizume et al., "Mortality risk attributable to high and low ambient temperature: a multicountry observational study," *The Lancet*, 2015, *386* (9991), 369–375.

Hersbach, Hans, Bill Bell, Paul Berrisford, Shoji Hirahara, András Horányi et al., "The ERA5 Global Reanalysis," *Quarterly Journal of the Royal Meteorological Society*, 2020, *146* (730), 1999–2049.

Mayer, Thierry and Soledad Zignago, "Notes on CEPII's Distances Measures: The GeoDist Database," 2011.

Nath, Ishan B., Valerie A. Ramey, and Peter J. Klenow, "How Much Will Global Warming Cool Global Growth?," 2025. Revise and Resubmit at the *American Economic Review*.

Park, R. Jisung, Joshua Goodman, Michael Hurwitz, and Jonathan Smith, "Heat and Learning," *American Economic Journal: Economic Policy*, 2020, *12* (2), 306–339.

Riahi, Keywan, Detlef P. van Vuuren, Elmar Kriegler et al., "The Shared Socioeconomic Pathways and their Energy, Land Use, and Greenhouse Gas Emissions Implications: An Overview," *Global Environmental Change*, 2017, *42*, 153–168.

Rohde, Robert A. and Zeke Hausfather, "The Berkeley Earth Land/Ocean Temperature Record," *Earth System Science Data*, 2020, *12*, 3469–3479.

Schlenker, Wolfram and Michael J. Roberts, "Nonlinear temperature effects indicate severe damages to U.S. crop yields under climate change," *Proceedings of the National Academy of Sciences*, 2009, *106* (37), 15594–8.

UNDESA, Population Division, "International Migrant Stock 2020: Destination and Origin," Dataset 2021.

Vicedo-Cabrera, Ana M., Noah Scovronick, Francesco Sera et al., "The burden of heat-related mortality attributable to recent human-induced climate change," *Nature Climate Change*, 2021, *11*, 492–500.